

PFAS REMOVAL FOR MUNICIPAL DRINKING WATER

By

ABIGALE MARIE BAHNICK

---

A Thesis Submitted to The W.A. Franke Honors College

In Partial Fulfillment of the bachelor's degree  
With Honors in

Chemical Engineering

THE UNIVERSITY OF ARIZONA

M A Y 2 0 2 5

Approved by:

Dr. Adrianna Brush  
Department of Chemical & Environmental Engineering

0

## **Abstract**

Poly- and perfluoroalkyl substances (PFAS) are hazardous synthetic chemicals that pose significant health risks and have contaminated water supplies in many communities, including a community in the Southside of Tucson, Summit, Arizona. In response, this project proposes a water treatment solution targeting the region's need for clean and safe drinking water. The REAL Water Treatment Plant combines granulated activated carbon filtration with advanced oxidation to effectively remove PFAS and other contaminant 1,4-dioxane. The treatment process effectively removes PFAS concentrations to levels well below the EPA drinking water regulations. To optimize efficiency, the system includes breakthrough modeling that extends the lifespan of filtration media, reduces waste, and minimizes operational costs. Environmental stewardship is central to the design, with a strong emphasis on reducing chemical waste and carbon emissions through media reactivation rather than landfill disposal. Safety protocols are also in place to manage potentially hazardous materials used in the oxidation process. This project provides a model for how communities can address PFAS contamination while promoting environmental responsibility and economic viability. Its successful implementation can serve as a blueprint for broader efforts to ensure universal access to clean water.

## Project Contributions

For this senior design project, I led the development of the advanced oxidation process (AOP) unit operation focused on 1,4-dioxane treatment. I was also responsible for the process description, sizing calculations, stream table data, equipment selection and rationale, process flow diagram (PFD), HAZOP analysis, and life cycle assessment (LCA) related to this unit. Additionally, I researched in detail the AOP design and its theoretical basis. Additionally, a deep dive of adsorption principles was conducted, including hand calculations using Langmuir and Freundlich models, and an analysis of kinetic and equilibrium dependencies of Freundlich parameters. I also explored technical concerns surrounding GAC reactivation in conjunction with AOP, incorporating theories on site occupation, particle diameter, pore size distribution, and their relationship to breakthrough behavior. The work further evaluated the correlation between media weight and treatment efficiency and concluded in conducting an economic hazard analysis specific to the AOP's implementation for 1,4-dioxane.

My teammates were responsible for the rest of the report. Reese contributed extensively to the granulated activated carbon (GAC) system, including unit operation design, process modeling in RStudio, and sizing calculations. She developed key technical documentation such as the process and instrumentation diagrams (PFD/BFD), equipment tables, and stream tables, and conducted both life cycle and economic analyses, including modeling breakthrough behavior and media optimization. Ellie focused on the backwash unit operation and its economic feasibility, contributing detailed calculations, economic summaries, and optimization strategies for reactivated GAC media. She also analyzed capital and annual costs and implemented media mass optimization through breakthrough modeling. Lizzy handled the sediment removal and ground well unit operations, produced foundational sections like the objective statement, introduction, and conclusion, and addressed system-wide concerns such as fouling, pressure balances, GAC media limitations, and environmental and social impacts. Together, these team members provided a comprehensive and integrated design across technical, economic, and sustainability domains.

**Process Proposal**  
**PFAS Removal for Municipal**  
**Drinking Water**

**Reese Arbitelle:**

*Reese Arbitelle*

---

**Ellie Holicky:**

*Ellie Holicky*

---

**Abigale Bahnick:**

*Abigale Bahnick*

---

**Lizzy Somer:**

*Lizzy Somer*

---

## Executive Summary

Poly- and perfluoroalkyl substances (PFAS) are synthetic organofluorides linked to serious human health risks. This proposal outlines a scalable water treatment solution for Summit, Arizona, one of the communities most closely affected by PFAS contamination in Southern Arizona. With water scarcity intensifying in the region, delivering clean, safe drinking water that meets the EPA's Maximum Contaminant Levels (MCLs) is essential.

The REAL Water Treatment Plant will treat 1.2 million gallons per day using granulated activated carbon (GAC) in a lead-lag configuration and an advanced oxidation process (AOP) to target PFAS and 1,4-dioxane. After treatment, PFAS levels were reduced to approximately  $\leq 2$  ppt, well below the EPA's MCL of  $\leq 4$  ppt for PFOA and PFOS,  $\leq 10$  ppt for PFHxS, PFNA, and GenX, and  $\leq 2000$  ppt for PFBS. 1,4-dioxane was reduced to  $< 0.1$  ppb. Breakthrough modeling for two long-chain PFAS compounds, PFOS and PFOA, was conducted to optimize GAC replacement for 318 days and a media weight of 30,000 pounds. This was found to reduce replacement time and waste generation, along with reducing cost to \$13.33 per milligram of PFAS treated.

The \$6.8 million capital investment yields a projected internal rate of return of 24.5%, with positive cash flow starting in year two. Though the cumulative present value remains negative for six years, future opportunities such as raw material substitution and public subsidies will enhance economic viability.

Safety efforts target hydrogen peroxide handling in the AOP zone but are also implemented throughout the system. Environmentally, the design prioritizes PFAS destruction and sustainable disposal, with reactivation technology utilized to break the PFAS waste cycle with less than 0.01 g of PFAS and 400 ft<sup>3</sup> of GAC sent to landfills each year. Reactivation also greatly reduces costs for media replacement by around 70% and emissions from 600 kg of CO<sub>2</sub> per year to 70 kg of CO<sub>2</sub> when compared to replacing GAC contactors with virgin media.

Access to clean water is a human right that remains unmet for many. This project carves a path toward fulfilling that right by addressing PFAS contamination, a growing threat not just for Summit, but worldwide. Scaling this solution can halt further devastation caused by PFAS.

## Overview of Contributions from each team member:

- Reese
  - GAC Unit Op
    - Process Description
    - Sizing Calculations
    - Stream Table - sediment
    - Equipment Table and Rationale
    - PFD
    - HAZOP
    - LCA
  - Executive Summary
  - BFD
  - Economic Analysis Including Economic Hazards of GAC
  - RStudio Breakthrough Curves + Modeling
  - Effects of various factors on breakthrough and removal efficiency
  - Recommendation
  
- Ellie
  - Backwash Unit Op
    - Process Description
    - Sizing Calculations
    - Stream Table - sediment
    - Equipment Table and Rationale
    - PFD
    - HAZOP
    - LCA
  - Economic Calculation
    - Capital Costs
    - Annual Costs
    - Cash Flow
  - Economic Analysis
  - GAC Headloss Cut Sheets
  - GAC Reactivated Media Implementation Cost Benefits
  - Media Mass Optimization via Breakthrough Curve Modeling
  
- Abby
  - AOP 1,4-dioxane Treatment Unit Op
    - Process Description
    - Sizing Calculations
    - Stream Table - sediment
    - Equipment Table and Rationale
    - PFD
    - HAZOP
    - LCA
  - Written Description of Process & Rationale
  - Langmuir & Freundlich Hand Calculations

- Kinetic & Equilibrium Dependence of Freundlich Parameters
- Concerns of Reactivation
- Theory of Sites Occupied, PSDFR, Particle Diameter, & Pore Size
- Correlation of Media Weight & Breakthrough
- Economic Hazards of 1,4-Dioxane Treatment
- Lizzy
  - Sediment Removal and Ground Well Unit Ops
    - Process Description
    - Sizing Calculations
    - Stream Table - sediment
    - Equipment Table and Rationale
    - PFD
    - HAZOP
    - LCA
  - Pressure Table Calculations
  - Objective Statement
  - Introduction
  - Executive Summary
  - Economic Hazards
  - Fouling Theory
  - Social and Environmental Impacts
  - GAC media weight feasibility limitation
  - Conclusions

## Table of Contents

<a href="#"><u>Executive Summary</u></a> .....	4
<a href="#"><u>Overview of Contributions from each team member:</u></a> .....	5
<a href="#"><u>Table of Contents</u></a> .....	7
<a href="#"><u>1. Introduction</u></a> .....	10
<a href="#"><u>1.1 Overview of PFAS</u></a> .....	10
<a href="#"><u>1.2 Overview of 1,4-Dioxane</u></a> .....	11
<a href="#"><u>1.3 Current Market</u></a> .....	11
<a href="#"><u>1.4 Objective Statement and Criteria and Constraints</u></a> .....	12
<a href="#"><u>1.5 Summary of Last Semester</u></a> .....	12
<a href="#"><u>5. Process Description</u></a> .....	13
<a href="#"><u>5.1 Quantitative Block Flow Diagrams</u></a> .....	13
<a href="#"><u>5.1.1 Overview of BFD</u></a> .....	13
<a href="#"><u>5.1.2 Block Flow Diagrams for First Part of Sediment Removal</u></a> .....	14
<a href="#"><u>5.1.3 Block Flow Diagram for Second Part of Sediment Removal</u></a> .....	15
<a href="#"><u>5.1.4 Block Flow Diagram for AOP Chamber</u></a> .....	16
<a href="#"><u>5.1.5 Block Flow Diagram for GAC and Backwash</u></a> .....	17
<a href="#"><u>5.2 Process Flow Diagrams</u></a> .....	18
<a href="#"><u>5.3 Equipment Tables</u></a> .....	19
<a href="#"><u>5.4 Stream Tables</u></a> .....	21
<a href="#"><u>5.5 Utility Table and Overall Energy Balance</u></a> .....	28
<a href="#"><u>5.6 Written Description of Process &amp; Rationale</u></a> .....	29
<a href="#"><u>6. Chemistry of PFAS and adsorption principles</u></a> .....	30
<a href="#"><u>6.1 PFAS Chemistry</u></a> .....	30
<a href="#"><u>6.2 Adsorption Principles</u></a> .....	31
<a href="#"><u>6.2.1 Equilibrium</u></a> .....	31
<a href="#"><u>6.2.2 Mass Transfer Considerations</u></a> .....	32
<a href="#"><u>7. Equipment Description and Rationale</u></a> .....	33
<a href="#"><u>7.1 Ground Wells</u></a> .....	33
<a href="#"><u>7.2 Solids Removal</u></a> .....	33
<a href="#"><u>7.3 1,4-dioxane treatment</u></a> .....	35
<a href="#"><u>7.4 GAC</u></a> .....	36
<a href="#"><u>7.5 Backwash</u></a> .....	38
<a href="#"><u>8. Overview of the Spring Semester and Optimizations</u></a> .....	39
<a href="#"><u>8.1 HALT Method</u></a> .....	39
<a href="#"><u>8.3 Modeling &amp; Breakthrough Curves</u></a> .....	41
<a href="#"><u>8.3.1 Modeling Focus Compounds</u></a> .....	41
<a href="#"><u>8.3.2 Langmuir &amp; Freundlich Theory</u></a> .....	41
<a href="#"><u>8.3.3 Overview of Hand Calculations</u></a> .....	42
<a href="#"><u>8.3.4 Langmuir Hand Calculations</u></a> .....	43
<a href="#"><u>8.3.5 Freundlich Hand Calculations</u></a> .....	44
<a href="#"><u>8.3.6 Equilibria &amp; Kinetic Dependence of the Freundlich Isotherm</u></a> .....	45
<a href="#"><u>8.3.7 Breakthrough Assumption</u></a> .....	47
<a href="#"><u>8.3.8 EPA Modeling Overview</u></a> .....	47
<a href="#"><u>8.4 Reactivation Overview</u></a> .....	51

<u>8.4.1 Concerns of Reactivation</u> .....	52
<u>8.4.2 Effects of Occupied Sites</u> .....	53
<u>8.4.3 Effects of Pore to Surface Diffusion Ratio (PSDFR)</u> .....	54
<u>8.4.4 Effects of GAC Particle Diameter</u> .....	55
<u>8.4.5 Effects of GAC Pore Size</u> .....	56
<u>8.5 Benefits of Implementation of Reactivation</u> .....	56
<u>8.5.1 Costing Savings with Reactivation</u> .....	56
<u>8.5.2 Emissions/Environmental Impact with Reactivation</u> .....	57
<u>8.7 Optimizing GAC Media Weights</u> .....	60
<u>8.7.1 Cost Optimization with Reactivated Media Weight</u> .....	60
<u>8.7.2 Media Weight Feasibility</u> .....	61
<u>8.7.3 Correlation of Media Weight &amp; Breakthrough</u> .....	62
<b><u>9. Safety Issues</u></b> .....	<b>63</b>
<u>9.1 Sediment Removal HAZ-OP</u> .....	63
<u>9.1.1 Ground Well Pump</u> .....	63
<u>9.1.2 Desander</u> .....	63
<u>9.1.3 Clarifier</u> .....	64
<u>9.1.4 Leak Addendum</u> .....	64
<u>9.2 1,4-Dioxane Treatment HAZ-OP</u> .....	64
<u>9.2.1 Hydrogen Peroxide Storage Tank</u> .....	64
<u>9.2.2 UV-AOP Chamber</u> .....	65
<u>9.3 GAC HAZ-OP</u> .....	65
<b><u>10. Environmental Impact Statement</u></b> .....	<b>67</b>
<u>10.1 Sediment Removal LCA</u> .....	68
<u>10.2 1-4 Dioxane Treatment LCA</u> .....	68
<u>10.3 GAC LCA</u> .....	69
<u>10.4 Backwash LCA</u> .....	70
<b><u>11. Final Economic Analysis (Including Economic Hazards)</u></b> .....	<b>71</b>
<u>11.1 Economic Hazards</u> .....	74
<u>11.1.1 GAC Cost</u> .....	74
<u>11.1.2 1,4-dioxane treatment</u> .....	74
<b><u>12. Global, Social, Cultural, and Public Health Impacts</u></b> .....	<b>74</b>
<b><u>13. Conclusions and Recommendations</u></b> .....	<b>76</b>
<b><u>14. References</u></b> .....	<b>78</b>
<b><u>16. Appendices</u></b> .....	<b>86</b>
<u>16.1 Nomenclature</u> .....	86
<u>16.1.1 Acronyms</u> .....	86
<u>16.1.2 Units</u> .....	86
<u>16.1.3 Symbols</u> .....	87
<u>16.2 Final Calculations</u> .....	87
<u>16.2.1 Spread Sheets with Explanations</u> .....	87
<u>16.2.3 Hand calculations that demonstrate correct order of magnitude for equipment</u> .....	87
<u>16.2.4 Hand calculations for GAC Contactor Head loss from cut sheets</u> .....	88
<u>16.2.5 Additional Information</u> .....	88
<u>16.3 Figures</u> .....	89

<a href="#"><u>16.4 Tables</u></a> .....	93
<a href="#"><u>16.5 HAZOP</u></a> .....	100
<a href="#"><u>16.5.1 Solids Removal Zone</u></a> .....	100
<a href="#"><u>16.5.2 AOP</u></a> .....	100
<a href="#"><u>16.5.3 GAC</u></a> .....	100
<a href="#"><u>16.5.4 Backwash</u></a> .....	100
<a href="#"><u>16.6 LCA</u></a> .....	100
<a href="#"><u>16.6.1 Desander</u></a> .....	100
<a href="#"><u>16.6.2 AOP</u></a> .....	100
<a href="#"><u>16.6.3 GAC</u></a> .....	100
<a href="#"><u>16.6.4 Backwash</u></a> .....	100

## 1. Introduction

### 1.1 Overview of PFAS

Per- and poly-fluoroalkyl substances (PFAS) are a group of manufactured chemicals developed in the 1940s to create durable coatings that resist heat, oil, stains, grease, and water, and act as fire retardants [1]. Their unique chemical structure features a hydrophilic "head" group, and a hydrophobic group consisting of a carbon chain bonded to fluorine atoms [2]. The carbon-fluorine bond, one of the strongest in organic chemistry due to fluorine's high electronegativity, makes PFAS highly resistant to degradation [3]. This structure enables PFAS to interact with water while forming extremely stable solutions. This durability makes water purification a feat, commonly requiring advanced and expensive treatment methods.

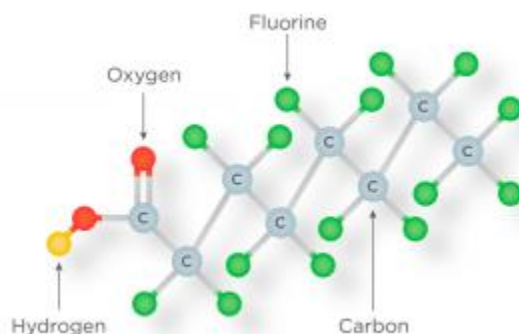


FIGURE 1: PFAS STRUCTURE SHOWCASING THE POLAR HEAD AND NONPOLAR TAIL. THE STRONG CARBON-FLUORINE BONDS ALONG THE CHAIN ARE ALSO SHOWN [4].

PFAS exposure is linked to a range of health risks, including developmental issues in children, increased cancer risk, immune system suppression, hormonal disruptions, and adverse effects on cholesterol levels and liver function [5]. The big six PFAS compounds found in Southern Tucson groundwater that pose notable health risks—PFBS, PFHxS, PFNA, PFOA, PFOS, and HFPO-DA (GenX) [2]—highlight significant contamination. Ground well samples detected concentrations of 17.5 ng/L for PFBS, 99.9 ng/L for PFHxS, 6.2 ng/L for PFOA, 30.4 ng/L for PFOS, and 2 ng/L for PFNA and GenX, most all of which exceed EPA standards. To mitigate the health and environmental risks posed by PFAs, the EPA has set limits at 10 ng/L for PFHxS, PFNA, GenX, 4 ng/L for PFOA and PFOS, and 2000 ng/L for PFBS, highlighting the drastic and urgent problem the region must face [1]. The types of PFAS varies by length, with shorter chain (PFHxS, PFBS, GenX) being more mobile and soluble in water, and long chain PFAs (PFOA, PFOS, PFNA) existing at higher levels in soil and the body [6]. Both necessitate a challenging and costly removal process.

Southern Arizona near Tucson sees unprecedented levels of PFOA and PFAS contamination in groundwater and soil owed to the Davis-Monthan Air Force Base. This contamination stems from historical industrial activities, including former aircraft and electronics manufacturing and firefighting foams [7]. Compounding the issue, groundwater in this area serves as the primary water source for domestic, industrial, and agricultural needs. This reliance

has become even more critical as the Colorado River faces increasing degradation, further limiting water resources in the region [8]. Addressing PFAS contamination in Southern Arizona is a vital environmental and public health challenge, requiring coordinated efforts to mitigate its impact on water supplies and surrounding ecosystems.

## 1.2 Overview of 1,4-Dioxane

1,4-Dioxane is a synthetic industrial chemical that has a widespread presence in groundwater throughout the United States [9]. Commonly known by synonyms such as dioxane, p-dioxane, diethylene dioxide, diethylene oxide, diethylene ether, and glycol ethylene ether [10]. This compound poses significant challenges for water treatment due to its persistence and complete miscibility in water. This is due to its molecular structure and strong polarity, allowing it to form strong hydrogen bonds with water molecules and preventing it from partitioning into soil or sediment [7]. Instead, it remains in the aqueous phase, dispersing easily through groundwater systems.

As a known carcinogen, 1,4-dioxane poses serious health risks, with its presence in drinking water sparking growing concerns. Currently, there is no federal regulation on the maximum contaminant level (MCL) of 1,4-dioxane in drinking water. However, the Environmental Protection Agency (EPA) has issued a health advisory suggesting a maximum concentration of 35 micrograms per liter ( $\mu\text{g/L}$ ) as a guideline for state agencies and public officials to consider [7]. The most common treatment is done using an advanced oxidation process (AOP), which forms hydroxyl radicals that chemically oxidize 1,4-dioxane molecules [11].

While this advisory is not legally enforceable, it raises the alarm for future regulatory action. Implementing treatment systems now, even in the absence of federal standards, would be a well-advised precautionary measure. With the likelihood of an official standard in the near future, early adoption of treatment technologies can help mitigate risks, ensure compliance, protect public health proactively, and set a global standard.

## 1.3 Current Market

Currently, the only PFAS and 1,4-Dioxane treatment zone in Southern Arizona is the Tucson Airport Remediation Project (TARP) facility, initially designed to prevent TCE from leaching into ground wells north of the plant. The implemented GAC beds were intended for hydrogen peroxide removal after the AOP, but this was before PFAs were discovered in the region's groundwater. As a result, the plant does not reduce PFAS levels to meet current EPA standards, rerouting the water to replenish the Santa Cruz River. This leaves an open market for households in the region.

The proposed water treatment process aims to fully serve Summit, Arizona, a smaller community of 5,000 households and its surrounding area [12], and improve waste disposal methods associated with GAC treatment. For instance, while systems like the Marana Picture Rocks plant effectively serve populations of up to 10,000 households, their disposal methods fall short, as fully contaminated GAC is disposed of in landfills. The REAL WTP will employ the

novel approach of third party reactivation to replenish GAC media, ultimately avoiding the long-term risk of PFAS leaching back into groundwater, perpetuating contamination for future generations [13].

#### 1.4 Objective Statement and Criteria and Constraints

PFAS exposure poses serious health risks and has earned the nickname “forever chemicals” due to their persistence in the environment. While the burden of managing PFAS contamination has largely fallen on consumers, this proposal offers a scalable treatment solution for Summit, Arizona—one of the most heavily impacted regions [8]. The proposed plant prioritizes removal efficiency, sustainability, cost-effectiveness, and reliability to ensure safe drinking water while meeting strict environmental and regulatory standards.

#### 1.5 Summary of Last Semester

Last semester, the team identified the target community and established the design basis and treatment goals for addressing PFAS contamination. This included evaluating the health impacts of PFAS exposure, particularly on residents near the Davis-Monthan Air Force Base. A daily treatment capacity of 1.2 million gallons was selected as the design flow rate. Site visits to the TARP and Marana Picture Rocks water treatment facilities provided critical insight into system components such as groundwater extraction, solids removal, AOP, PFAS removal, and backwash management. All major equipment was sized accordingly to ensure high removal efficiency, operational safety, and long-term sustainability. After reviewing multiple PFAS treatment technologies and applying a weighted criteria analysis, the team selected GAC as the most suitable method at this scale. However, challenges related to GAC’s adsorption behavior and disposal frequency, particularly the risk of PFAS leaching from spent media, emerged as key concerns. These risks became a major goal for the spring semester, as many local treatment plants still landfill their used GAC. To address this, the team prioritized modeling GAC adsorption and breakthrough behavior to better understand replacement frequency and explore more sustainable media and waste solutions.

## 5. Process Description

### 5.1 Quantitative Block Flow Diagrams

#### 5.1.1 Overview of BFD

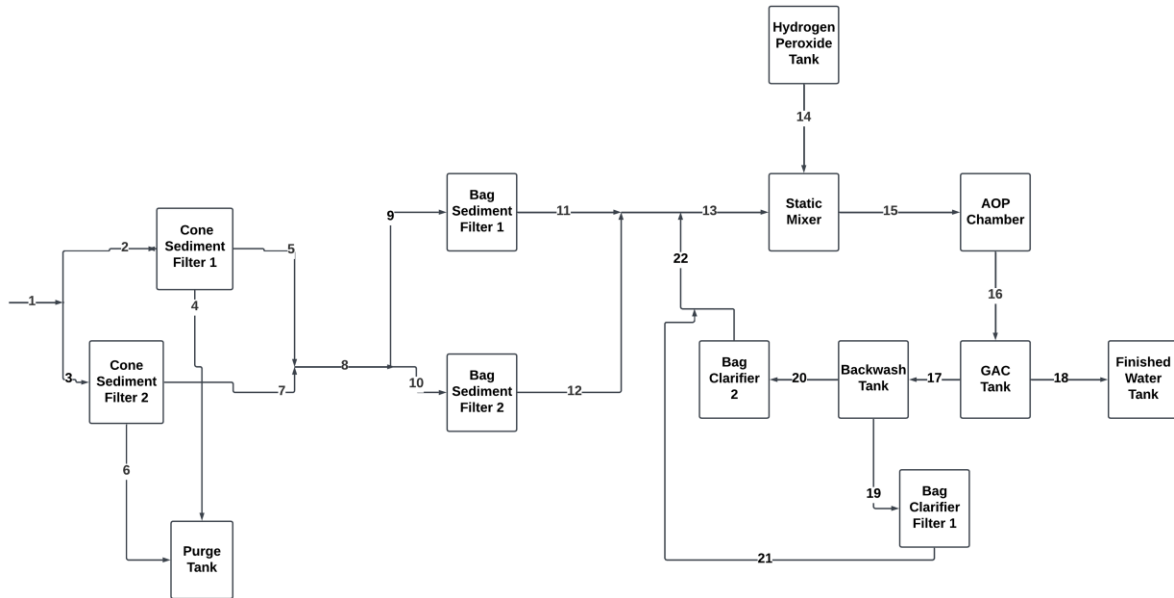


FIGURE 2: COMPLETE OVERVIEW OF THE BLOCK FLOW DIAGRAM FOR THE PROPOSED PROCESS.

### 5.1.2 Block Flow Diagrams for First Part of Sediment Removal

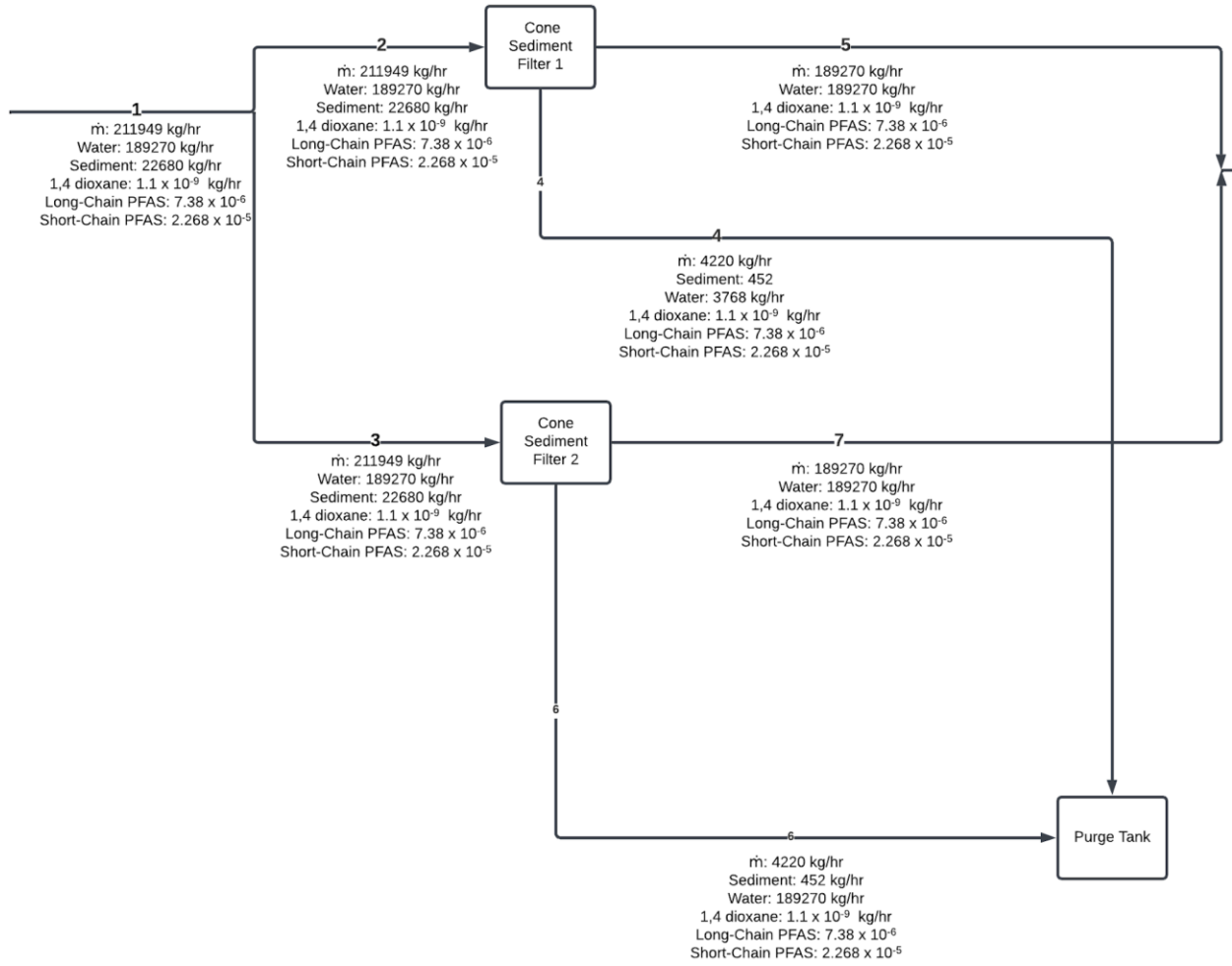


FIGURE 3: SEDIMENT REMOVAL BLOCK FLOW DIAGRAM, INCLUDING SHORT-CHAIN AND LONG-CHAIN PFAS, 1,4-DIOXANE, WATER, SEDIMENT, AND TOTAL MASS FLOW RATES.

### 5.1.3 Block Flow Diagram for Second Part of Sediment Removal

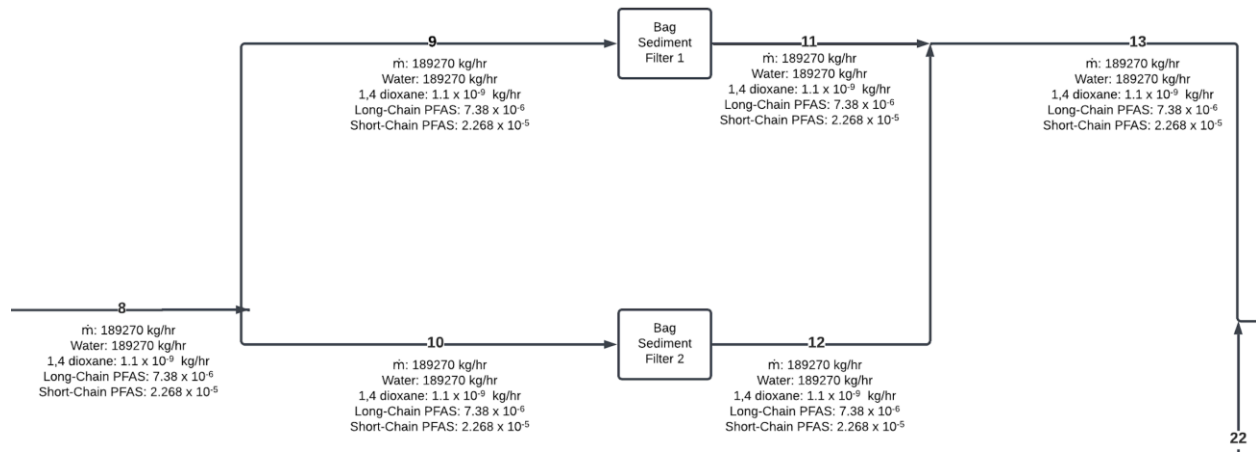


FIGURE 4: SEDIMENT REMOVAL BLOCK FLOW DIAGRAM, INCLUDING SHORT-CHAIN AND LONG-CHAIN PFAS, 1,4-DIOXANE, WATER, SEDIMENT, AND TOTAL MASS FLOW RATES.

### 5.1.4 Block Flow Diagram for AOP Chamber

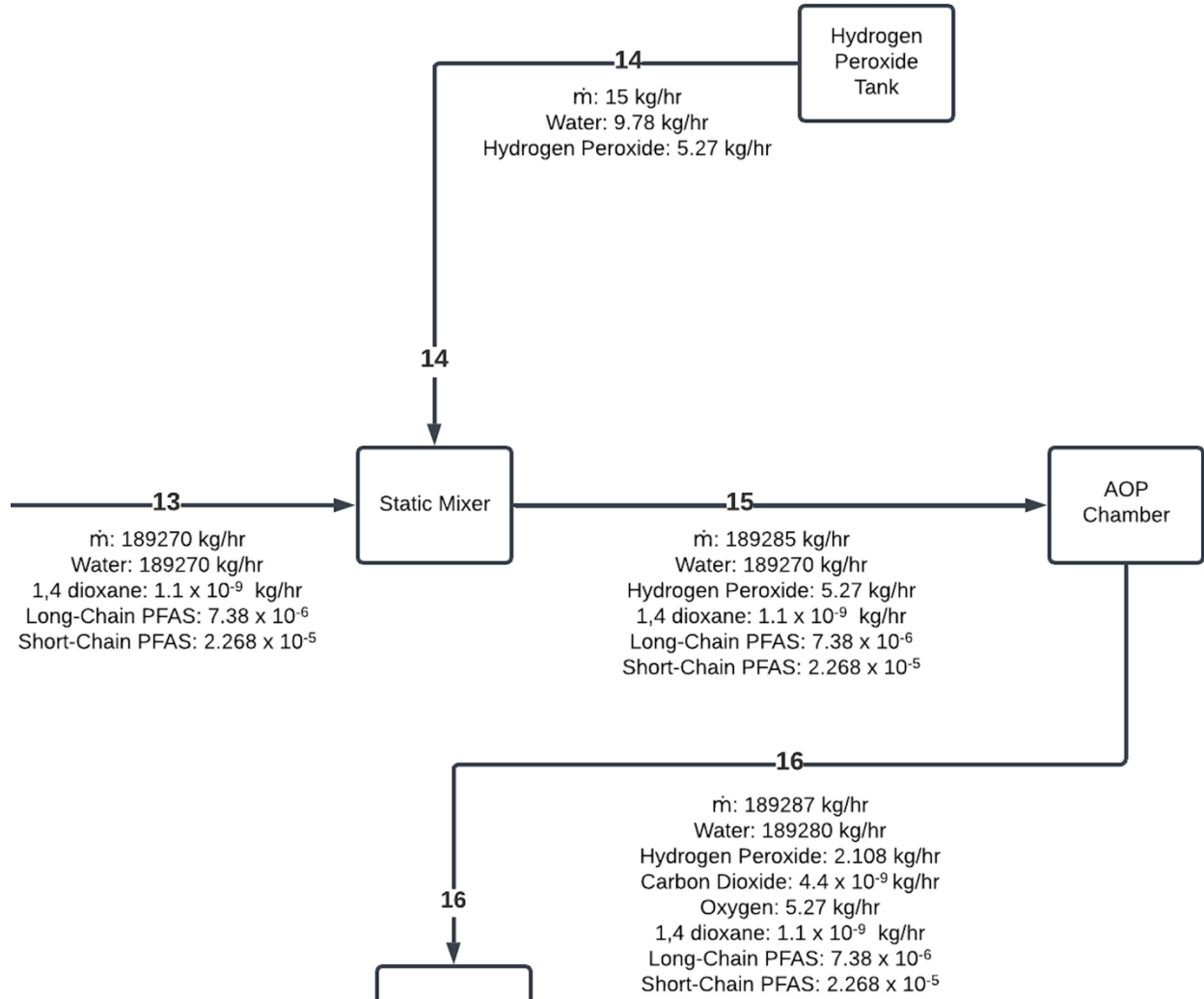


FIGURE 5: AOP BLOCK FLOW DIAGRAM, INCLUDING SHORT-CHAIN AND LONG-CHAIN PFAS, 1,4-DIOXANE, WATER, SEDIMENT, AND TOTAL MASS FLOW RATES.

### 5.1.5 Block Flow Diagram for GAC and Backwash

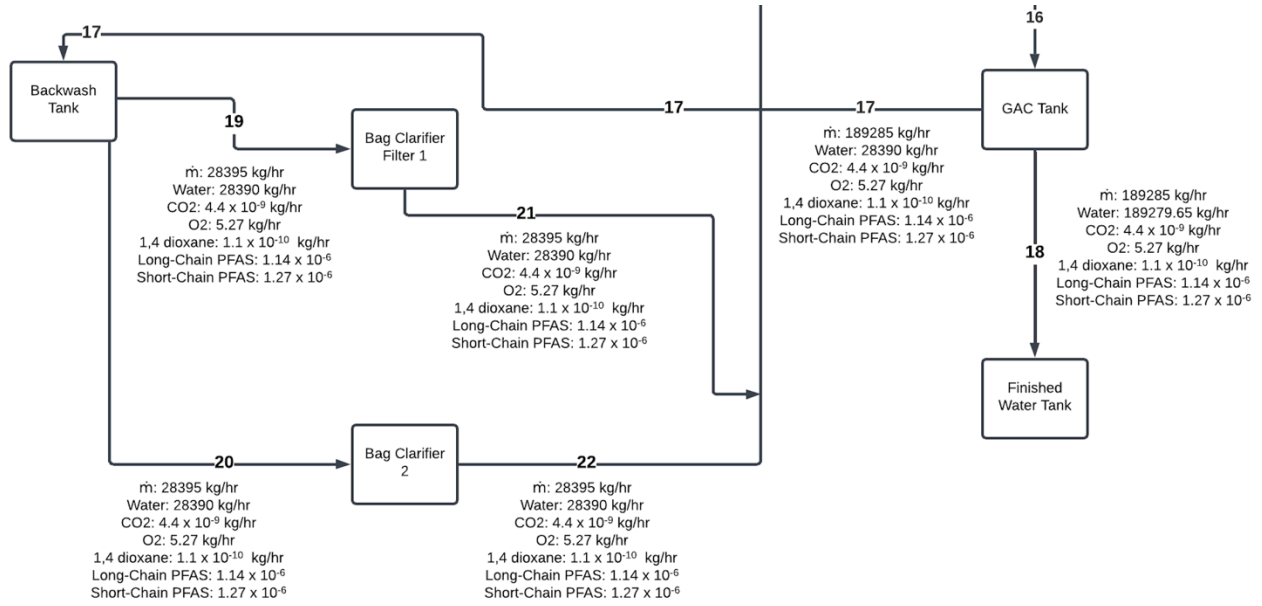


FIGURE 6: GAC BLOCK FLOW DIAGRAM, INCLUDING SHORT-CHAIN AND LONG-CHAIN PFAS, 1,4-DIOXANE, WATER, SEDIMENT, AND TOTAL MASS FLOW RATES.

## 5.2 Process Flow Diagrams

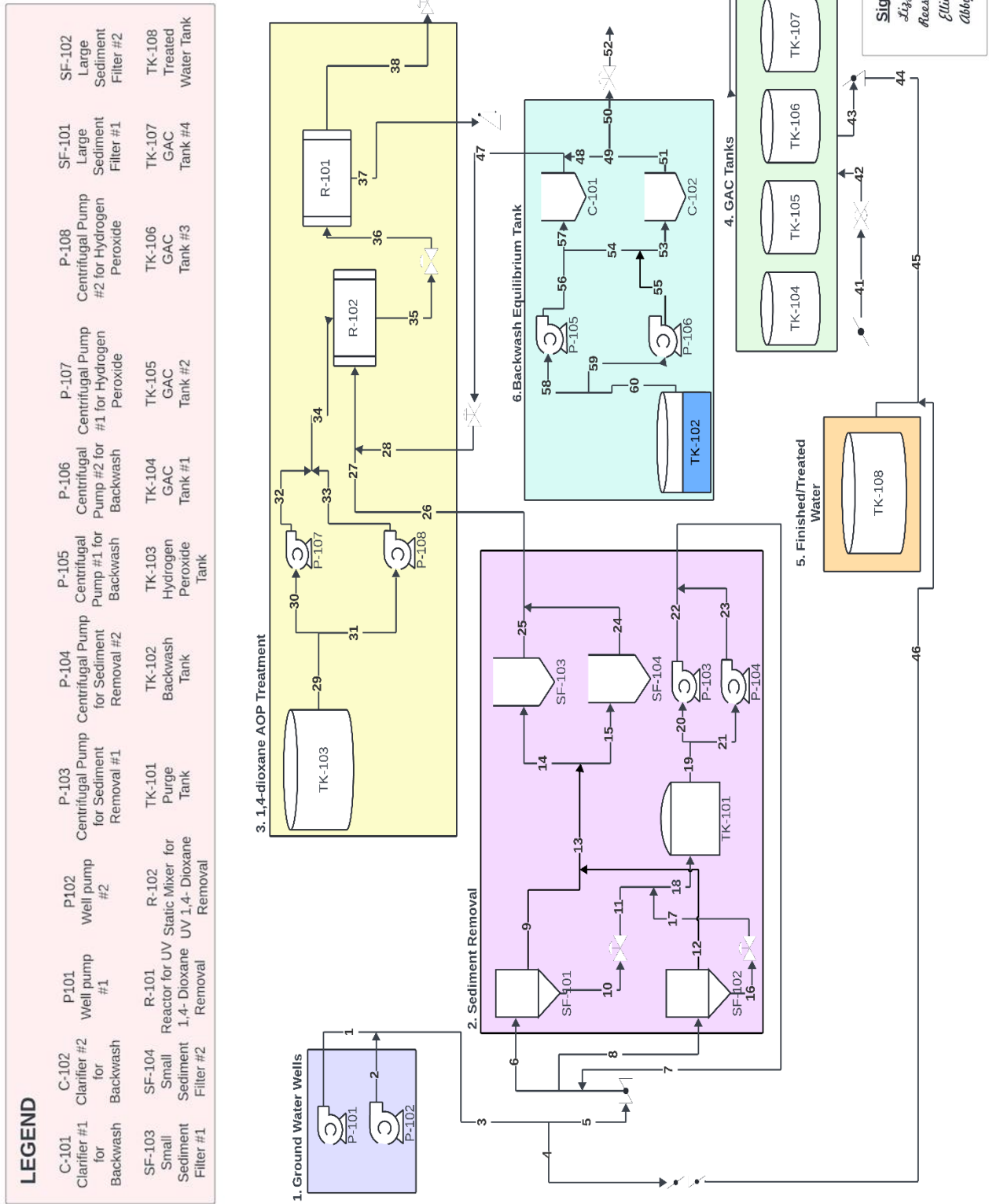


FIGURE 7: COMPLETE OVERVIEW OF THE PROCESS FLOW DIAGRAM SEPARATED BY UNIT-OP.

### 5.3 Equipment Tables

Clarifiers/Reactors	units	SF-101	SF-102	SF-103	SF-104	R-101 (AOP)	R-102 (Static Mixer)
Temperature	C	27	27	27	27	20	20
Pressure	psi	35	35	2	2	15	15
Volume	m <sup>3</sup>	N/A	N/A	N/A	N/A	2	0.0815
MOC		Carbon-Steel	Carbon-Steel	Polypropylene Felt	Polypropylene Felt	N/A	Stainless Steel
Fluid Flow	gpm	833	833	833	833	833	833
Fluid Flow	kg/hr	204116	204116	189270	189270	318002	189002
Fluid Density	kg/m <sup>3</sup>	1078	1078	1000	1000	1000	1000
Head Loss	ft	0	0	5	5	1.34	1.35

Pumps	units	P-101	P-102	P-103	P-104
Temperature	C	50	50	27	27
Type		Well	Well	Centrifugal	Centrifugal
MOC		Steel	Steel	Steel	Steel
Fluid Flow	gpm	833	833	16.6	16.6
Flow	kg/hr	204116	204116	4066	4066
Fluid Density	kg/m <sup>3</sup>	1078	1078	1000	1000
Power	hp	131	131	1	1
Efficiency		0.85	0.85	0.85	0.85
Head Loss	ft	N/A	N/A	N/A	N/A
P(in)	psi	40	40	15	15
P(out)	psi	121	121	50	50

Pumps	units	P-105	P-106	P-107	P-108
Temperature	C	27	27	20	20
Type		Centrifugal	Centrifugal	Peristaltic	Peristaltic
MOC		steel	steel	Stainless Steel	Stainless Steel
Fluid Flow	gpm	125	125	0.055	0.055
Flow	kg/hr	28302	28302	15	15
Fluid Density	kg/m <sup>3</sup>	1000	1158	1158	1158
Power	hp	3	3	N/A	N/A
Efficiency		0.65	0.65	N/A	N/A
Head Loss	ft	N/A	N/A	N/A	N/A
P(in)	psi	15	15	15	15
P(out)	psi	0	0	15	15

Tanks	units	TK-101	TK-102	TK-103	TK-104	TK-105
Temperature	C	27	27	27	27	27
Pressure	psi	15	15	15	15	15
Height	m	56	7.32	2.41	4.88	4.88
Diameter	m	86	5.33	2.44	3.66	3.66
Volume	m <sup>3</sup>	3.75	14	11	18	18
MOC		Polyethylene	carbon steel	HDPE	Carbon Steel	Carbon Steel
Head loss	ft	N/A	N/A	N/A	14.0	14.0

Tanks	units	TK-106	TK-107
Temperature	C	27	27
Pressure	psi	15	15
Height	m	4.88	4.88
Diameter	m	3.66	3.66
Volume	m <sup>3</sup>	18	18
MOC		Carbon Steel	Carbon Steel
Head loss	ft	14.0	14.0

TABLE 1: EQUIPMENT DATA TABLES.

### 5.4 Stream Tables

Stream Number	1	2	3	4	5	6	7	8	9	10
Pressure (PSI)	121.2	121.2	121.2	121.2	121.2	121.2	-	121.2	121.2	-
Mass Flow rate (kg/hr)	21112 4	21112 4	21112 4	21112 4	21112 4	21112 4	18927 0	21112 4	18927 0	4066
Sediment	21854	21854	21854	21854	21854	21854	0	21854	0	435
Water	18927 0	18927 0	18927 0	18927 0	18927 0	18927 0	18927 0	18927 0	18927 0	3631
Hydrogen Peroxide	0	0	0	0	0	0	0	0	0	0
Carbon Dioxide (CO2)	0	0	0	0	0	0	0	0	0	0
Oxygen (O2)	0	0	0	0	0	0	0	0	0	0
1,4 dioxane	1.1E-09	1.1E-09	1.1E-09	1.1E-09	1.1E-09	1.1E-09	1.1E-09	1.1E-09	1.1E-09	1.1E-09
PFBS	3.3E-06	3.3E-06	3.3E-06	3.3E-06	3.3E-06	3.3E-06	3.3E-06	3.3E-06	3.3E-06	3.3E-06
PFHxS	1.9E-05	1.9E-05	1.9E-05	1.9E-05	1.9E-05	1.9E-05	1.9E-05	1.9E-05	1.9E-05	1.9E-05
PFNA	3.8E-07	3.8E-07	3.8E-07	3.8E-07	3.8E-07	3.8E-07	3.8E-07	3.8E-07	3.8E-07	3.8E-07
PFOA	1.2E-06	1.2E-06	1.2E-06	1.2E-06	1.2E-06	1.2E-06	1.2E-06	1.2E-06	1.2E-06	1.2E-06
PFOS	5.8E-06	5.8E-06	5.8E-06	5.8E-06	5.8E-06	5.8E-06	5.8E-06	5.8E-06	5.8E-06	5.8E-06
HFPO-DA (Gen X)	3.8E-07	3.8E-07	3.8E-07	3.8E-07	3.8E-07	3.8E-07	3.8E-07	3.8E-07	3.8E-07	3.8E-07

Stream Number	11	12	13	14	15	16	17	18	19	20
Pressure (PSI)	-	121.2	121.2	121.2	121.2	-	-	-	-	-
Mass Flow rate (kg/hr)	4066	1.9E5	1.9E5	1.9E5	1.9E5	4066	4066	4066	4066	4066
Sediment	435	0	0	0	0	435	435	435	435	435
Water	3631	18927 0	18927 0	18927 0	18927 0	3631	3631	3631	3631	3631
Hydrogen Peroxide	0	0	0	0	0	0	0	0	0	0
Carbon Dioxide (CO2)	0	0	0	0	0	0	0	0	0	0
Oxygen (O2)	0	0	0	0	0	0	0	0	0	0
1,4 dioxane	1.1E-09	1.1E-09	1.1E-09	1.1E-09	1.1E-09	1.1E-09	1.1E-09	1.1E-09	1.1E-09	1.1E-09
PFBS	3.3E-06	3.3E-06	3.3E-06	3.3E-06	3.3E-06	3.3E-06	3.3E-06	3.3E-06	3.3E-06	3.3E-06
PFHxS	1.9E-05	1.9E-05	1.9E-05	1.9E-05	1.9E-05	1.9E-05	1.9E-05	1.9E-05	1.9E-05	1.9E-05
PFNA	3.8E-07	3.8E-07	3.8E-07	3.8E-07	3.8E-07	3.8E-07	3.8E-07	3.8E-07	3.8E-07	3.8E-07
PFOA	1.2E-06	1.2E-06	1.2E-06	1.2E-06	1.2E-06	1.2E-06	1.2E-06	1.2E-06	1.2E-06	1.2E-06
PFOS	5.8E-06	5.8E-06	5.8E-06	5.8E-06	5.8E-06	5.8E-06	5.8E-06	5.8E-06	5.8E-06	5.8E-06
HFPO-DA (Gen X)	3.8E-07	3.8E-07	3.8E-07	3.8E-07	3.8E-07	3.8E-07	3.8E-07	3.8E-07	3.8E-07	3.8E-07

Stream Number	21	22	23	24	25	26	27	28	29	30
Pressure (PSI)	-	-	-	119.2	119.2	119.2	119.2	-	15	15
Mass Flow rate (kg/hr)	4066	4066	4066	18927 0	18927 0	18927 0	18927 0	2839 0	15	15
Sediment	435	435	435	0	0	0	0	0	0	0
Water	3631	3631	3631	18927 0	18927 0	18927 0	18927 0	2839 0	9.7 8	9.7 8
Hydrogen Peroxide	0	0	0	0	0	0	0	0	5.2 7	5.2 7
Carbon Dioxide (CO2)	0	0	0	0	0	0	0	0	0	0
Oxygen (O2)	0	0	0	0	0	0	0	0	0	0
1,4 dioxane	1.1E-09	1.1E-09	1.1E-09	1.1E-09	1.1E-09	1.1E-09	1.1E-09	0	0	0
PFBS	3.3E-06	3.3E-06	3.3E-06	3.3E-06	3.3E-06	3.3E-06	3.3E-06	0	0	0
PFHxS	1.9E-05	1.9E-05	1.9E-05	1.9E-05	1.9E-05	1.9E-05	1.9E-05	0	0	0
PFNA	3.8E-07	3.8E-07	3.8E-07	3.8E-07	3.8E-07	3.8E-07	3.8E-07	0	0	0
PFOA	1.2E-06	1.2E-06	1.2E-06	1.2E-06	1.2E-06	1.2E-06	1.2E-06	0	0	0
PFOS	5.8E-06	5.8E-06	5.8E-06	5.8E-06	5.8E-06	5.8E-06	5.8E-06	0	0	0
HFPO-DA (Gen X)	3.8E-07	3.8E-07	3.8E-07	3.8E-07	3.8E-07	3.8E-07	3.8E-07	0	0	0

Stream Number	31	32	33	34	35	36	37	38	39	40
Pressure (PSI)	15	15	15	15	133.63	133.63	-	133.63	133.63	-
Mass Flow rate (kg/hr)	15	15	15	15	189285	189285	189287	189287	189287	189285
Sediment	0	0	0	0	0	0	0	0	0	0
Water	9.78	9.78	9.78	9.78	189280	189280	189280	189280	189280	189280
Hydrogen Peroxide	5.27	5.27	5.27	5.27	5.27	5.27	2.108	2.108	2.108	0
Carbon Dioxide (CO2)	0	0	0	0	0	0	4.4E-09	4.4E-09	4.4E-09	4.4E-09
Oxygen (O2)	0	0	0	0	0	0	5.27	5.27	5.27	5.27
1,4 dioxane	0	0	0	0	1.1E-09	1.1E-09	1.0E-10	1.0E-10	1.0E-10	1.0E-10
PFBS	0	0	0	0	3.3E-06	3.3E-06	3.3E-06	3.3E-06	3.3E-06	4.7E-07
PFHxS	0	0	0	0	1.9E-05	1.9E-05	1.9E-05	1.9E-05	1.9E-05	4.2E-07
PFNA	0	0	0	0	3.8E-07	3.8E-07	3.8E-07	3.8E-07	3.8E-07	3.8E-07
PFOA	0	0	0	0	1.2E-06	1.2E-06	1.2E-06	1.2E-06	1.2E-06	3.8E-07
PFOS	0	0	0	0	5.8E-06	5.8E-06	5.8E-06	5.8E-06	5.8E-06	3.8E-07
HFPO-DA (Gen X)	0	0	0	0	3.8E-07	3.8E-07	3.8E-07	3.8E-07	3.8E-07	3.8E-07

Stream Number	41	42	43	44	45	46	47	48	49	50
Pressure (PSI)	-	-	109	109	109	-	-	-	-	-
Mass Flow rate (kg/hr)	189285	189285	189285	189285	189285	189285	28395	28395	28395	28395
Sediment	0	0	0	0	0	0	0	0	0	0
Water	189280	189280	189280	189280	189280	189280	28390	28390	28390	28390
Hydrogen Peroxide	0	0	0	0	0	0	0	0	0	0
Carbon Dioxide (CO2)	4.4E-09	4.4E-09	4.4E-09	4.4E-09	4.4E-09	4.4E-09	4.4E-09	4.4E-09	4.4E-09	4.4E-09
Oxygen (O2)	5.27	5.27	5.27	5.27	5.27	5.27	5.27	5.27	5.27	5.27
1,4 dioxane	1E-10	1E-10	1E-10	1E-10	1E-10	1E-10	1E-10	1E-10	1E-10	1E-10
PFBS	4.7E-07	4.7E-07	4.7E-07	4.7E-07	4.7E-07	4.7E-07	4.7E-07	4.7E-07	4.7E-07	4.7E-07
PFHxS	4.2E-07	4.2E-07	4.2E-07	4.2E-07	4.2E-07	4.2E-07	4.2E-07	4.2E-07	4.2E-07	4.2E-07
PFNA	3.8E-07	3.8E-07	3.8E-07	3.8E-07	3.8E-07	3.8E-07	3.8E-07	3.8E-07	3.8E-07	3.8E-07
PFOA	3.8E-07	3.8E-07	3.8E-07	3.8E-07	3.8E-07	3.8E-07	3.8E-07	3.8E-07	3.8E-07	3.8E-07
PFOS	3.8E-07	3.8E-07	3.8E-07	3.8E-07	3.8E-07	3.8E-07	3.8E-07	3.8E-07	3.8E-07	3.8E-07
HFPO-DA (Gen X)	3.8E-07	3.8E-07	3.8E-07	3.8E-07	3.8E-07	3.8E-07	3.8E-07	3.8E-07	3.8E-07	3.8E-07

Stream Number	51	52	53	54	55	56	57	58	59	60
Pressure (PSI)	-	-	-	-	-	-	-	-	-	-
Mass Flow rate (kg/hr)	28395	28395	28395	28395	28395	28395	28395	28395	28395	28395
Sediment	0	0	0	0	0	0	0	0	0	0
Water	28390	28390	28390	28390	28390	28390	28390	28390	28390	28390
Hydrogen Peroxide	0	0	0	0	0	0	0	0	0	0
Carbon Dioxide (CO2)	4.4E-09	4.4E-09	4.4E-09	4.4E-09	4.4E-09	4.4E-09	4.4E-09	4.4E-09	4.4E-09	4.4E-09
Oxygen (O2)	5.27	5.27	5.27	5.27	5.27	5.27	5.27	5.27	5.27	5.27
1,4 dioxane	1E-10	1E-10	1E-10	1E-10	1E-10	1E-10	1E-10	1E-10	1E-10	1E-10
PFBS	4.7E-07	4.7E-07	4.7E-07	4.7E-07	4.7E-07	4.7E-07	4.7E-07	4.7E-07	4.7E-07	4.7E-07
PFHxS	4.2E-07	4.2E-07	4.2E-07	4.2E-07	4.2E-07	4.2E-07	4.2E-07	4.2E-07	4.2E-07	4.2E-07
PFNA	3.8E-07	3.8E-07	3.8E-07	3.8E-07	3.8E-07	3.8E-07	3.8E-07	3.8E-07	3.8E-07	3.8E-07
PFOA	3.8E-07	3.8E-07	3.8E-07	3.8E-07	3.8E-07	3.8E-07	3.8E-07	3.8E-07	3.8E-07	3.8E-07
PFOS	3.8E-07	3.8E-07	3.8E-07	3.8E-07	3.8E-07	3.8E-07	3.8E-07	3.8E-07	3.8E-07	3.8E-07
HFPO-DA (Gen X)	3.8E-07	3.8E-07	3.8E-07	3.8E-07	3.8E-07	3.8E-07	3.8E-07	3.8E-07	3.8E-07	3.8E-07

TABLE 2: STREAM TABLE FOR EVERY STREAM NOTED IN THE PFD. THE GREEN INDICATES BEFORE PFAS REMOVAL TREATMENT AND PURPLE REFERS TO AFTER PFAS REMOVAL TREATMENT.

The stream table operates on the assumption that the REAL water treatment plant will produce 1.2 million gallons of treated water per day. The goal for the project is to achieve 2 ppt of each of the big 6 PFAS compounds, notably PFOS and PFOA, at breakthrough, which was used as a basis for the stream table calculations. This also assumes that the system removes a 1,4-dioxane concentration of 1.1 ppb down to 0.1 ppb. The specific calculations regarding the reaction that takes place in the AOP chamber can be found in the hand calculations of the Appendix section. Also, as seen in several of the streams and depicted in the PFD, multiple of the sets of pumps include one operating and one on standby. Therefore, the inlet and outlet streams of the pumps are equal, but not in operation at the same time. Other assumptions made in the completion of the stream table include that the concentration of 1,4-dioxane and PFAS compounds from the backwash tank (stream 28) are negligible due to backwash tank only as needed. The concentration of sediment going into the clarifiers is negligible compared to the sand content that was removed from the desanders, and that there is an overdose of H<sub>2</sub>O<sub>2</sub> added in the AOP process, so the system is assumed to only remove 60% of H<sub>2</sub>O<sub>2</sub> in the AOP chamber and the other 40% is removed in the GAC tanks.

Stream	Pressure (PSI)	Stream Number	Pressure (PSI)	Stream Number	Pressure (PSI)	Stream Number	Pressure (PSI)
1	121	16	-	31	15	46	-
2	121	17	-	32	15	47	-
3	121	18	-	33	15	48	-
4	121	19	-	34	15	49	-
5	121	20	-	35	134	50	-
6	121	21	-	36	134	51	-
7	-	22	-	37	-	52	-
8	121	23	-	38	134	53	-
9	121	24	119	39	134	54	-
10	-	25	119	40	-	55	-
11	-	26	119	41	-	56	-
12	121	27	119	42	-	57	-
13	121	28	-	43	109	58	-
14	121	29	15	44	109	59	-
15	121	30	15	45	109	60	-

TABLE 3: PRESSURE OF EACH STREAM DURING NORMAL OPERATING HOURS (16 HOURS A DAY). DASHES REPRESENT STREAMS THAT ARE DRY DURING NORMAL OPERATION.

Stream	Pressure (PSI)	Stream Number	Pressure (PSI)	Stream Number	Pressure (PSI)	Stream Number	Pressure (PSI)
1	-	16	-	31	-	46	-
2	-	17	-	32	-	47	77.75
3	-	18	-	33	-	48	77.75
4	-	19	-	34	-	49	77.75
5	-	20	-	35	77.75	50	77.75
6	-	21	-	36	77.75	51	77.75
7	-	22	-	37	-	52	-
8	-	23	-	38	77.75	53	79.74
9	-	24	-	39	77.75	54	79.74
10	-	25	-	40	53.51	55	79.74
11	-	26	-	41	-	56	79.74
12	-	27	77.75	42	-	57	79.74
13	-	28	77.75	43	-	58	53.51
14	-	29	-	44	-	59	53.51
15	-	30	-	45	-	60	53.51

TABLE 4: PRESSURE OF EACH STREAM DURING BACKWASH OPERATION. DASHES REPRESENT STREAMS THAT ARE DRY DURING BACKWASH OPERATION.

Initially, the streams operate at the pressure provided by the ground well pump. The rationale for the pressure of 121 psi is detailed in Section 6.1. Water pressurized to this level exits the well pump and flows toward the sedimentation zone, entering the desander, where head loss is negligible. Subsequently, the stream passes through the bag filters, which cause a head loss of 2 psi when they are clean. Stream 27 then merges with the streams from the AOP system in a mixer with negligible head loss. The AOP system operates at ambient pressure but introduces hydrogen peroxide into the stream. After exiting the mixer, the pressure increases to 134 psi due to the addition from the AOP system. From here, the water proceeds to the GAC zone, where significant head losses occur, as explained in Section 6.4. Finally, the fully treated water moves to the finished water tank at a pressure of 70 psi. This pressure exceeds the expected ambient level, possibly due to sizing assumptions and the exclusion of piping pressure losses.

### 5.5 Utility Table and Overall Energy Balance

The energy balance consists solely of the electrical needs of the treatment plant. As we are a municipal water treatment plant, we will not need to pay for the water we are treating. The total annual cost of our electricity is \$68,689 for the pump motors and AOP unit. Of this electricity cost, the most expensive aspect is the groundswell pumps, P101 and P102. These pumps push the water through our entire system, overcoming the system's head loss, and pull it up from the ground, so they require a large amount of energy. The uncertainty in the utility table is rooted in the assumptions. The first important assumption is that the plant will be charged a flat rate for electricity at \$0.0832/kWh. The second important assumption that the plant is running for 16 hours daily. An increase in either of these assumed values would increase the plants overall utility costs.

				TEP \$/kWh	0.0832
<b>Motors for Pumps</b>					
	P101/102	P103/P104	P105/P106	P107/P108	units
FL Amp	224.00	-	2.90	15.20	amps
Voltage	460.00	-	575.00	120.00	volts
Kilowatts	103.04	1.10	1.67	1.82	kW
Usage	16.00	1.00	2.26	16.00	hours
kWh	1648.64	1.10	3.77	29.18	kWh
Days of operation	365	12	4	365	days
Total kWh	601754	13.20	15.07	10652	kWh
Annual Cost	\$50,065.90	\$ 1.10	\$ 1.25	\$ 886.26	USD

<b>AOP Chamber</b>		
	Lamps	Panels
Number	72	1
Voltage	0.25	18.5
Kilowatts	16	16
Usage	4	296
Days of Operation	365	365
Total kWh	105120	108040
Annual Cost	\$ 8,745.98	\$8,988.93

<b>Total Annual Cost</b>	<b>\$68,689.42</b>
--------------------------	--------------------

TABLE 5: COMPLETE OVERVIEW OF PROCESS FLOW DIAGRAM. ASSUMPTION BASED ON DATA FROM TUCSON ELECTRIC AND POWER COST.

## 5.6 Written Description of Process & Rationale

The overall process flow of the REAL water treatment plant is depicted in the PFD found in section 9.2. The treatment process begins by pumping the raw, contaminated water from two ground wells. The water then flows through a solid removal zone. The purpose of the solid removal zone is to protect downstream equipment, primarily the AOP and GAC treatment zones—from gravel, sand, and other solids that may be pumped from the groundwater well. These are solids that cannot be dissolved in water known as total suspended solids (TSS). Additionally, the system is designed to return concentrated sediment slurry for further treatment and ultimate off-site disposal. While the EPA does not have a primary health standard for TSS in drinking water, removing these solids ensures the longevity and reliability of the treatment system.

Next, an AOP chamber is used to remove 1,4-dioxane from the water, breaking down 1,4-dioxane into harmless byproducts using a powerful oxidant of hydrogen peroxide and UV

light. The resulting products of this process are water, carbon dioxide, and oxygen. The AOP system removes 1,4-dioxane treatment from a concentration of 1.1 ppb down to 0.1 ppb.

The water then undergoes PFAS removal through granular activated carbon (GAC) adsorption tanks, where PFAS compounds adsorb to the carbon material. The GAC treatment reduces the PFAS compounds down to a concentration of approximately less than 2 ppt. To remove trapped contaminants and restore filter efficiency, a backwash system runs once a month. While the backwash system is running, the water is directed through the bottom of the GAC vessels. They are backwashed one at a time, after which the wastewater is stored in a tank. The solids are allowed to settle before the water is returned to the system. To return the backwash water to the system, the system must be running, and the backwash water is filtered before returning into the system. Finally, the last step of the process sends the treated water to a dedicated tank, after a chlorination process, ensuring it is ready for safe distribution to consumers.

This system is modeled like the existing water treatment plants the group toured this semester, the Marana Picture Rocks plant, and the TARP plant [14]. The entire plant was sized based on an assumption of 1.2 million gallons of water per day; a flowrate determined to service a population of 10,000 households. The plant is designed to operate for 16 hours per day, a schedule determined by analyzing the daily operation patterns of the Marana Picture Rocks Plant and the TARP Plant. These facilities run for extended periods to meet peak water demand during the early and late parts of the day. Based on this observed demand cycle, the team selected a 16-hour operational basis for the system. This operational timeframe is considered in the calculations for energy consumption and cost requirements, ensuring the design aligns with practical and economic considerations.

## **6. Chemistry of PFAS and adsorption principles**

### **6.1 PFAS Chemistry**

The most widely accepted definition of PFAS is “a substance that contains at least one fully fluorinated methyl group ( $-\text{CF}_3$ ) or fully fluorinated methylene group ( $-\text{CF}_2-$ ) without any hydrogen, chlorine, bromine, or iodine atom attached to it” [15]. PFAS can be broadly categorized into two classes: polymers and non-polymers. The PFAS species targeted in water treatment plants are classified as non-polymeric and belong to the subclass of perfluoroalkyl substances [16].

Perfluoroalkyl substances are characterized by an alkyl chain in which all hydrogen atoms on the carbon backbone have been fully replaced with fluorine atoms, with the chain attached to a functional group. Within this subclass, the perfluoroalkyl acids (PFAAs) represent the majority of compounds routinely monitored by commercial analytical methods and are the primary focus of health-based regulatory standards at the federal and state levels [16]. Structurally, PFAAs are among the least complex PFAS species and exhibit exceptional environmental stability, with negligible degradation under normal environmental conditions. Due to their chemical persistence

and resistance to transformation, they are often referred to as “terminal PFAS” or “terminal transformation products” [16].

Common subgroups within the PFAA class include the perfluorosulfonic acids (PFSAs) and perfluorocarboxylic acids (PFCAs), which are distinguished by their sulfonic acid and carboxylic acid functional groups, respectively. The classification of PFAS as long-chain or short-chain varies depending on the group: for PFCAs, compounds with eight or more carbons are considered long-chain, while for PFSAs, six or more carbons constitute a long-chain structure. Short-chain PFAS contain seven or fewer carbons for PFCAs and five or fewer for PFSAs [17].

The head of a PFAS molecule contains the functional group, which consistently includes oxygen, although the specific chemical configuration varies between species. In this project, the primary PFAS of interest are PFOA, featuring a carboxylic acid group, and PFOS, featuring a sulfonic acid group. The functional head is highly polar and extremely hydrophilic [18], while the hydrophobic tail, composed of a carbon–fluorine (C–F) backbone, is highly electronegative due to the presence of fluorine atoms. A detailed understanding of PFAS chemistry provides a foundation for evaluating their physical properties, which govern their fate and transport in water treatment processes.

## 6.2 Adsorption Principles

Adsorption is a separation process in which atoms, ions, or molecules from a gas, liquid, or dissolved solid adhere to the surface of a material known as the adsorbent. The species retained on the surface is referred to as the adsorbate [19]. In the case of PFAS removal, the PFAS molecule acts as the adsorbate, while the GAC particle serves as the adsorbent. PFAS adsorption is a complex process primarily driven by physical types of adsorption such as electrostatic and hydrophobic interactions [20]. Electrostatic interactions are most relevant for the removal of short-chain PFAS. PFAS exhibits anionic characteristics because of the negative charge buildup from oxygen atoms at the molecular heads and fluorine atoms along the carbon chain [21]. The adsorbent is positively charged, allowing for electrostatic interactions to occur between the two [1]. For long chain PFAS, hydrophobic interactions play a dominant role. The C-F chain results in hydrophobic properties, and as the chain length increases, so does the hydrophobic effect. As concentrations increase, hydrophobic aggregation can lead to the formation of micelles. These are spherical structures in which hydrophobic tails cluster internally while hydrophilic heads face outward [18]. Understanding the physical adsorption mechanisms of PFAS is critical for predicting their removal efficiency in treatment systems and optimizing adsorbent selection.

### 6.2.1 Equilibrium

In the adsorption process, equilibrium behavior must also be considered. For PFAS removal using GAC, adsorption can be described as the partitioning of PFAS molecules between the water phase and the GAC surface [22]. After sufficient contact time, the system reaches equilibrium. The amount of PFAS adsorbed onto the GAC can be expressed as a function of the PFAS concentration in water at a constant temperature—a relationship known as an adsorption isotherm. The Langmuir and Freundlich models use this assumption, which is discussed in depth later in this report.

### *6.2.2 Mass Transfer Considerations*

For PFAS removal using GAC, operation begins with a clean adsorption bed containing virgin GAC. Once PFAS-contaminated influent enters the GAC bed, mass transfer starts immediately, and the PFAS concentration in the water decreases along the length of the bed until it reaches zero [22]. As fresh influent continues to flow, the section of the bed that is initially contacted by the feed reaches equilibrium with the influent PFAS. Once a section of the bed reaches equilibrium, it is considered “spent” or “exhausted,” and no further adsorption occurs in that portion of the bed. When the influent reaches a portion of bed that has not yet experienced equilibrium, mass transfer resumes and the PFAS concentration decreases with increasing bed length. The region where this concentration change occurs is called the mass-transfer zone (MTZ) [22]. The MTZ marks where active mass-transfer is still happening. As more media becomes saturated and less effective for PFAS removal, the MTZ advances through the length of the GAC bed. Eventually, PFAS will begin to appear in the effluent – a phenomenon known as breakthrough [22]. Breakthrough is typically measured by plotting effluent PFAS concentrations as a function of time. Prior to breakthrough, the effluent PFAS concentration remains near zero, but rises as the MTZ reaches the end of the GAC bed and exits the column.

Rather than defining breakthrough as the first detectable appearance of PFAS in the effluent, the REAL Water Treatment Plant defines breakthrough as the point when the effluent concentration reaches the internal goal of approximately 2 ppt. This operational definition extends the effective lifespan of the GAC within the contactor tank while ensuring that effluent concentrations remain below the EPA's maximum contaminant level (MCL) of 4 ppt.

A critical factor influencing the advancement of the MTZ and the timing of breakthrough is the empty bed contact time (EBCT). EBCT is calculated as the volume of the GAC bed divided by the flow rate of the system [23]. It determines how long the water remains in contact with the media and therefore controls how much time is available for PFAS molecules to diffuse into the pores and adsorb onto active sites [24], [25]. Longer EBCTs provide greater opportunity for mass transfer and deeper penetration of PFAS into the media, which can help slow the progression of the MTZ. For PFAS removal using GAC, an EBCT of at least 10 minutes is typically recommended [24], [25], though this value can vary depending on water quality and the specific GAC product used.

## 7. Equipment Description and Rationale

### 7.1 Ground Wells

Water in Tucson is collected from ground wells which are replenished by the Colorado River. The targeted treatment city, Summit, lies in the Tucson water Basin which has an average depth to water of 153 feet [26]. To overcome head loss from both the elevation gain as well as losses throughout the entire system, primarily in the solids removal, AOP, and GAC treatment zones, the well pump will need to operate at 121 psi. This pressure was found through the pump curve for a J11HC well pump (National Pump Company). The well pumps (P-101 and P-102) will operate in a duty/standby configuration based on the liquid level in the finished water reservoir. Based on the total dynamic head losses of TDH, the system will need a HP horsepower pump with an efficiency of 85% to successfully ensure water flows through the entire system with an output of 1.2 million gallons per day of water to supply Summit, AZ and its surrounding area, a total population of 10,000 households.

### 7.2 Solids Removal

This solids removal process will be achieved using two desanders supporting one duty unit and one standby unit. Desanders function like cyclones: their internal cone-shaped housing forces the liquid to flow in a spiral pattern, which “spits out” large particles into an outer housing that serves as an accumulation tank while maintaining a consistent flow rate. The system divides the incoming flow into two streams: an overflow stream (treated water) and an underflow stream (which contains purged solids). Periodically, the underflow is purged using system feed pressure to transfer solids from the accumulator tank to the purge tank.

Assuming an incoming flow rate of 1.2 million gallons per day and a freshly drilled well with low-weight drilling fluid (8 ppg water), a desander with a 6-inch inlet can effectively remove 99% of particles measuring 86 microns or larger [27]. For reference, the average fine sand particle measures 125 microns, while gravel particles measure approximately 8,000 microns [28]. Therefore, a desander with a 6-inch inlet is sufficient to remove these large TSS from the downstream process, ensuring system performance and protecting the more sensitive downstream equipment. As the ground well ages, more sediment will be pumped through, leading to a higher-density slurry. The maximum density of sediment the desander can support while maintaining proper flowrate is 475 ppg, which is far above the average ground well slurry density of 11 ppg [29].

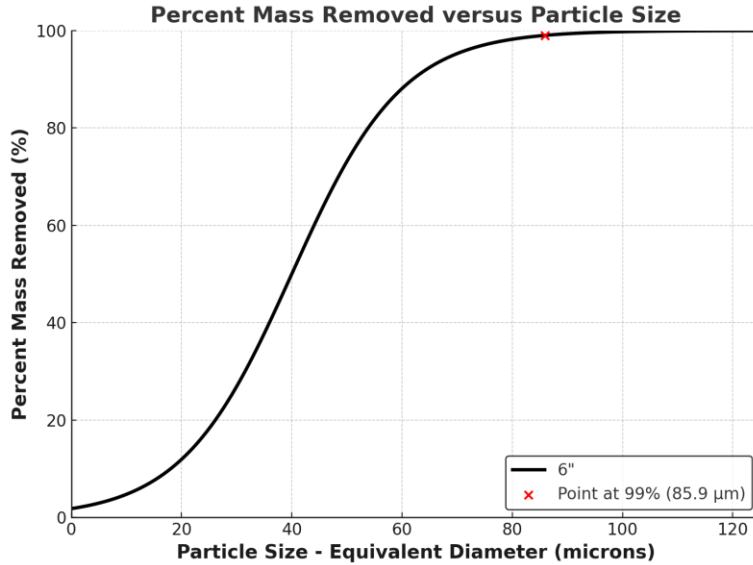


FIGURE 8: THE REMOVAL EFFICIENCY OF SOLIDS FROM A RELATIVELY LOW-WEIGHT DRILLING FLUID (8 PPG) FOR A DESANDER WITH A 6" INLET DIAMETER [28].

Another added benefit of the desander is that the fluid will always have the same velocity within the cone if the same head is delivered to the desander inlet. This maintains the high-water delivery rate through the system, while ensuring consistent solids removal.

A single purge tank is in the sediment removal area to manage the underflow concentrated sediment slurry from the desander. The slurry is first directed into the sediment accumulator on the desander's outer housing, where it is temporarily held before being periodically purged into the tank. This periodic purging minimizes the flow rate into the purge tank, allowing for a reasonably sized design. The 4-inch discharge piping and tank configuration reduce the flow velocity, promoting the settling of solids, while the 2-inch return piping recycles the liquid portion of the slurry. Pumps, configured in parallel with duty and standby operation, recycle the purge water back to the desanders. To ensure TSS does not get drawn back into the desanders, the tank's volume must provide adequate residence time for settling. A volume of 185 gallons was determined to be sufficient to allow complete the calculated settling time of 12 minutes for the slurry.

As shown in Figure 2, desanders are less efficient at removing smaller particles. To address this, bag filters are installed downstream in a parallel configuration, supporting one duty and one standby unit. Each housing contains 14 bags capable of filtering particles as small as 5 microns. When clean, the bag filters cause minimal head loss (~5 ft), but this increases to 35 ft as they become dirty. To monitor performance, pressure gauges will alert staff when filter replacement is needed [30].

### 7.3 1,4-dioxane treatment

1,4-dioxane is an industrial chemical that is the byproduct of products such as hand sanitizers, cosmetics, hygienic products, and dyes. The treatment of 1,4-dioxane has grown increasingly important in recent years. As 1,4-dioxane releases into the air, the compound breaks down quickly. However, when it is released into soil and water, it becomes much harder to break down. This compound is commonly found in groundwater throughout the United States and is a carcinogen, posing great health risks to communities. Currently, there is no federal regulation on the maximum contamination level of 1,4-dioxane in drinking water. However, the EPA has issued a health advisory to provide specific suggestions or standards for state agencies and other public officials to enforce at the state level. The EPA Health Advisory suggested standard for 1,4-dioxane is a maximum concentration of 35 micrograms per liter ( $\mu\text{g/L}$ ) for drinking water [9]. Due to the chosen area of concern for the project, near the airport, the group is basing the assumed 1,4-dioxane concentration in the untreated water off of recent reports by the TARP water treatment plant, which is also located near the airport. According to the TARP Water Quality Report from July through September 2024 [4], the average 1,4-dioxane contaminant level of the raw water is 1.1 ppb and drops to 0.1 ppb after treatment. Going forward, the equipment sizing of the treatment system was based on this goal for 1,4-dioxane removal, achieving the EPA-suggested standard as well.

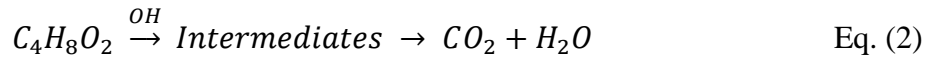
Several methods exist for treating 1,4-dioxane in groundwater, including reverse osmosis, chlorination, ion exchange resins, and advanced oxidation processes (AOPs). Among these, AOPs are the most effective for removing 1,4-dioxane due to their high efficiency in degrading the compound and their scalability for industrial applications. The treatment of 1,4-dioxane using Advanced Oxidation Processes (AOPs) involves the addition of hydrogen peroxide ( $\text{H}_2\text{O}_2$ ) in conjunction with a UV AOP system. The UV-hydrogen peroxide system achieves up to 94% destruction of 1,4-dioxane, making it highly efficient in removal compared to other AOP systems [31]. Specifically, the low-pressure, high-output (LPHO) ultraviolet system facilitates the degradation of 1,4-dioxane in raw, untreated water. Hydrogen peroxide is used because 1,4-dioxane is highly susceptible to chemical oxidation.

The degradation first begins with the decomposition of hydrogen peroxide ( $\text{H}_2\text{O}_2$ ) as it is exposed to UV light decomposing into reactive hydroxyl radicals ( $\cdot\text{OH}$ ) [32]. These hydroxyl radicals produced in the first step, Equation 1, play a central role in the breakdown of 1,4-dioxane. The radicals are extremely reactive and can break the carbon-oxygen bonds of the dioxane ring. The reaction that takes place is an oxidative cleavage of the 1,4-dioxane ring, resulting in the formation of various degradation products, leading to further instant oxidation of intermediates. These reactions happen rapidly; thus they are ultimately negligible compared to the final reaction between the organic intermediates into non-toxic compounds such as water ( $\text{H}_2\text{O}$ ) and carbon dioxide ( $\text{CO}_2$ ). This reaction is demonstrated in Equation 2. As a result of the  $\text{H}_2\text{O}_2$  decomposition, oxygen ( $\text{O}_2$ ) is also produced, as seen in Equation 3.

### Formation of Hydroxyl Radicals



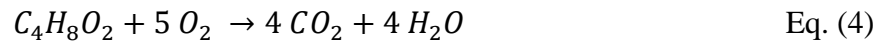
### Complete Destruction Process of 1,4-dioxane



### Balanced Equation of Breakdown of Hydrogen Peroxide



### Balanced Equation of 1,4-dioxane



One of the most common UV AOP chambers used in drinking water treatment is the TrojanUV AOP system, which is currently used at the Marana Picture Rocks Water Treatment Plant in Marana, AZ and TARP in Tucson, AZ. Under the assumption of treating 1.2 million gallons of water per day, which is modeled after the Marana plant, the equipment needed for this scope of 1,4-dioxane treatment is the Trojan UVPhox system. This particular system is used at the Marana plant and is sized to achieve a 1.25-log reduction of 1,4-dioxane, which reaches a final concentration of less than 0.1 ppb [14]. This sizing also takes into account a 25% safety factor applied to the treated water to reach the concentration goal. This sizing aligns with the project's assumed goal of reducing the 1,4-dioxane concentration of 1.1 ppb in the untreated water down to a concentration of 0.1 ppb. The calculations of this unit operation can be found in section 16.1 of the Appendix. The peristaltic pump used to push the H<sub>2</sub>O<sub>2</sub> and water solution to the static mixer operates at inlet and outlet pressures of 15 psi. To calculate the equipment sizing, head loss, and flow rates, the AOP chamber was modeled as a shell and tube heat exchanger. This assumption was made due to the UV lamps modeled as tubes, with the shell-side modeled as the water flowing through.

### 7.4 GAC

The decision matrix developed in CHEE 442 initially guided the team toward selecting granular activated carbon (GAC) adsorption as the most effective method for removing PFAS from drinking water. At the REAL Water Treatment Plant (WTP), four GAC contactors are used, arranged as two lead-lag pairs operating in parallel. Each lead-lag pair consists of two vessels in series. Water first flows through the lead vessel, or “worker bed,” which removes the majority of PFAS contaminants [33], followed by the lag vessel, which further polishes the water by adsorbing any remaining PFAS. This series configuration increases the total empty bed contact time (EBCT), enhancing adsorption capacity and providing protection against premature breakthrough [34].

Each contactor tank is 7.32 m in height and 3.66 m in radius, resulting in an individual volume of 967 ft<sup>3</sup>. With four contactors in operation, the system is designed to treat a total flow rate of 1.2 million gallons per day, enough to serve the town of Summit, Arizona, and surrounding areas. Because the lead-lag pairs operate in parallel, the total flow is evenly split between them, resulting in a flow rate of 416 gallons per minute (gpm) through each pair. By splitting the total flow between two pairs in parallel, each handling half the influent rate, the flow rate through each individual pair is reduced. This lower flow improves adsorption capacity by increasing contact time between the PFAS-contaminated water and the GAC media, which enhances overall treatment performance. If all four contactors were operated in series, the first tank would be exposed to the full PFAS load and would reach breakthrough much more quickly, while the last tank would remain largely unused. This creates an imbalance where the front tanks are exhausted rapidly and require frequent replacement, while the downstream tanks have barely adsorbed any PFAS. Replacing all four tanks just because the first one is spent would be inefficient and costly. Using parallel lead-lag pairs ensures more even utilization of the GAC and avoids premature media replacement, making the system more economical and effective.

Each GAC contactor contains 30,000 pounds of granular activated carbon. The media selected is Calgon's Filtrasorb 400 (F400), a 12x40 mesh, reagglomerated bituminous coal-based carbon. F400 is one of the most widely used and cost-effective GAC types available, making it a practical choice for large-scale water treatment applications [35]. Re-agglomeration creates artificial cracks and crevices in GAC, mimicking the transport pore structures essential for efficient contaminant removal. These transport pores, with diameters exceeding 100 angstroms, do not contribute significantly to adsorption but serve as pathways guiding contaminants to smaller, high-energy adsorption pores. The re-agglomeration process enhances the number and volume of these transport pores, increasing surface area and adsorption efficiency [35]. By using re-agglomerated bituminous coal, both long chain and short chain removal is achieved [36]. While short-chain PFAS molecules have fewer carbon atoms and molecular weight than their long chain variants. Short chains can be removed using re-agglomerated bituminous coal because of the transport pores created during re-agglomeration. This results in both short and long chain PFAS becoming trapped within the high-energy adsorption pore within the internal pore structure. In studies simulating systems with a similar amount of GAC (approximately 23,500 lbs), bituminous coal-based GAC outperformed coconut-based alternatives in removing PFOA and PFOS. The inferior performance of coconut-based GAC was attributed to its narrower transport pores, which limit effective contaminant transport rather than its adsorption pore structure.

These tank specifications, GAC media weight, and flow rate yield a breakthrough time of 453.5 days (15.2 months) for PFOA and 381 days (12.7 months) for PFOS. To ensure the safety of the REAL WTP's customers, GAC media will be replaced every 12 months.

The Ergun equation was used to estimate head loss through the packed GAC bed, using the specified column height, diameter, and flow rate. This calculation yielded a relatively small head loss of approximately 0.9 feet through a single tank. To better represent actual system performance, a heuristic of 1 to 2 feet of head loss per foot of carbon bed was applied during

CHEE 442. This rule of thumb provided a more realistic estimate and helped strengthen the pressure drop values reported in the pressure table.

This heuristic was shared by Viking Edeback, a Carollo engineer whom the team met during a tour of the TARP water treatment plant. Viking is considered a reliable source due to his extensive experience with PFAS treatment systems. He has led more than a dozen PFAS projects, including detailed design work, operational planning, and maintenance coordination for full-scale facilities such as TARP [37]. Beyond the heuristic guidance, Viking has been a valuable resource to the team through frequent email correspondence and two formal meetings. In the first meeting, he informed the team that Calgon, a major producer of GAC media, publishes technical cut sheets with key information about their products. These sheets include parameters such as effective size, uniformity coefficient, apparent density, and importantly, a graph showing typical pressure drop through a bed of F400 GAC. Using data from Calgon's cut sheet, the pressure drop through a 24-foot bed (7.32 meters) containing 30,000 pounds of GAC was calculated to be 14 feet, equivalent to a head loss of 6.072 PSI [38]. Although this value is lower than the heuristic estimate, it falls closer in magnitude and is more representative of the specific media and system design. Therefore, a head loss of 6.072 PSI was used for each GAC contactor bed in the pressure table.

## 7.5 Backwash

Backwashing the GAC filtration system is used to remove any accumulated solids that may have clogged the contactor vessels and reduce head losses through the GAC contactors. The backwash operation consists of a tank to hold the backwash water and allows dislodged solids to settle, a pump that recirculates the water back into the process once backwashing is complete, and bag filters that ensure no dislodged solids re-enter the system. During backwashing, the piping manifolds are reconfigured to reverse the normal flow direction, allowing water from the ground well pumps to flow upward through the GAC beds. This upward flow removes accumulated solids. It is important to note that if backwashing occurs too frequently, it can disturb the transfer zones. Transfer zones refer to horizontal sections of the GAC media that have similar adsorption characteristics based on the amount of PFAS previously removed. Preserving these zones is critical for maintaining consistent filtration performance.

The primary purpose of the GAC backwash recycle system is to reduce waste and protect downstream equipment by recirculating the backwash water. This system helps safeguard the UV chamber and GAC contactors from debris removed during the backwashing process. After the backwash water is collected, it can either be returned upstream of the UV chambers through the recycle system or sent off-site for disposal by tank truck. Within the recycle system, solids are allowed to settle in the backwash equalization tank, and additional sediment is removed using bag filters before the water is reused. The accumulated solids in the equalization tank are periodically removed using a vacuum truck to maintain system efficiency and cleanliness.

Backwashing frequency cannot be estimated and will be determined by the operators based on system performance [39]. In this system, backwashing will be initiated when the head loss through a GAC contactor has doubled from its clean-bed value of 6 psi. Therefore, when a

head loss of 12 psi is observed across a single GAC contactor, operators will perform the backwash to prevent excessive resistance through the media bed.

## **8. Overview of the Spring Semester and Optimizations**

### **8.1 HALT Method**

At the end of the first semester, the team planned to incorporate a comparative study between PFAS removal using GAC through adsorption and the newly developed Hydrothermal Alkaline Treatment (HALT) method for PFAS destruction. Building upon the progress made in the first semester, extensive research was conducted to develop a deeper understanding of the HALT destruction process. Additionally, the team established a connection with Aquagga, a start-up company founded in 2019 that develops pilot-scale PFAS destruction systems using HALT.

The HALT method was particularly appealing due to its potential to address the persistent, cyclic nature of PFAS waste. HALT is considered an effective PFAS destruction technology, offering several benefits, such as its demonstrated ability to reduce both long- and short-chain PFAS to non-detectable levels, while also producing no air emissions or hazardous byproducts. Its effectiveness lies in its capacity to break down PFAS compounds and achieve defluorination through the use of high pressure and temperature, coupled with a highly alkaline environment to drive destruction in the aqueous phase [40]. Specifically, the HALT process operates at around 25 MPa and 350 °C, with a pH greater than 14 [41]. In simpler terms, the system utilizes hot, compressed, and alkaline water to cleave the strong carbon-fluorine bonds present in PFAS. This method has been shown to reduce total PFAS levels, including PFOS and PFOA, by more than 99%.

The team met with a representative from Aquagga, gaining valuable insights into the HALT process and its potential applications. The discussion also provided an overview of the company's perspective on PFAS treatment, the role HALT could play in the future of water treatment, and Aquagga's expansion goals involving both public and private sector partnerships. The representative shared updates on exciting new pilot-scale projects and future plans to scale HALT technology to industrial-scale applications. Aquagga has collaborated with various universities to support the development of their pilot-scale systems and with corporations, including companies like 3M, to implement on-site PFAS removal solutions.

However, after further evaluation, the team decided to pursue a different direction for the semester. This decision was influenced by several factors, including the early-stage nature of HALT technology, limited availability of water quality testing data, and the fact that HALT is currently designed primarily for wastewater treatment, rather than groundwater applications. Another key constraint was the high cost due to the energy demand of a high temperature, high pressure system. Nonetheless, the opportunity to research the HALT method provided the team with a deeper appreciation for PFAS destruction technologies and highlighted the innovation and future possibilities emerging in the field.

## 8.2 Investigating Desorption and Leaching

At the beginning of the spring semester, the team focused on investigating adsorption and identifying specific areas within this topic to explore. Building on last semester's work, the team recognized that PFAS waste (via landfill, incinerating, etc.) and its cyclical nature was a large problem that was mainly unaddressed. In January, this concern guided the team toward preliminary research on desorption and leaching, with the intent of making these processes a central focus of the project.

The team began their investigation by researching PFAS desorption in saturated and unsaturated soil. The leaching potential of PFAS from soils is largely governed by their desorption characteristics [42]. Under saturated conditions, anionic PFAS compounds are particularly prone to leaching. However, desorption behavior varies significantly based on the chemical structure of the PFAS, soil composition, and the surrounding solution chemistry. Short-chain PFAS generally exhibit high mobility due to easier desorption, while long-chain PFAS do not readily desorb, especially in acidic environments. These long-chain species often accumulate in the soil matrix, acting as persistent sources for potential long-term leaching. Most existing desorption and leaching studies have been conducted under saturated conditions, leaving knowledge gaps regarding behavior under unsaturated scenarios.

Additionally, the team also investigated PFAS desorption back into water. PFAS compounds adsorbed onto GAC were found to be desorbed back into the water, even after initial removal [43]. PFAS adsorbed onto GAC can desorb back into water, even after initial removal [43]. As with soils, short-chain PFAS demonstrated higher desorption potential, while long-chain species exhibited stronger binding due to hydrophobic interactions, resulting in lower desorption ratios. Additional factors such as competitive displacement, pore blockage, natural organic matter (NOM) content, flow dynamics, and biodegradation further contributed to desorption variability and uncertainty [43]. In a meeting with Dr. Karanikola, whose research focuses on PFAS, it was noted that desorption remains an under-researched area and may be particularly difficult to characterize quantitatively. This observation is consistent with the findings from the reviewed literature: limited published research exists on PFAS desorption in soils [42], and the relationship between desorption behavior and PFAS physical properties in water remains unclear [43]. Based on these findings, the team decided to shift away from pursuing desorption and leaching as the project's primary focus, was on adsorption and modeling and generating breakthrough curves.

## 8.3 Modeling & Breakthrough Curves

### 8.3.1 Modeling Focus Compounds

PFOS and PFOA were chosen as the primary PFAS compounds for modeling due to their widespread use, well-documented adsorption behavior, and relevance to local contamination. Both compounds were key ingredients in legacy formulations AFFF, which was heavily used by the Davis–Monthan Air Force Base in Tucson, Arizona. Consistent AFFF use led to persistent PFOS and PFOA contamination in the surrounding groundwater. From a modeling standpoint, PFOS and PFOA are particularly well-suited for adsorption modeling due to the availability of reliable experimental data and their relatively simple, predictable behavior at low concentrations.

### 8.3.2 Langmuir & Freundlich Theory

In CHEE 420, the team was introduced to fundamental adsorption concepts and isotherms, including the Langmuir adsorption isotherm. To evaluate feasible modeling approaches, the team also consulted Patrick Lohr, a chemical engineering Ph.D. candidate. He confirmed that the Langmuir isotherm could be applied and explained that calculating the number of occupied adsorption sites could help estimate breakthrough time—assuming breakthrough corresponds to full bed saturation. The team reached out to their CHEE 420 professor, Dr. Suchol Savagatrup, to discuss the Langmuir adsorption model and other potential modeling approaches. He confirmed that Langmuir would be a good starting point due to its simplicity but also suggested exploring more advanced models, such as the Freundlich isotherm, which allows for multilayer adsorption. He also noted that experimental values for parameters like the equilibrium constant  $K$  could likely be found in literature.

Additionally, to support the modeling and design of the two specific compounds the team decided to model, PFOA and PFOS, Dr. Vicky Karanikola and PhD candidate McKenna Dunmyer provided relevant data and literature on adsorption theory and model application. PFOS and PFOA's strong affinity for activated carbon stems from long hydrophobic fluorocarbon chains and negatively charged head groups, which drive both hydrophobic and electrostatic interactions. Their larger molecular size compared to short-chain PFAS also enhances van der Waals forces, increasing surface contact with the carbon and strengthening adsorption [44]. Though individually weak, these forces become significant when combined with the extensive molecular surface area of PFOS and PFOA. Together, these properties explain their consistent isotherm behavior, which aligns well with equilibrium models like Langmuir and Freundlich [45], [46]. Importantly, at low concentrations typical of drinking water systems, PFOS and PFOA remain as monomers and do not form surface aggregates, which allows equilibrium-based models to be applied without needing to account for kinetics, which can get extremely complicated to model [46].

The Langmuir model assumes adsorption occurs as a monolayer onto a fixed number of uniform sites, characterized by a maximum adsorption capacity ( $q_{\max}$ ) and an affinity constant ( $K_L$ ). The linearized equation is shown below.

$$\frac{1}{q_e} = \left( \frac{1}{K_L \cdot q_{max}} \right) \cdot \frac{1}{C_e} + \frac{1}{q_{max}}$$

In contrast, the Freundlich model is an empirical equation that describes multilayer adsorption behavior, using parameters that reflect adsorption strength ( $K_F$ ) and surface heterogeneity ( $1/n$ ). The linearized equation is shown below.

$$\log q_e = \frac{1}{n} \log C_e + \log K_F$$

Additional parameters shown are  $C_e$ , concentration at equilibrium and  $q_e$ , adsorption capacity at equilibrium.

### 8.3.3 Overview of Hand Calculations

As discussed previously, the two models that best describe PFAS adsorption onto granular activated carbon are the Langmuir and Freundlich isotherms. The team's first step in applying these models involved manually calculating the isotherm adsorption parameters using experimental water treatment data. By providing experimental values of  $C_e$  and  $q_e$  over a time interval from literature, the aim was to back-calculate the specific isotherm parameters by rearranging the original equations into a linear form. The primary objective of these hand calculations was to generate isotherm curves and determine whether the system's adsorption behavior aligns more closely with the Langmuir or Freundlich model.

A major challenge in developing initial breakthrough curves stemmed from the critical factors required for accurate PFAS modeling, whether via hand calculations or coding methods. Key considerations included selecting the most appropriate isotherm model for the system, sourcing reliable experimental data from published studies, and ensuring the data reflected groundwater PFAS concentrations typical of industrial-scale water treatment and the use of comparable media, specifically Calgon F400 GAC, as used at the REAL plant. Furthermore, as elaborated later in the discussion of hand calculations, the Langmuir and Freundlich isotherm constants vary depending on the media type, reiterating the importance of matching experimental conditions as closely as possible.

One important distinction to make is that adsorption isotherms describe the amount of solute adsorbed per unit mass of adsorbent (the dependent variable) as a function of the solute concentration at equilibrium (the independent variable), rather than the initial concentration [47]. This means that the isotherm models are only valid once the equilibrium concentration has been determined. Therefore, in industrial and experimental systems, it is often more useful to predict removal efficiency based on the initial experimental conditions, including the initial solute concentration, solution volume, and adsorbent mass [47]. Another option also includes calculating the amount of adsorbent needed to achieve a specific removal target. This can be seen in the results of the hand calculations detailed below.

### 8.3.4 Langmuir Hand Calculations

The first step involved modeling the system using the simplest model: the Langmuir isotherm. As stated before, this model incorporates several key parameters:  $C_e$ , the solute concentration at equilibrium;  $q_e$ , the mass of solute adsorbed per unit mass of adsorbent at equilibrium;  $K_L$ , the Langmuir equilibrium constant; and  $q_{max}$ , representing the maximum adsorption capacity [47]. It is important to note that, prior to beginning these calculations, the team recognized that the monolayer, homogeneous surface adsorption assumption might not be suitable for PFAS behavior in this system. This expectation was based on an understanding that PFAS does not adhere to a monolayer assumption on GAC surfaces, as discussed in detail in the report section reviewing PFAS chemistry.

After a thorough review of published PFAS data, the team identified a suitable experimental dataset that met key criteria: it included concentrations representative of a groundwater industrial-scale treatment plant, utilized media with similar characteristics to F400, and provided equilibrium data for the two long-chain PFAS compounds of interest, PFOA and PFOS. To manually model both the Langmuir and Freundlich isotherms, the team used data from the paper "Kinetic and isotherm study for the adsorption of PFAS on activated carbon in the low ng/L range" by [48]. Specifically, the dataset from Table S.9 in the Supplemental Information was used, providing experimental equilibrium data for PFAS adsorption on SRD activated carbon, including equilibrium concentrations ( $c$ , ng/L) and adsorbent loadings ( $q$ , ng/mg) across a range of concentrations [48].

It is important to note that the SRD activated carbon used in this study is not identical to the Calgon F400 media used at the REAL plant. However, based on mesopore distribution data from Figure S.1 in the Supplemental Information of the Pranic et. al paper, the SRD carbon exhibits a pore size distribution most similar to F400. Given the lack of available equilibrium data for F400, the team determined that SRD carbon data was appropriate for preliminary hand calculations. The dataset was also selected due to the broader range of equilibrium concentrations it covered compared to other published data, which was often limited or incomplete.

To better reflect real-world conditions, initial concentrations from TARP water quality data were used: 6.2 ng/L for PFOA and 30.4 ng/L for PFOS. Several assumptions were necessary due to differences between the experimental setup and actual plant conditions. For Langmuir modeling, the team graphed adsorbent loading ( $q$ ) versus equilibrium concentration ( $c$ ) and applied the linearized Langmuir equation, where the slope corresponds to  $\frac{1}{K_L * q_{max}}$  and the y-intercept to  $\frac{1}{q_{max}}$  [48]. Using these relationships,  $K_L$  and  $q_{max}$  were calculated. Based on visual inspection and the relatively low  $R^2$  value of 0.7276, the data was found not to fit the Langmuir model well. The resulting  $K_L$  and  $q_{max}$  values for PFOS were 0.187 L/mg and 49.02 mg/g respectively. The resulting  $K_L$  and  $q_{max}$  values for PFOA were 0.338 L/mg and 20.62 mg/g respectively. Using these parameters, they can be used to either predict the final solute concentration and removal efficiency or estimate the amount of adsorbent needed in a fixed solution volume to achieve a desired removal efficiency based on initial conditions. To explore this, removal efficiency (%) was plotted against adsorbent mass (mg). However, the resulting curves did not resemble the

classic breakthrough curves the team originally aimed to generate; instead, the curve shape was the opposite of what is typically seen in breakthrough behavior. Additionally,  $C/C_0$  was graphed vs. time to model breakthrough using the Langmuir isotherm. However, this resulted in an incorrect breakthrough shape which is further discussed in the EPA modeling section of the report. An example of this incorrect shape can be found in Figure 9 in section 8.3.5, as the figure of the Freundlich isotherm had a similar shape to Langmuir. As a result, it was determined that additional research and modeling efforts would be necessary to generate true breakthrough curves, plotting concentration versus time. Furthermore, recognizing that PFAS adsorption typically does not conform to the monolayer, homogeneous surface assumptions of Langmuir, the team then moved to a more appropriate model for PFAS behavior: the Freundlich isotherm.

### 8.3.5 Freundlich Hand Calculations

As stated before, the Freundlich equation takes into account the parameters of  $K_F$ , the constant of the Freundlich isotherm and  $1/n$ , the Freundlich exponent, in addition to the same parameters of the Langmuir equation,  $C_e$  and  $q_e$  [47]. As with the Langmuir isotherm, the linearized form of the Freundlich equation can be used to assess whether the adsorption behavior fits the Freundlich model and to determine the model's constants. If the experimental data displays a strong linear relationship when plotted, it suggests that the adsorption process follows the Freundlich isotherm. Once the isotherm parameters are obtained from a set of experimental results, they can be used to either predict the final solute concentration and removal efficiency or estimate the amount of adsorbent needed in a fixed solution volume to achieve a desired removal efficiency based on initial conditions, similar to Langmuir [47].

Similar to the Langmuir hand calculations, the team used the same experimental equilibrium dataset from SRD activated carbon to model the Freundlich isotherm. Specifically, data from Table S.9 in the Supplemental Information was used, which provides equilibrium concentrations ( $c$ , ng/L) and adsorbent loadings ( $q$ , ng/mg) across a range of PFAS concentrations [47]. The initial concentrations applied were again taken from TARP water data: 6.2 ng/L for PFOA and 30.4 ng/L for PFOS. For the Freundlich modeling,  $\log(q)$  was plotted against  $\log(c)$  using the linearized form of the Freundlich equation, where the slope corresponds to  $1/n$  and the y-intercept to  $\log(K_F)$ . From the resulting plot, the Freundlich parameters were determined. Compared to the Langmuir model, the Freundlich fit showed a slight improvement, with an  $R^2$  value of 0.7972. For PFOS, the calculated  $K_F$  was  $7.85 \text{ L}^{\frac{1}{n}} \text{mg}^{(1-1/n)} / \text{g}$  and  $1/n$  was 1.26 (unitless). For PFOA,  $K_F$  was  $5.61 \text{ L}^{\frac{1}{n}} \text{mg}^{(1-1/n)} / \text{g}$  and  $1/n$  was 1.34 (unitless).

As with the Langmuir calculations, removal efficiency (%) was plotted against adsorbent mass (mg), but again, the resulting curves did not exhibit the typical breakthrough behavior; the shape of the curve was opposite to what is expected for breakthrough curves. Additionally,  $C/C_0$  was graphed vs. time to model breakthrough using the Freundlich isotherm. However, this resulted in an incorrect breakthrough shape which is further discussed in the EPA modeling section of the report. This can be seen in Figure 9 below. While working through these hand calculations, the team also continued searching for time-dependent concentration data under similar conditions. This led to a connection with a representative at the EPA, who provided supplemental published data for comparison [49]. Table 2 in the referenced study reports Freundlich parameters for

PFAS adsorption onto Calgon F400 media. For PFOS, the reported values were  $K_F = 15.0$  and  $1/n = 0.65$ , while for PFOA,  $K_F = 9.08$  and  $1/n = 0.67$ . Although the hand-calculated values were of the same order of magnitude, discrepancies are expected due to differences in media type (SRD vs. F400) and the narrower concentration range used in the preliminary dataset. Moving forward, the team determined that the EPA data—based on Calgon F400 and more representative groundwater conditions—would provide a stronger foundation for accurate breakthrough modeling.

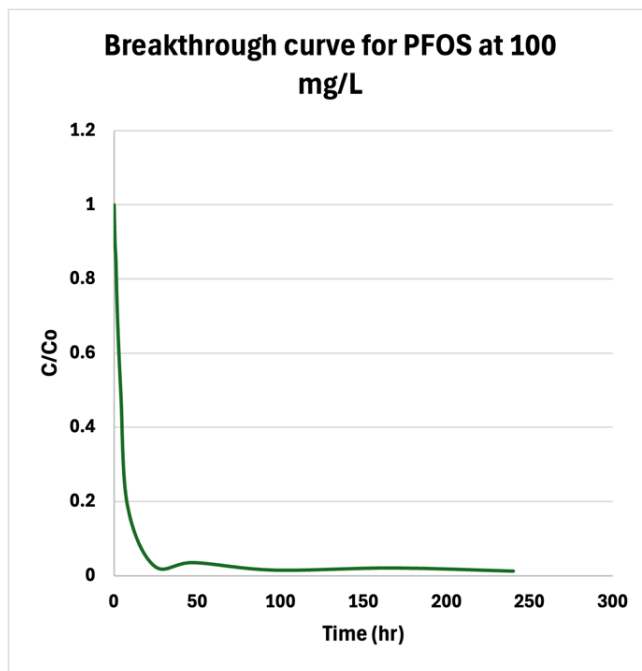


FIGURE 9 HAND CALCULATED BREAKTHROUGH GRAPH USING THE FREUNDLICH ISOTHERM. (REPRESENTS THE INCORRECT BREAKTHROUGH SHAPE FOR MODELING PURPOSES)

### 8.3.6 Equilibria & Kinetic Dependence of the Freundlich Isotherm

As described in sections above, PFAS adsorption onto granular activated carbon is often modeled using isotherms like the Freundlich and Langmuir equations, which describe equilibrium behavior. The Freundlich isotherm is particularly useful for modeling because it models heterogeneous surfaces, like GAC, and assumes non-uniform adsorption energies [47]. Since the breakthrough curves and RStudio modeling in this analysis are based on the Freundlich model, it's important to understand the parameters that drive the model.

The Freundlich constant, in this case  $K_F$ , is related to the adsorption capacity of the adsorbent. The constant  $K_F$  increases with the overall capacity of the GAC to adsorb PFAS. A higher  $K_F$  suggests a stronger affinity or more available surface area or pore volume, which extends breakthrough time [50]. As the parameter  $K_F$  is increased, the breakthrough time increases as a result. This relationship is supported through our modeling data, seen in Figure 10 below. This

parameter is media specific. A higher  $K_F$  value suggests greater adsorption capacity, meaning the adsorbent can hold more of the adsorbate at equilibrium [51]. The value of  $K_F$  depends on the capacity of the media, meaning how many sites and strength of adsorption sites, as well as the media's attraction to its adsorbent. Therefore, the main factors that influence  $K_F$  are the surface area and porosity of the media, surface chemistry such as the functional on the adsorbent surface, and hydrophobicity of the adsorbent surface [52]. As explained in detail in section regarding the chemistry of PFAS, PFAS is hydrophobic and adsorbents with hydrophobic surfaces tend to have higher  $K_F$  values due to the stronger interactions [20]. These factors contribute as to why GAC has moderate to high  $K_F$  values for PFAS adsorption, attributed to its high surface area and hydrophobic nature [52]. Additionally, most ion exchange resins have a higher  $K_F$  value due to strong due to electrostatic interactions between the resin's positively charged functional groups and the anionic PFAS molecules, as well as exhibit better adsorption for short-chain PFAS [52]. However, as conducted in last semester's decision matrix, this removal method is less favorable in industrial-size systems due to its high production expense for media and energy purposes.

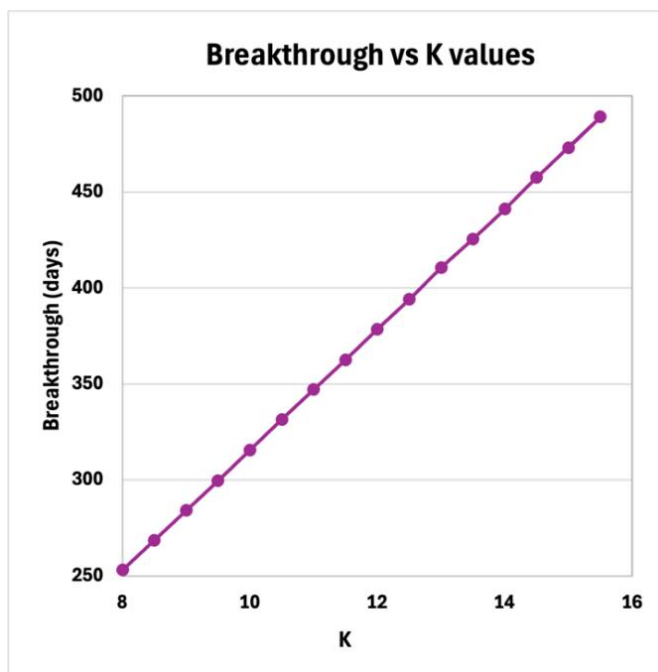


FIGURE 10 VARIOUS K VALUES EFFECT ON BREAKTHROUGH FOR THE STANDARD OPERATING CONDITIONS OF 30,000LBS OF CALGON F400 GAC MEDIA.

The other Freundlich parameter,  $n$ , is an empirical constant related to the heterogeneity of the adsorbent surface [50]. The exponent  $1/n$  reflects how adsorption energy varies across the GAC surface. If  $1/n < 1$ , it indicates favorable adsorption, meaning more PFAS adsorbs at lower concentrations, which is typical for PFAS compounds on GAC [53]. While the Freundlich model is empirical and does not explicitly define concentration dependence, it effectively captures how adsorption varies with changing PFAS concentrations.

Although the Freundlich model describes equilibrium behavior, kinetics still play a critical role in determining how quickly that equilibrium is achieved. In practice, adsorption does not happen

instantaneously. Factors such as film diffusion, intraparticle diffusion, and specific chemical interactions can influence the rate of PFAS uptake. For instance, PFAS molecules must first diffuse across a boundary layer surrounding the GAC particle (film diffusion) and then travel through the internal pore network to reach available adsorption sites (intraparticle diffusion) [54]. Strong interactions, such as electrostatic attractions, can actually slow down this process, meaning that even a favorable equilibrium scenario might take longer to reach in real-world systems.

### *8.3.7 Breakthrough Assumption*

The REAL WTP will be located on a greenfield site, meaning the groundwater will be undisturbed and low in sediment and natural organic matter (NOM). This minimizes early fouling of the GAC, helping extend the lifespan of both the media and the treatment equipment. Fouling occurs when organic material or solids accumulate on the GAC surface, reducing adsorption efficiency by blocking pores and slowing mass transfer. While fouling at this site is assumed to be negligible for many years, ground wells eventually garner more sediment upheaval leading to performance decline. According to Burkhardt et al. (2021), fouling can be incorporated into GAC performance modeling by adjusting parameters like the Freundlich constant ( $K_F$ ) and diffusion coefficients. Fouling lowers  $K_F$  over time, meaning the carbon becomes less effective at holding onto PFAS. In the model, this is shown as a reduced adsorption capacity. The diffusion coefficients ( $d_s$  and  $K_F$ ) control how quickly PFAS molecules move into the carbon particles. Fouling clogs pores and slows down this movement, so the model reduces these values as well. These adjustments affect breakthrough curve predictions and help determine when GAC replacement will be needed. For now, the clean source water allows for longer replacement intervals, but breakthrough recalculations with new modeling parameters will be needed as fouling becomes more likely.

### *8.3.8 EPA Modeling Overview*

After performing hand calculations for Freundlich and Langmuir, the team realized that they were highly inaccurate. One of the main indicators that these results were incorrect was the shape of the breakthrough curves generated from the hand calculations. Typically, a breakthrough curve has a symmetrical S-shape, especially if it follows theoretical expectations [22]. However, when plotting effluent PFAS concentration over time, the graph resembled an exponential decay curve, as seen in Figure 9, rather than the expected S-shape. One team member discussed the design project with a former coworker, Anton Gomenuic, a licensed Water/Wastewater PE. They reached out due to his experience with PFAS-contaminated groundwater remediation and the design performance of adsorption systems. He recommended using AdDesignS to help model adsorption more accurately and generate realistic breakthrough curves. AdDesignS, originally developed by Michigan Tech in the mid to late 1990s, allows users to model liquid-phase adsorption in fixed-bed adsorbers using equilibrium and mass transfer models [55]. The EPA later adapted this software into code on GitHub, which can now be used in Python and RStudio environments.

During CHEE 442 and early in 443, the team was unsure how to scale equilibrium and kinetic data. AdDesignS addresses this by enabling proper scaling for full-scale systems, allowing the

team to use equilibrium data in a more practical context. It's worth noting that this software was initially developed for modeling breakthrough of trichloroethylene (TCE) in water, which may present limitations when applied to other contaminants like PFAS.

The EPA's code adaptations are based off of the Pore Surface Diffusion Model (PSDM), which the original AdDesignS also utilized. The PSDM makes several assumptions: (1) the adsorption equilibrium of each compound can be described by the Freundlich isotherm, (2) IAST accounts for competition between compounds, (3) there are no interactions between adsorbing compounds during diffusion, (4) flow rate remains constant, and (5) local adsorption equilibrium exists between the solute adsorbed on the GAC particle and the solute in the intra-aggregate stagnant fluid. Modeling adsorption with PSDM requires equilibrium and kinetic parameters, as well as physical properties for both the adsorbent and the contaminant [55]. On GitHub, several versions of the EPA's water treatment models are available. One of these is a Python-based PSDM that reads input from Excel.

There was some confusion about the input parameters, so the team contacted Jonathan Burkhardt, an Environmental Engineer at the EPA and the author of the code. In their meeting, the team reviewed several Excel inputs. For each compound of interest, the model requires Freundlich parameters  $K$ ,  $1/n$ , and  $q$ . Jonathan clarified that  $K$  and  $1/n$  are *essential*, while  $q$  is simply a reported value from the curve fitting process and is not directly used in the model. He also reminded the team that "all models are wrong, but some are useful," emphasizing that while these models provide insight into system behavior, they are not exact. At the REAL water treatment plant, the water being treated is sourced from a greenfield groundwater site. Because of this, the team assumed the water has a low natural organic matter (NOM) content. However, finding published Freundlich isotherm values that exactly match the conditions at the REAL plant (specifically for full-scale groundwater treatment using F400 GAC) has been difficult. To determine appropriate  $K$  and  $1/n$  values for PFOA and PFOS, the team referred to Burkhardt's 2022 paper on full-scale water treatment design. They used data from Column 1 (C1), which included raw inlet water and equilibrium data for F400 GAC. For PFOA, they used a  $K$  value of 9.08 and a  $1/n$  of 0.67. For PFOS, they used a  $K$  of 15 and a  $1/n$  of 0.65 [49]. These were the most comparable published values the team could find, as they reflected full-scale operation using F400 GAC, which are two of the most critical factors. While the study used surface water as its influent, the model's breakthrough results are likely conservative, as groundwater generally contains fewer competing contaminants than surface water. The meeting with Jonathan also encouraged the team to focus on GAC media usage rate by analyzing the resulting breakthrough curves.

### 8.3.9 Python Model

First, the team began by running the PSDM model in Python. This model assumes a non-competitive environment (i.e., effective single-solute conditions), since it would be too complex to characterize variables such as water chemistry and the actual species competing for adsorption sites. The model was run using a flow rate of 416 gpm, a GAC weight of 40,000 pounds, a column height of 9.76 m, and a column radius of 3.66 m. Both the GAC weight and column height were doubled from 20,000 to 40,000 pounds and from 4.88 to 9.76 meters to account for adsorption through both the lead and lag tanks.

The GAC weight and height were doubled from 20,000 to 40,000 lbs and 4.88 m to 9.76 m to account for adsorption through both the lead and lag tanks. When consulting expert Viking Edeback, he confirmed that this method was appropriate, as it essentially models the system as one continuous bed representing both tanks in series. The team's customer size is the same as the Marana Picture Rocks Campus, which led them to assume an initial basis of 20,000 lbs of GAC (which was further optimized to 30,000lbs, as discussed later in the report). Since the system includes two sets of lead and lag contactor vessels operating in parallel, the total flow of 832 gpm was split in half (416 gpm) to reflect the flow through each set of tanks. From the resulting breakthrough curves (Figures 11 & 12), the modeled time until breakthrough for both tanks was unexpectedly short. Breakthrough was defined as the point when the effluent concentration reached the target value of approximately 2 ppt. For PFOA, breakthrough occurred at approximately 38 days, and for PFOS, around 35 days. A timeline this short is realistically not feasible, and is much shorter than the replacement time of TARP, who has relatively high influent concentrations of PFAS.

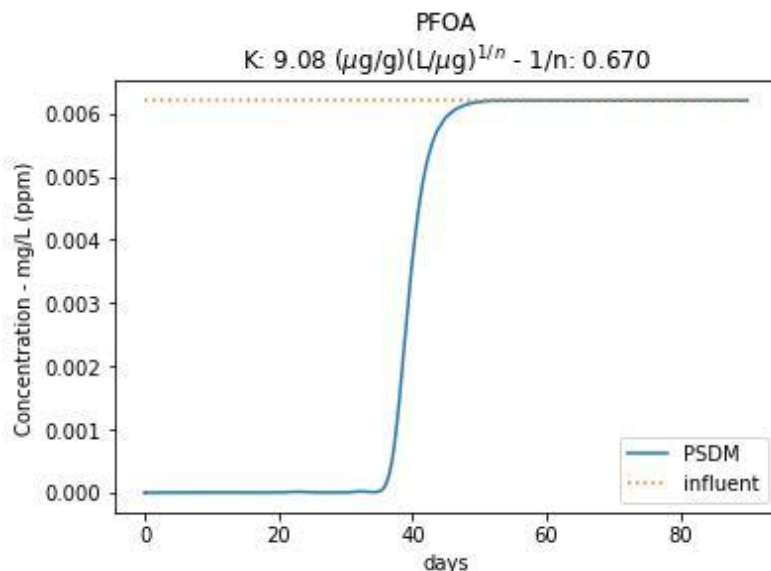


Figure 11. Breakthrough curve through two tanks for PFOA, at 20,000 lbs of GAC using the PSDM modeling tool in Python.

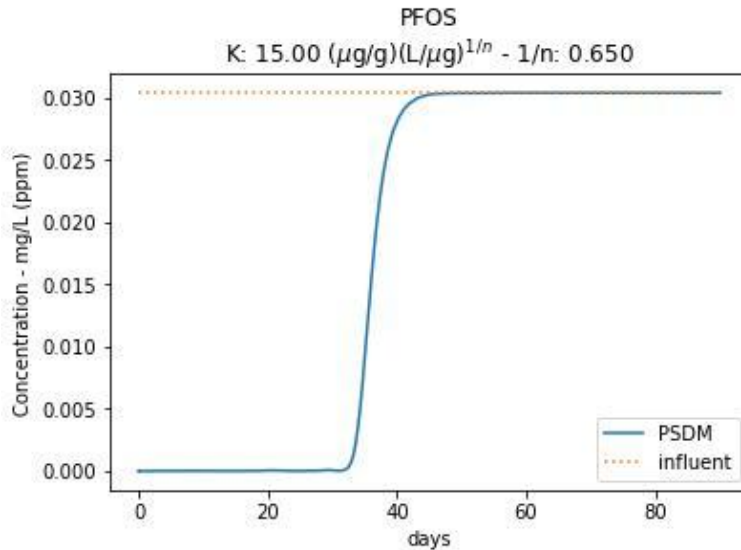


Figure 12. Breakthrough curve through two tanks for PFOS, at 20,000 lbs of GAC using the PSDM modeling tool in Python.

### 8.3.10 RStudio Model

The team then decided to try modeling breakthrough curves using the ShinyGAC water treatment model from the GitHub. The ShinyGAC modeling tool models GAC in a drinking water plant, which most accurately reflects the system at the REAL water treatment plant. This modeling tool also incorporates a PSDM to predict breakthrough behavior for the unit op design. This model uses R and reads from a Python engine. This model was also primarily of interest, since it opens a graphical user interface (GUI) within RStudio making it more interactive and user friendly when analyzing breakthrough curves and adjusting inputs or units. The following conditions were run for this: a flow rate of 416 gpm, a height of 4.88 m, a radius of 3.66 m, and a GAC weight of 20,000 lbs. Breakthrough was also measured at the target concentration level of approximately 2 ppt. For PFOA, through one tank the breakthrough at 2 ppt was 138.25 days, and for PFOS it was 145 days. When these values are doubled, representing breakthrough through both tanks it results in 276.5 and 290 days for PFOA and PFOS, respectively. The one tank values were doubled after running it through RStudio, because if the user tries to double the tank height and GAC weight, then the R session terminates immediately and gives an error saying that “R Session aborted.” The reason for this termination is unclear, however, it appears to be a limitation of the model for this scenario and a few others that the team has encountered during the modeling process. These results were significantly better than those from the Python PSDM model, increasing the predicted breakthrough time from about one month to approximately nine months. After establishing this as a baseline, the team tested different configurations of flow rates, heights, and column sizes to identify the most optimal setup. The original parameters yielded the best overall results (Table 6, 7). Using this RStudio, the overall system was optimized further, as discussed in later sections of the report.

PFOA					
Flow rate (gpm)	Height (m)	Weight of GAC (lbs)	Breakthrough at 2 ppt (days)	Breakthrough at 2 ppt (months)	Notes
1,664	9.76	40,000	66.00	2	Quadruple flow, double height, double weight
416	9.76	40,000	0	0	Double height, doubled weight
832	9.76	40,000	139.75	4.658	Double flow, height, weight
416	4.88	20,000	138.25	4.608	Standard conditions
832	4.88	20,000	65.25	2.175	Double flow

TABLE 6: PFOA BREAKTHROUGH TIMES UNDER VARYING FLOW RATES, GAC WEIGHTS, AND COLUMN HEIGHTS AT A BREAKTHROUGH THRESHOLD OF 2 PPT. RESULTS SHOW THAT INCREASING GAC WEIGHT AND COLUMN HEIGHT GENERALLY EXTENDS BREAKTHROUGH TIME, WHILE HIGHER FLOW RATES REDUCE IT. THE STANDARD CONDITION (416 GPM, 4.88 M HEIGHT, 20,000 LBS GAC) YIELDS ~138 DAYS UNTIL BREAKTHROUGH. DOUBLING FLOW UNDER STANDARD GEOMETRY NEARLY HALVES THE BREAKTHROUGH TIME, WHILE DOUBLING BOTH HEIGHT AND WEIGHT RESTORES PERFORMANCE. AT QUADRUPLE FLOW WITH DOUBLE GEOMETRY, BREAKTHROUGH DROPS SIGNIFICANTLY, ILLUSTRATING NONLINEAR SCALING EFFECTS.

PFOS					
Flow rate (gpm)	Height (m)	Weight of GAC (lbs)	Breakthrough at 2 ppt	Months at 2 ppt	Notes
1,664	9.76	40,000	66	2.2	Quadruple flow, double height, double weight
416	9.76	40,000	0	0	Double height, doubled weight
832	9.76	40,000	151.5	5.05	Double flow, height, weight
416	4.88	20,000	145	4.833	Standard conditions
832	4.88	20,000	61.75	2.0583	Double flow

TABLE 7

*PFOS BREAKTHROUGH TIMES AT A THRESHOLD OF 2 PPT UNDER VARYING FLOW RATES, GAC WEIGHTS, AND COLUMN HEIGHTS. THE STANDARD SETUP (416 GPM, 4.88 M HEIGHT, 20,000 LBS GAC) ACHIEVES ~145 DAYS BEFORE BREAKTHROUGH. DOUBLING THE FLOW RATE UNDER THE SAME GEOMETRY REDUCES BREAKTHROUGH TO ~62 DAYS. WHEN BOTH THE COLUMN HEIGHT AND GAC WEIGHT ARE DOUBLED, BREAKTHROUGH TIME IS RESTORED AND IMPROVED. AT QUADRUPLE FLOW, DESPITE DOUBLED GEOMETRY, PERFORMANCE DROPS TO ~66 DAYS, UNDERSCORING THE COMPOUNDING EFFECTS OF HIGH FLOW ON ADSORPTION EFFICIENCY.*

## 8.4 Reactivation Overview

Reactivation is the process of restoring spent GAC so that it can be reused rather than disposed of. According to [56], reactivation involves thermal treatment of used GAC at high temperatures up to 1800°F with steam and/or carbon dioxide. This process decomposes and removes the

contaminants trapped in the GAC's pores, effectively clearing the adsorption sites for reuse. Reactivation is not a new process; it has commonly been used in destruction of TCE and other contaminants since the 80s [57]. However, after discussing with two professionals in the water treatment industry, Viking Edeback (Corolla Engineering) and Johnathon Burkhardt (EPA), the team found that reactivation however is a relatively new process for PFAS destruction and not many treatment sites are utilizing it. However, reactivation is an increasingly exciting innovation that can transform the future of waste, economic impact, and emissions of PFAS destruction.

When GAC reaches the end of its functional lifespan and becomes ultimately spent, it is a common practice to thermally treat the spent media, known as the reactivation process. This involves exposing carbon to elevated temperatures that volatilize and degrade the adsorbed contaminants, effectively restoring the material to a near-virgin state, allowing it to be reused. In recent years, the emergence of regulations surrounding PFAS has raised important questions about whether traditional reactivation methods are sufficient to break down these highly persistent compounds. Due to PFAS' notable resistance to thermal degradation and the limited research on this specific application, a comprehensive evaluation was undertaken at a commercial-scale GAC facility, Calgon Carbon Corporation. The Calgon system, operating under standard conditions, demonstrated complete removal of PFAS from the GAC and achieved destruction efficiencies exceeding 99.99% through the thermal processing and emission control systems [58].

It is also important to clarify that carbon reactivation is a defined process and is not classified as incineration under current regulatory definitions, as well as not the same as regeneration. Carbon reactivation involves high-temperature thermal treatment, reaching up to 1800°F, to remove and destroy adsorbed contaminants on spent activated carbon [58]. Compounds that do not volatilize during this process are typically converted into char, ensuring the carbon is restored to a near-virgin state suitable for reuse [59]. In contrast, carbon regeneration relies on lower temperature treatments, generally below 400°F, using steam, inert gases, or mild chemical methods to remove only a fraction of the adsorbed compounds [58]. These regeneration methods are often carried out in place and work by cycling between adsorption and desorption, resulting in carbon that may still retain some, or even most, of the original contaminants [60]. Overall, thermal reactivation remains a well-established and effective method for restoring spent activated carbon. However, it is important to ensure a thorough understanding of the critical factors that influence adsorption behavior. These considerations are discussed in detail in the following sections.

#### *8.4.1 Concerns of Reactivation*

Looking ahead, before recommending and integrating a reactivation process into the REAL water treatment plant's system for PFAS removal, it is important to evaluate a key hypothetical: what if reactivation is not fully effective? Although Calgon reports that their reactivation process removes and destroys more than 99.99% of PFAS, effectively restoring full media capacity, the implications if this efficiency were lower must be considered. For example, this could be 90% or even 80% removal. In such cases, some adsorption sites would remain occupied, reducing the overall effectiveness of the reactivated GAC. This raises further questions about how partial reactivation may influence breakthrough times and the frequency of media replacement. In addition to sites occupied, there are possible other factors that could be affected by an incomplete

reactivation. To explore this, the team identified four critical parameters that could be influenced and, in turn, affect adsorption performance: the number of sites occupied, the pore-to-surface diffusion ratio (PSDFR), particle diameter, and pore size.

Using the ShinyGAC modeling tool in R, the team simulated these variables under a range of values to assess their impact on adsorption behavior in the event that reactivation falls short of ideal performance. By evaluating these factors, the team aims to determine which are the most sensitive to variation and whether the system can still function effectively even when media characteristics are slightly altered. This approach is particularly relevant given that thermal reactivation for PFAS removal is still an emerging technology, and real-world variability should be expected. Ultimately, this analysis helps build confidence in reactivation as a viable option, even under less-than-optimal conditions.

#### *8.4.2 Effects of Occupied Sites*

As discussed previously, a critical factor influencing PFAS adsorption efficiency, particularly under conditions of incomplete media reactivation, is the number of adsorption sites occupied on the GAC media. During reactivation, the goal is to thermally destroy adsorbed contaminants and restore adsorption to its full capacity. However, if the process fails to reach the reported >99.99% PFAS destruction, a significant fraction of adsorption sites may remain occupied. This directly reduces the number of available sites for new PFAS molecules to adsorb, thereby impacting both the kinetics and equilibrium of the adsorption process.

From an adsorption modeling perspective, the Freundlich isotherm offers insight into how site occupancy affects equilibrium concentrations. As explained earlier in the report, the Freundlich isotherm is modeled by where  $q$  is the mass of PFAS adsorbed per unit mass of GAC,  $C$  is the equilibrium concentration in the aqueous phase, and  $K_F$  and  $n$  are empirical constants. A lower number of unoccupied sites effectively reduces  $q$ , meaning the system reaches equilibrium at a higher aqueous PFAS concentration[61]. In other words, this results in faster breakthrough times and reduced bed life.

Additionally, adsorption kinetics are influenced by site availability. With fewer active sites, the initial adsorption rate is decreased, as the driving force for mass transfer into the GAC is reduced [62]. Studies using the same ShinyGAC software have shown that even a small reduction in available sites (10–20%) leads to shorter breakthrough times, especially for longer-chain PFAS like PFOS and PFOA, which rely more heavily on micropore interactions [63]. The relationship between the pore size and adsorption is addressed in the sections below. To reflect this study into the team's R model, various scenarios were run reducing the number of sites under the REAL Water Treatment Plant's conditions. The R model in turn supported this theory, showing that any decrease in available sites decreases the time until breakthrough. Overall, the number of sites occupied have a key role in adsorption behavior and are critical in the case of incomplete reactivation.

To address the hypothetical scenario where Calgon does not remove and destroy more than 99.9% of PFAS, the team performed calculations to estimate the efficiency of the media and the time until breakthrough if a certain percentage of adsorption sites remain occupied after

reactivation. As mentioned by Dr. Brush, the most accurate way to represent this would be to modify the R code directly by changing the initial number of occupied sites from zero to the desired value. However, although this method is precise, she advised against it due to its complexity. To represent sites occupied after reactivation, the initial GAC weight was multiplied by the percentage of unoccupied sites. This adjusted weight reflects how much of the media is still available for adsorption. In all cases, the tank height, radius, and flow rate were kept the same, and only the weight of GAC was changed. It is assumed that this reduced amount of GAC behaves the same as if the model directly accounted for a portion of occupied sites, allowing the team to evaluate the impact on breakthrough behavior.

For example, to model 10 percent of sites being occupied after reactivation, the initial weight of 30,000 pounds was multiplied by 0.9, yielding 29,700 pounds. This method was applied in 10 percent increments, modeling scenarios where 10 to 90 percent of sites remained occupied. As observed in the study by Abulikemu, even a 10 to 20 percent reduction in available sites resulted in noticeably earlier breakthrough for long-chain PFAS. From 0 to 10 percent of sites occupied, breakthrough occurred 45.5 days earlier for PFOA and 57 days earlier for PFOS. Increasing to 20 percent occupied led to breakthroughs 91 days earlier and 113.5 days earlier for PFOA and PFOS, respectively. These model results are discussed further in the recommendation section of the report.

#### *8.4.3 Effects of Pore to Surface Diffusion Ratio (PSDFR)*

Another factor is the pore-to-surface diffusion ratio (PSDFR). This concept refers to the importance of both pore diffusion, which is intraparticle transport, and surface diffusion, which is movement along the internal GAC surface. PFAS molecules, especially long-chain compounds modeled in the team's system, PFOA or PFOS, are moderately hydrophobic [20]. They also can strongly adsorb once inside GAC and experience surface diffusion along the pore walls [54]. The two driving factors in this ratio, surface diffusion and pore diffusion, have a direct impact on adsorption. If surface diffusion dominates, it results in faster kinetics and adsorption is quick, because PFAS can "slide" along the GAC surfaces after initial entry [64]. If pore diffusion dominates, there are slower kinetics, so mass transfer is limited, and breakthrough time is extended [64]. Therefore, a higher PSDFR, meaning pore diffusion dominates, the longer time until breakthrough and more gradual saturation of the media, which is reflected in the results of the modeling tests [54]. However, it is important to note that as the PSDFR was increased, the breakthrough time was not affected as drastically compared to when other factors, like media weight, were altered. Additionally, the PSDFR is a parameter of the GAC media used, therefore if a different type of media was used, or if reactivation influenced the ratio, the breakthrough time would be affected as a result.

According to Jonathan Burkhardt (EPA), a typical PSDFR value for GAC ranges from 3 to 5. A value of 5 was used for all standard experiments involving GAC weight and tank height optimization. To isolate the effect of PSDFR on breakthrough time, only the PSDFR was varied, while flow rate (416 gallons per minute), tank height (7.32 m), radius (3.66 m), and GAC weight (30,000 pounds) were kept constant.

Lower PSDFR values between 1 and 4 resulted in earlier breakthroughs, with breakthrough time increasing as PSDFR increased, which is consistent with theoretical expectations. The effect was more pronounced when PSDFR increased from 1 to 5 compared to increases from 5 to 10 for PFOA. For example, increasing PSDFR from 1 to 2 extended breakthrough by nine days, while increases from 2 to 3 and 3 to 4 added five and three days, respectively. A further increase from 4 to 5 also added three days. In contrast, increasing PSDFR from 5 to 10 yielded smaller gains in breakthrough time, with each unit increase adding only about one to one and a half days. A similar trend was observed for PFOS. Increasing PSDFR from 1 to 2 extended breakthrough by 26.5 days, while increases from 2 to 3 and 3 to 4 added 13 and 8 days, respectively. An increase from 4 to 5 extended breakthrough by six days. As with PFOA, gains in breakthrough time from 5 to 10 were smaller, with increases of 4, 3, 3, 2.5, and 1.5 days per unit.

These results suggest that while diffusion kinetics influence breakthrough, equilibrium within the packed bed plays a more dominant role. They may also help explain why typical PSDFR values fall between 3 and 5: values above 5 provide diminishing returns in breakthrough time, while values below 3 can reduce breakthrough by one to two weeks.

#### *8.4.4 Effects of GAC Particle Diameter*

Among the critical parameters affecting PFAS adsorption, particle diameter of the GAC is another important factor when implementing reactivation. Particle diameter directly influences both the available surface area and the mass transfer dynamics during adsorption [63]. Smaller GAC particles offer a greater surface area-to-volume ratio, which enhances external mass transfer and provides more accessible adsorption sites [63]. In contrast, larger particles reduce the external surface area and introduce longer intraparticle diffusion paths [63]. This in turn can delay equilibrium and decrease overall adsorption capacity, especially when some adsorption sites remain occupied due to incomplete reactivation, as discussed earlier in this section.

Additionally, according to the study by [63] it has been shown that PFAS molecules, particularly longer-chain compounds like PFOA and PFOS, exhibit slower diffusion into the internal pore structure of larger GAC particles, leading to earlier breakthrough and shorter bed life [63]. In the same study, it was demonstrated that the PFOS surface diffusion coefficient increased with increasing particle diameter [63]. In other words, as described in the PSDFR section, the surface diffusion factor dominates, decreasing the time until breakthrough, with the use of larger particles. The simulations run using the ShinyGAC model support this theory. The model was run at various partial reactivation scenarios in which the diameter was changed and resulted in the systems using smaller particle diameters maintained longer breakthrough times compared to systems using larger particles.

The particle radius for Calgon F400 is 0.0513 cm. To observe the effects of particle radius on breakthrough, the team conducted hypothetical situations where the particle size decreases, for example when it is a certain percentage of the original size. When the particle radius was decreased from the original size, breakthrough time was extended, aligning with expectations from theory since a greater surface area to volume ratio provides more accessible adsorption

sites. For example, when the radius of PFOS is decreased by 10%, the breakthrough time for two tanks increases by 13.5 days. A 20% decrease in radius yields an increase in 26 days. For PFOA, when the particle radius is decreased by 60%, breakthrough increases by 25.5 days.

#### *8.4.5 Effects of GAC Pore Size*

As explained above in the overview of the Freundlich isotherm and its equilibrium and kinetic effects, the pore size of the media directly influences adsorption behavior. It is important to note that the overall characterization of specific pore sizes for GAC media is generally nuanced. The pore size of F400 12x40 media ranges from a combination of micropores (< 2 nm) and mesopores (2–50 nm) on one singular particle [65]. The larger pore sizes in other types of media include macropores (> 50 nm). During the reactivation process, the pore structure of the GAC can change, specifically the pores tend to widen over time [54]. In micropores, the proximity of the pore walls allows their attractive forces to overlap, which can enhance the adsorption of smaller molecules [54]. As a result, a high volume of micropores is typically associated with increased surface area and strong adsorption performance for small organic contaminants [54]. However, in water treatment applications, larger organic molecules may also be present, making mesopores beneficial as well [54].

Particularly for PFAS adsorption, smaller pore sizes have been linked to higher adsorption abilities [66]. Since GAC pores have been shown to widen during thermal reactivation, problems arise when repeated reactivation cycles gradually convert micropores into mesopores, potentially reducing the GAC's capacity to adsorb smaller species [54]. Over time, this can lead to decreased performance or even structural degradation. Therefore, the reactivation process has its limitations after long performance, meaning the GAC media cannot be reactivated indefinitely. Unfortunately, there is no way to model pore size in the R model. Therefore, at this time the team can only connect this parameter to theory and make a general recommendation as to how long the reactivated GAC media can last until new virgin GAC must be cycled through. However, as discussed in the cost analysis of reactivation, it remains more economically viable than purchasing virgin GAC for every replacement cycle. These findings and their implications are further addressed in the recommendation section, supported by these theoretical pore size principles.

### 8.5 Benefits of Implementation of Reactivation

#### *8.5.1 Costing Savings with Reactivation*

To estimate the cost savings associated with reactivation, the team referenced activated carbon pricing data from the course textbook, *Product and Process Design Principles* by W. D. Seider. The cost of virgin GAC was first estimated by multiplying the required volume by a factor of 41, resulting in a purchase cost ( $C_p$ ) of \$36,000 for 30,000 pounds of virgin GAC. This value was then adjusted using the Chemical Engineering Plant Cost Index (CE Index) to reflect current prices, increasing the estimated cost to \$56,000 [67]. The CE Index accounts for inflation and material cost fluctuations over time, allowing historical cost data to be updated to present-day values. The cost of transportation for the media is estimated within the annual maintenance costs, further explained in the economic analysis.

This updated cost of \$56,000 per 30,000 pounds served as a baseline for evaluating reactivation savings. According to Calgon Carbon, the plant's current media supplier, reactivation costs are approximately 30% of the cost of virgin media [68]. Additionally, it is assumed that 10% of the media is lost during each reactivation cycle and must be replaced with new virgin media. Therefore, each time the media is reactivated, the plant purchases an additional 3,000 pounds of virgin GAC. Accounting for both the 70% cost reduction from reactivation and the replacement cost of lost media, the total estimated cost per tank of reactivated GAC is approximately \$22,000 per 30,000 pounds.

To calculate the cost to treat per milligram of PFAS, the team began by doubling the number of days until breakthrough as predicted by the RStudio software for one GAC contactor, based on its height and media mass. Then, 365 days were divided by the adjusted breakthrough time to determine how many times the media would need to be replaced each year. Using this, the team calculated the total annual amount of GAC media required for all 4 contactors.

Next, the team estimated the annual cost of both virgin and reactivated GAC media. As previously mentioned, each time the media is reactivated, 10% of its original weight must be replaced with new virgin media, and the cost of reactivation is 30% of the original virgin media price. These principles were used to calculate the annual cost of virgin and reactivated media separately, which were then added together to determine the total media cost per year. This entire process was repeated for both PFOS and PFOA, the two modeled PFAS compounds. Finally, the total media cost was divided by the amount of PFAS treated annually to determine the cost to treat per milligram of PFAS. Based on this analysis, using 30,000 pounds of GAC media was identified as the most cost-effective option.

To confirm that 30,000 pounds of GAC was the more financially viable option, the team compared the original capital investment and cash flow projections for the 20,000-pound system with reactivated media to those of the 30,000-pound system. This comparison provided a more comprehensive view of the economic benefits, especially in understanding how capital costs are impacted by the increased media purchase. Many capital and annual expenses were estimated using bare module cost correlations, which increase with media weight. Additionally, as noted in the economic summary, annual maintenance costs were influenced by the transportation costs of GAC media. Taking all of these factors into account, the team concluded that 30,000 pounds of GAC represents the most optimized and cost-effective media quantity for the system.

The team compared the 20,000 pound and 30,000 pound GAC systems to evaluate which offered better long-term economic performance. While the 30,000-pound system required a higher initial capital investment, it produced greater annual net earnings and a higher 20 year NPV of \$7 million compared to \$6.2 million for the 20,000 pound system. With a slightly improved IRR and reduced media replacement frequency, the 30,000 pound system was determined to be the more financially advantageous option over the project's lifetime.

### *8.5.2 Emissions/Environmental Impact with Reactivation*

Reactivation leads to a small material loss—typically about 10% of the GAC mass—because part of the carbon structure is burned off during cleaning. In comparison, virgin GACs like

Calgon F400 involve intensive processing by steam activation of pulverized and agglomerated bituminous coal and around a 60% loss of raw material during activation [69]. These two materials were considered when optimizing the environmental impacts of the REAL WTP.

To first understand the emissions of GAC, the WTP had to know the annual GAC consumption. Total GAC consumption was calculated based on four 30,000-pound tanks, each replaced upon breakthrough. When GAC is reactivated, only 10% of the original 30,000 pounds must be replaced with virgin GAC, as detailed previously. This limited replacement results in approximately 400 cubic feet of GAC sent to the landfill per year, compared to 4000 cubic feet per year if virgin GAC were used exclusively. With less GAC entering the landfill, the risk of PFAS leaching is also significantly reduced. Importantly, the 10% of reactivated GAC destroyed during reactivation is 99.9% free of PFAS, leading to less than 0.01 grams of PFAS entering the landfill annually [69]. In contrast, using only virgin GAC replacement would result in over 500 grams of PFAS being sent to the landfill each year. These distinctions in consumption result in vastly different environmental impacts.

Table 9 summarizes the environmental impacts of virgin and reactivated GAC assessed over one- and five-year periods [70], using LCA emission factors from [56]. Notably over five years, virgin GAC use emits nearly ten times more carbon dioxide (CO<sub>2</sub>) than reactivated GAC. Energy consumption is also significantly higher for virgin GAC, at 255 kg carbon monoxide (COE) vs. 93.5 kg COE. Across all impact categories—acidification, ozone formation, eutrophication, and toxicity—reactivation reduces environmental burdens by 50–90%. These estimates reflect real use rates at the plant and highlight the sustainability benefits of choosing GAC reactivation over landfill disposal and virgin replacement.

Virgin		Reactivated		
1 year	5 years	1 year	5 years	
51.0	255	18.7	93.5	kg COE
623	3115	66.3	331	kg CO <sub>2</sub>
0.07	0.34	0.03	0.15	kg C <sub>2</sub> H <sub>4</sub>
0.33	1.64	0.10	0.51	kg SO <sub>2</sub>
0.03	0.15	0.02	0.08	kg PO <sub>4</sub> <sup>3-</sup>
2.38E-06	1.19E-05	1.81E-06	9.06E-06	kg As

TABLE 9: 8 VIRGIN VERSUS REACTIVATED GAC LCA COMPARISON FOR GAC CONSUMPTION AT THE REAL WTP AFTER ONE YEAR AND AFTER FIVE YEARS.

For improved optimization in the future, alternatives like coconut-based GAC are more sustainable, especially in terms of global warming potential, acidification, and energy use. However, as of now this option comes at a high cost as Catalytic CAT coconut shell runs at five to six dollars per pound versus virgin GAC at around 50 cents per pound (*Viking*, Carollo Engineers). Also, it is less efficient at removing PFAS and PFOA as stated earlier in section 7.4.

## 8.6 Recommendation for Optimal Media

Based on analysis of adsorption theory, kinetics, and material characteristics, the following parameters represent the most effective conditions for extending the time until PFAS breakthrough in granular activated carbon (GAC) treatment systems. Reducing the particle diameter enhances external mass transfer by increasing the available surface area for adsorption. A smaller particle radius improves access to active sites, which delays breakthrough. In the model used, decreasing the particle radius by 20% to 0.041 cm extended the breakthrough time for PFOS from 15.8 to 16.6 months, and from 14.2 to 14.5 months for PFOA. Although pore size could not be adjusted within the model, literature suggests that optimal GAC media should contain a distribution of both micropores (< 2 nm) and mesopores (2-50 nm). The high surface area of micropores enables effective PFAS adsorption, while the larger dimensions of mesopores facilitate the transport and capture of bulkier organic molecules. A combination of both pore types is optimal, allowing the GAC media to efficiently target a broader spectrum of contaminant sizes. Equilibrium behavior also plays a significant role. An increase in the equilibrium constant ( $K_f$ ) increases adsorption capacity, where the GAC is able to hold more PFAS at equilibrium. For example, increasing  $K$  from 15 to 19.5 raised the breakthrough time for PFOS to 115.5 days, which is nearly four months.

The REAL Water Treatment Plant's selection of Calgon Filtrasorb 400 (F400) is strongly supported when considered alongside theoretical modeling and commercial alternatives. F400 contains approximately 63% micropores and 29% mesopores [63]. As discussed previously this is favorable because the micropores provide high surface area for PFAS adsorption, while the mesopores enhance mass transfer and facilitate access to internal sites, resulting in improved adsorption efficiency and delayed breakthrough. In contrast, coconut shell-based GAC such as Evoqua AC1230CX consists of approximately 78% micropores and only 14 % mesopores (Abulikemu), which limits the ability and effectiveness to treat larger PFAS contaminants. Furthermore, the effective particle diameter of F400 (0.55–0.75 mm) [38] is smaller than that of AC1230CX (0.6–0.85 mm) [71], which supports improved breakthrough performance due to enhanced mass transfer at smaller particle sizes. Cost is also a critical consideration. According to Viking Edeback of Carollo Engineering, catalytic coconut-based GAC is priced at \$5 to \$6 per pound, while bituminous coal-based F400 is available at approximately \$0.56 per pound. Considering these factors, Calgon F400 represents the most effective and economically viable option for PFAS removal at the REAL Water Treatment Plant.

Incorporating reactivation into the PFAS treatment process offers several operational, economic, and environmental advantages. As previously stated, it is significantly more cost-effective than relying solely on virgin GAC. The cost of reactivating spent carbon is approximately 30% of the cost of purchasing new media, representing substantial long-term savings. Additionally, reactivation significantly reduces solid waste generation. Assuming that 10% of the spent GAC cannot be reactivated and must be landfilled, reactivation still results in a 90% reduction in landfill disposal volume. Without reactivation, an estimated 3,870 ft<sup>3</sup> of spent media would be disposed of, whereas with reactivation, only 387 ft<sup>3</sup> would be sent to landfill.

From a contaminant destruction standpoint, Calgon reports that greater than 99.9% of PFAS is removed and destroyed during reactivation. Even under more conservative assumptions,

reactivation remains viable. Calculations were performed to evaluate the performance of reactivated carbon in scenarios where PFAS destruction efficiency is significantly lower than claimed. For instance, if 50% of adsorption sites remain occupied after reactivation, the breakthrough time for PFOA in a two-tank system would be 199.5 days. This is comparable to 15,000 lbs of virgin GAC, which is half of the plant's 30,000lbs operating conditions, which yields a breakthrough of 201.5 days. For PFOS, if 80% of sites remain occupied, breakthrough occurs at 38.5 days, which is similar to the performance of 5,000 lbs of virgin GAC with a 33.5 day breakthrough. These results demonstrate that even under the worst-case conditions, reactivated GAC can perform comparably to smaller doses of virgin material. Even when reactivated media retains more occupied sites than Calgon's claims, the comparable breakthrough times demonstrate that reactivation remains the more cost-effective option compared to purchasing virgin GAC alone.

In addition to cost and performance, reactivation contributes to sustainability goals by reducing the demand for new carbon production and lowering the environmental burden associated with mining, manufacturing, and transportation. It also ensures more predictable supply availability, which is especially important given the rising demand for PFAS treatment technologies. Given the comparable adsorption performance, reduced environmental impact, and cost savings, integrating reactivation into the PFAS treatment process is a highly advantageous and justifiable strategy.

## 8.7 Optimizing GAC Media Weights

### *8.7.1 Cost Optimization with Reactivated Media Weight*

The team used break through curves to optimize the amount of reactivated GAC media and the size of the contactor tanks. In the RStudio software previously mentioned, the tank radius (3.66 m), flow rate (416 gpm), inlet PFAS concentrations (30.4 ppt for PFOS and 6.2 ppt for PFOA), F400 particle characteristics, and Freundlich parameters were kept constant through the optimization process. The only two parameters that were changed in the model were tank height and reactivated media weight. The tank was scaled up in height to accommodate the media based on our original sizing of 20,000 pounds in a tank with a volume of 51.2 m<sup>3</sup>. The values of tank height and media mass tested can be seen in **Table 10**. To generate these values, the team took into account the cost of reactivated media after each replacement, an addition of 10% of virgin media added to each replacement, and annual capital costs. Using the initial concentrations of the compounds treated, as well as the modeled breakthrough time of the media, the cost to treat per milligram of PFOA and PFOS was totaled to find that 30,000 pounds of regenerated media was the most cost effective at \$13.33 per milligram of PFOS and PFOA.

Tank Height (m)	GAC (lbs)	PFOA Breakthrough at 2 ppt	PFOS Breakthrough at 2 ppt	Annual Cost to treat per mg of PFOA	Annual Cost to treat per mg of PFOS	Annual Cost to treat per mg of PFAS TOTAL
		days	days	(\$/mg)	(\$/mg)	(\$/mg)
1.22	5,000	55.5	33.5	\$4.87	\$14.40	\$19.27
2.44	10,000	127.5	114	\$2.86	\$12.54	\$15.40
3.66	15,000	201.5	200.5	\$2.44	\$11.90	\$14.34
4.88	20,000	276.5	290	\$2.25	\$11.57	\$13.81
6.1	25,000	351	381	\$2.14	\$11.39	\$13.53
7.32	30,000	426	473	\$2.07	\$11.26	\$13.33

TABLE 109: SUMMARY OF THE ANNUAL COST TO TREAT PFAS DEPENDING ON THE WEIGHT OF GAC MEDIA.

### 8.7.2 Media Weight Feasibility

Although costs continue to go down with increasing media weight as shown in Appendix **Figure VI**, there are other factors to consider for maintaining the weight within feasible limits. The pressure required to move the treated water through to the finishing tanks prior to the GAC contactors must remain above zero. If the GAC media weight is too great the head losses will be greater than the head the ground well pumps can deliver, which is 121 psi. **Figure 11** shows the trend of head loss as media weight increases. At 140,000 pounds of media in each of the four tanks, the pressure leaving the tanks drops below 20 psi. The EPA model was only capable of modeling up to 30,000 pounds, meaning that breakthrough would be unknown in tanks of greater size. Also, tanks that are 140,000 pounds can introduce safety concerns and logistic issues upon replacement. At approximately 25 feet tall [72], filling the tank would involve an operator working at heights and potential engulfment if they were to fall inside. It would also require new equipment such as cranes or grain elevators to draw up media to that height. The importance of breakthrough modeling to ensure maximum removal efficiency, safety, and effective operations requires that 30,000 pounds be the feasible amount of GAC for the REAL WTP.

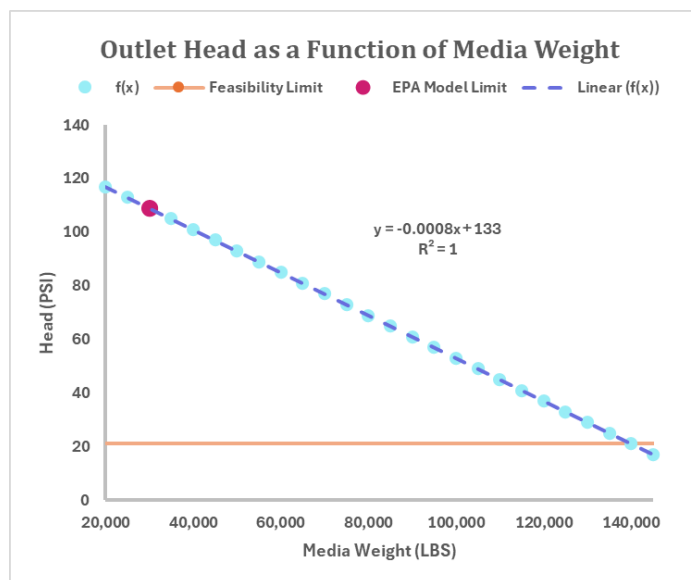


FIGURE 13 OUTLET HEAD PRESSURE FROM THE FOUR GAC CONTACTORS AS A FUNCTION OF MEDIA WEIGHT. THE ORANGE LINE INDICATES THE MINIMUM HEAD REQUIRED TO TRANSFER WATER TO THE FINISHING TANKS, WHILE THE PINK DOT MARKS THE EPA MODEL'S FEASIBILITY LIMIT. THE LINEAR TREND LINE ( $R^2 = 1$ , SLOPE  $= -0.0008$ ) DEMONSTRATES A PERFECT INVERSE RELATIONSHIP. FEASIBILITY IS EXCEEDED AT 140,000 POUNDS OF GAC MEDIA.

### 8.7.3 Correlation of Media Weight & Breakthrough

A key trend observed after running the model in R at various GAC media weights, under consistent flow conditions, was the strong correlation between media weight and breakthrough time. As expected, increasing the weight of granular activated carbon (GAC) led to longer breakthrough times for PFOA and PFOS at the 2 parts per trillion (2 ppt) contaminant level. This conceptually makes sense: at a constant flow rate, a larger GAC mass offers more adsorption sites, allowing the system to delay contaminant breakthrough and extend media life.

However, this relationship is not linear. The breakthrough time does not increase in direct proportion to the amount of GAC media added. In other words, doubling or tripling the GAC weight does not double or triple the breakthrough time. This is due to decreasing returns in adsorption efficiency as more media is added, a phenomenon consistent with adsorption behavior described by the Freundlich isotherm equation, which models non-linear adsorption on heterogeneous surfaces. The equation suggests that as adsorbate concentration increases, the rate of additional adsorption slows, and this explains why gains in breakthrough time begin to level out with increasing GAC weight [47].

The model's data supports this theory as well. For example, for PFOA, increasing GAC from 1,000 to 5,000 lbs yields a breakthrough time increase from 1.5 to 55.5 days, which is 37 times gain in performance. However, in the higher weight range (10,000 to 30,000 lbs), breakthrough time increases more predictably, adding about 74–75 days for every 5,000-lb increment. This suggests that while the system still benefits from additional media at larger

scales, the increasing breakthrough slightly plateaus as the system approaches its adsorption capacity limits.

Despite this non-linear trend, the model supports that increasing GAC media weight does effectively extend breakthrough time, which directly translates into longer system lifespan and less frequent media replacement. This has significant operational and economic impacts. While purchasing more GAC upfront raises the initial media costs, those costs are ultimately offset by reduced maintenance intervals and fewer media changeouts over time. This tradeoff between capital investment and long-term operational savings is further discussed in the cost analysis section.

## **9. Safety Issues**

After performing a Hazard and Operability study (HAZOP) on every unit operation in the REAL WTP, it was found that among all treatment zones, the AOP system presents the greatest safety risks due to its reliance on concentrated hydrogen peroxide (H<sub>2</sub>O<sub>2</sub>). Hydrogen peroxide can decompose explosively under heat, pressure, or in the presence of contaminants, and it can cause severe burns or respiratory harm upon contact. According to [73], the hydrogen peroxide standard from OSHA, the limit before worker endangerment is 1 ppm as an 8-hour time-weighted average. In the UV-AOP process, H<sub>2</sub>O<sub>2</sub> is used at elevated concentrations and pressurized for injection, which magnifies the danger of leaks, spills, or over pressurization. Storage tank failures or dosing errors could result in chemical exposure, corrosive damage to equipment, or uncontrolled reactions. Also, the AOP system is early in the treatment process, so any shutdown due to peroxide flow or UV malfunction not only halts 1,4-dioxane removal but also disrupts downstream operations like GAC adsorption.

### **9.1 Sediment Removal HAZ-OP**

#### *9.1.1 Ground Well Pump*

The well pump poses low-likelihood risks related to both flow and pressure. If the well runs low or a blockage occurs upstream, flow may cease, causing the pump to run dry and halt the entire treatment process. This can lead to cavitation, which reduces pump efficiency, increases vibration and wear, and ultimately requires maintenance or replacement. Pressure Indicators should be installed at the pump discharge to monitor abnormal pressures. A Pressure Control Valve can be used to regulate excessive discharge pressure and protect downstream units like the AOP and GAC. To mitigate failures, backup pumps should be on standby, and flow can be diverted to the finished water tank during troubleshooting.

#### *9.1.2 Desander*

The desanders face low-to-medium likelihood risks from blockages, pump failures, or variable sediment inflow, which can lead to the unit running dry or sending unseparated solids

downstream. This contamination can clog or damage the AOP and shorten GAC media life. Pressure Indicators should be placed at the inlet and outlet to detect pressure drops that indicate blockages or drying out. A Pressure Control Valve can be installed to relieve high pressure caused by unexpected flow resistance. If finer sediments are present and separation becomes inadequate, units should be shut down and inspected, and backup desanders should be activated as needed.

### *9.1.3 Clarifier*

Main risks for the clarifier involve full or clogged filter bags, leading to restricted flow, elevated pressures, or sediment bypass. These issues compromise treatment and damage downstream units. Installing Pressure Indicators before and after the filter housings enables early detection of pressure differentials, signaling clogged bags. A Pressure High High Alarm should notify operators when pressures exceed safe thresholds. Preventive maintenance includes scheduled bag replacement and activating parallel units during bag turnover or suspected upstream issues.

### *9.1.4 Leak Addendum*

Leaks across the solids removal system can reduce flow and pressure, potentially causing pump shutdowns or system inefficiencies. Over time, even small leaks increase wear on components and reduce treatment reliability. Local Pressure Indicators near joints, valves, and seals can help identify drops associated with leaks. Regular inspection and maintenance of all connections, along with installing drainage collection pans and level switches, can prevent unmonitored leakage from escalating.

## 9.2 1,4-Dioxane Treatment HAZ-OP

The two main study nodes of the HAZOP include the hydrogen peroxide storage tank and the UV-AOP chamber.

### *9.2.1 Hydrogen Peroxide Storage Tank*

The H<sub>2</sub>O<sub>2</sub> storage tank is critical for dosing the oxidant into the AOP system. Potential deviations such as low or high level, pressure, or flow were identified, often resulting from pump malfunctions, sensor failures, or line blockages. For example, a low peroxide level due to a broken outlet pump could lead to inadequate oxidant dosing. Without alarms and automatic shutdowns, this would result in incomplete oxidation of 1,4-dioxane, potentially allowing harmful contaminants to enter the water supply. Similarly, an unnoticed high tank level could result in overfilling, posing both chemical exposure and spill hazards. Excessive pressure, possibly from regulator malfunction, could damage piping or lead to rupture, while low pressure would inhibit peroxide delivery altogether. The HAZOP ensure that these consequences are generally mitigated by sensors and interlocks, but emphasizes that in their absence, system failure could have severe health and safety consequences. Another important consideration is the ripple effect of system shutdowns. While shutting down the UV-AOP process in response to

flow or concentration deviations prevents immediate harm, it also halts water treatment downstream, impacting the overall throughput of the water treatment facility. This can be considered a downstream consequence of a safeguard.

### *9.2.2 UV-AOP Chamber*

The UV-AOP chamber, where hydrogen peroxide reacts with UV light to degrade 1,4-dioxane, is equally vulnerable to flow and level deviations. Issues such as a blocked static mixer or malfunctioning pump could restrict oxidant or water flow into the chamber, making the oxidation process ineffective. If undetected, this could result in untreated water passing through to distribution. Low flow, especially from upstream sources like the sedimentation zone, may trigger automatic shutdowns, but without these systems, the chamber might run dry or operate under suboptimal conditions. High levels in the chamber, possibly from downstream blockage or holdup, could cause system flooding or equipment damage. Importantly, halting the UV-AOP process affects not just local treatment performance but can also result in upstream pressure buildup or downstream gaps in disinfection. This reinforces the need for careful coordination between safeguards and real-time process monitoring. The HAZOP makes clear that while automatic shutdowns protect the system, their activation has broader implications, such as stopping water treatment and requiring manual intervention for recovery.

## 9.3 GAC HAZ-OP

The HAZOP analysis on the GAC treatment zone focused on deviations in critical process parameters, including flow, pressure, and level. Each deviation was evaluated for its potential causes, safety and operational consequences, and appropriate corrective or preventive actions.

For flow deviations, a complete loss of flow may result from pump failure or an inlet line blockage. If the pump fails, upstream pressure can build, potentially causing pipe rupture and exposing operators to contaminated pressurized water. A blockage can also cause the pump to run dry, which may lead to overheating and mechanical failure that could escalate into a fire hazard. To prevent these outcomes, flow sensors with alarms and pressure relief valves should be installed. Thermal protection and automated pump shutdowns should be included as additional safeguards. Low flow may result from an undersized or degraded pump, a partially blocked line, or fouling of the GAC media. An improperly sized or degraded pump increases the risk of cavitation and failure. Flow instability may disrupt downstream operations, and insufficient contact time due to a blocked line can result in PFAS breakthrough above EPA limits. Fouling in the media increases head loss and pressure drop, which stresses upstream equipment and contributes to treatment inefficiencies. Recommended actions include installing flow and pressure monitoring, implementing regular backwashing, and developing procedures for detecting and clearing partial blockages. High flow conditions may be caused by excessive upstream flow. If not controlled, the tank can overflow and the packed bed may flood, creating slip hazards, damaging electrical equipment, and risking personnel safety. Preventive measures include installing high-level alarms, flow monitoring elements, and a diversion stream for excess water.

Pressure deviations also pose safety risks. Low pressure may result from pump cavitation or entrained air. Cavitation can damage impellers and lead to sudden pump failure. Air pockets may cause water hammer effects that stress piping. To prevent these conditions, cavitation detection with automatic shutdown and properly located pressure relief valves should be used. High pressure can occur due to media fouling, a closed or blocked outlet valve, or over pressurization from upstream pumps. If flow resistance increases, the upstream pump may be forced to operate at a higher pressure than the tank is rated for, leading to potential rupture, seal failure, or high-pressure leaks that could injure personnel. Recommended safeguards include pressure relief valves on the inlet and outlet, properly sized pumps, bypass lines, and regular media maintenance to control pressure buildup.

Level deviations present both operational and safety concerns. Low tank levels can be caused by failed pumps, over-opened valves, or over-controlled outlet valves. If the level drops too low, contact time is reduced and PFAS may not be fully adsorbed, leading to regulatory violations. Air entrainment from rapid draining can also disrupt downstream units. To manage this, a level element (LE), low-level alarm (LALL), and a feedback loop on the outlet valve should be used. Outlet valves should be reviewed to prevent opposing control signals or excessive outflow. The LE can be cascaded to a flow element (FE) to improve control responsiveness. High tank levels may result from blocked outlet flow or excessive inlet flow. These conditions can lead to flooding, electrical shock hazards, and possible tank rupture due to wall stress. If the outlet is blocked, backwashing should be performed. An overflow drain, LAHH alarm, and air-fail-to-open (AFO) actuator on the outlet valve are recommended. Installing a LE and cascading it to an FE at either the tank inlet or outlet can verify proper flow rates. If an FE is installed downstream, a feedback loop can be created using a flow control valve to maintain safe operating levels.

#### 9.4 Backwash HAZ-OP

The main safety issues in the backwash system were identified with HAZOP analysis, which highlighted potential risks such as high-pressure buildup, reduced flow from clogged or damaged bag filters, and pump malfunctions. There is also a risk that torn bag filters could allow GAC media or dislodged sediment to pass through, potentially causing damage to downstream systems such as the AOP Chamber. To address these concerns, the system was updated to include all necessary alarms. A high-pressure alarm is located immediately downstream of the pump before the bag filters to detect blockages. In addition to this, a low-pressure alarm after the pump ensures early warning in the event of a pump failure or a significant leak in the tank or piping manifolds. Level alarms are installed on the backwash tank to monitor for both high and low levels. The high-level alarm prevents overfilling and potential spills, while the low-level alarm helps protect the pump from running dry. Finally, the control logic was configured to allow automatic switching to a standby pump and bag filters in the event of a primary equipment failure. Although these safety measures are important, the risks in the backwash unit operations are relatively low because it involves groundwater and non-hazardous chemicals.

## 10. Environmental Impact Statement

The details of each unit operation Life Cycle Assessment (LCA) can be found below, but the following presents a summary of the significant emissions. The desander (SF-101) contributes minimally, using 1,375 kg of steel over a 10-year lifespan, resulting in a resource depletion of around 500 kg CO<sub>2</sub>/year. For the AOP chamber (R-101), GREET analysis shows around 900 kg CO<sub>2</sub>/year from stainless steel construction and approximately 15 kg CO<sub>2</sub>/year from the static mixer, assuming a 10-year equipment life. The AOP's emissions total around 900 kg CO<sub>2</sub> and 12,000 MJ of energy over its lifetime. A smaller static mixer used upstream (15 kg stainless steel) contributes an additional 15 kg CO<sub>2</sub> and 195 MJ. The dominant contributor by far is hydrogen peroxide, estimated at 55,000 kg CO<sub>2</sub>/year and 800,000 MJ/year, consistent with previous energy calculations (~213,000 kWh/year). The process also generates 10,000 kg/year of oxygen (~140,000 MJ/year), which does not negatively impact the environment. The GAC contactors (TK-104,105,106,107) will need 289 kg steel over a 10-year lifespan, and 40,000 lbs (18,144 kg) of GAC/year. While the model reported large negative emissions due to recycled steel and treated water credits (e.g., -6,000 kg CO<sub>2</sub> from engineering steel), these are likely artifacts of OpenLCA assumptions. The backwash tank (TK-102) contributes 3,000 kg CO<sub>2</sub>/year from truck transport, 800 kg CO<sub>2</sub>/year from steel production, and 200 kg CO<sub>2</sub>/year from electricity use during manufacturing. The tank's steel production also used approximately 4,000 MJ/year (~1,000 kWh/year). Although no equipment changes were made solely for environmental reasons, the results suggest that local sourcing and the use of renewable energy could significantly reduce the plant's overall carbon footprint.

To minimize the significant impact from the AOP hydrogen peroxide requirements a chlorine substitute could be considered. UV/Cl<sub>2</sub> offers environmental advantages over UV/H<sub>2</sub>O<sub>2</sub> in certain scenarios by increasing oxidative efficiency and reducing the amount of chemical required. However, careful control of chlorine dose and pH is necessary to minimize the formation of chlorate and other byproducts [74]. The formation of byproducts does not meet the criteria of removal efficiency which takes precedence over sustainability for the project currently.

Another environmental consideration is GAC disposal and replacement frequency because of desorption and leaching. Long-chain PFAS like PFOS and PFOA can leach from GAC, particularly under alkaline conditions or where GAC is physically disturbed. Though PFOS shows stronger binding than PFOA, both compounds exhibit measurable release, which poses a risk of soil and groundwater contamination if spent GAC is disposed of in unlined or poorly engineered [75]. At the current breakthrough, around 500 grams of PFAS will go into landfill every 318 days, which is the time until breakthrough. Using the LCA from Bayer Et. Al. and with the replacement frequency calculated for 30,000 pounds of GAC this translates to 600 kg CO<sub>2</sub>/year. Using Calgon's reactivation method to replace the media tanks after the initial breakthrough results in a deduction to <0.01 grams of PFAS into the landfill each year and around 70 kg CO<sub>2</sub>/year. Table 6 summarizes the amount of waste from each disposal method. Although landfill characteristics are unknown and desorption kinetics in spent GAC minimal and under-researched, as confirmed by Dr. Karanikola, this optimized media eliminates concern for leaching back into the environment as well as decreased emissions and ecotoxicity summarized

in Table 11. The goal to find a novel and environmentally friendly way to dispose of spent GAC has been met by utilizing reactivated media.

<b>Amount of Waste Every Year to Landfill</b>			
<b>Reactivated</b>		<b>Virgin</b>	
PFAS		PFAS	
<0.01	g	517	g
GAC Media		GAC Media	
387	ft <sup>3</sup>	3871	ft <sup>3</sup>

TABLE 11 THE AMOUNT OF WASTE, BOTH GAC AND PFAS, SENT TO THE LANDFILL EACH YEAR AT REAL WTP. THIS SERVES AS A COMPARISON BETWEEN THE REACTIVATED MEDIA AND VIRGIN MEDIA.

### 10.1 Sediment Removal LCA

The desander manufacturing process contributes minimally, using 1,375 kg of steel over a 10-year lifespan, resulting in a resource depletion of around 500 kg CO<sub>2</sub>/year. Running the desander uses minimal electricity, as the head from the pumps is sufficient for efficient separation. Compared to AOP and GAC emissions, the desander’s emissions are negligible.

### 10.2 1-4 Dioxane Treatment LCA

The LCA for the treatment of 1,4-dioxane focuses on the AOP chamber (R-101) used in the treatment system operating with UV radiation and hydrogen peroxide (H<sub>2</sub>O<sub>2</sub>). The assessment, conducted using GREET software, quantifies emissions, energy demand, and resource use related to both the chamber's construction and its operational inputs. While hydrogen peroxide emerged as the dominant contributor to annual environmental impact, this analysis also emphasizes the complexity and challenge of modeling an accurate water treatment system in tools like GREET, which are not inherently designed for such applications.

The AOP chamber, assumed to be constructed entirely from stainless steel, weighs approximately 953 kg. Using GREET's well-to-use data, its embodied emissions total around 879.33 kg CO<sub>2</sub> and 12,389 MJ of energy over its lifetime. A smaller static mixer used upstream (15 kg stainless steel) contributes an additional 13.84 kg CO<sub>2</sub> and 195 MJ. These values, though not insignificant, are relatively modest compared to annual operational emissions. They represent one-time impacts that, when spread over the chamber’s entire life, are far less influential than recurring inputs like hydrogen peroxide. Nonetheless, these figures show the importance of selecting durable, long-life materials to minimize environmental costs.

Hydrogen peroxide is the most environmentally intensive input in the AOP process. Based on estimated usage of 17,520 gallons per year, GREET data indicate it is responsible for roughly 55,238.67 kg CO<sub>2</sub>/year and 813,273 MJ/year of energy use. These numbers are much greater than every other component in the analysis of the unit operation, including construction materials and operational electricity demands. Notably, this energy usage aligns closely with the calculations of AOP power demand from last semester (approximately 213,000 kWh/year), suggesting internal consistency in energy scaling. However, it also raises questions about

potential overestimation by GREET, given the modeling constraints and lack of process specificity.

While the primary focus was on input-derived emissions, the AOP process also produces gaseous byproducts. CO<sub>2</sub> emissions from oxidation are negligible ( $4.45 \times 10^{-5}$  g/year), whereas O<sub>2</sub> generation, though more substantial (9,836 kg/year, 137,895 MJ/year), does not contribute negatively to the overall environmental impacts. These outputs, while accounted for, have little influence on overall LCA outcomes and are presented primarily for completeness and total system modeling.

Modeling the LCA of this water treatment system using the GREET software presented many challenges. The software is not specifically designed for unit operations like UV-AOP, and its output categories do not fully match the operations of drinking water treatment, particularly given that water itself is not a trackable output in the tool. It is also understood by the team that GREET estimates the energy and emissions associated with producing chemicals and materials, not their actual use in treatment, which can differ the results significantly. As such, it is likely that the values reported, especially for hydrogen peroxide, may be overestimated.

### 10.3 GAC LCA

A LCA was conducted for a single GAC contactor over the span of one year using the worldsteel\_2020 database in OpenLCA. For inputs, engineering steel was used to represent the tank material, carbon for the GAC media, and groundwater as the water source. Input ratios for each material were calculated. To estimate the mass of steel for the GAC tank, a back-of-the-envelope calculation was done. First, the internal and external tank volumes were determined, and their difference gave the volume of steel. Using the density of steel, the mass was then calculated and divided by 10 to account for a 10-year tank lifespan, resulting in an estimated 289 kg of steel per year. Assuming GAC is replaced every six months, and each tank holds 20,000 lbs, a total of 40,000 lbs of GAC would be used annually. The REAL water treatment plant treats 1.2 million gallons of water per day, or 438 million gallons per year. Since the GAC tanks operate in parallel, the flow was halved, giving 219 million gallons per year per contactor.

LCA outputs were measured in mass (kg) and included steel scrap, hazardous waste (PFAS-contaminated GAC), and treated drinking water. The volume of water was multiplied by density to determine its output mass (829,005,000 kg). Input volumes remained unchanged, especially for water, since no water is lost in the treatment process. Emissions were assessed for carbon dioxide (fossil) and groundwater. Interestingly, carbon itself was not a direct contributor to any emissions. This could be due to the database treating carbon as a natural resource rather than an emissions source.

The CO<sub>2</sub> emissions results were negative overall. This may be due to recycling credits, system boundary choices, or other assumptions in the model that reduce the calculated footprint. One possibility is carbon sequestration by materials in the model. Engineering steel was a major factor here, accounting for 97.96% of total emissions and contributing -5875.66 kg CO<sub>2</sub>. The model likely assumes that steel scrap is recycled, crediting avoided emissions from new steel production. Similarly, steel cold-rolled coil showed -122.21 kg CO<sub>2</sub>. Surprisingly, treated

drinking water contributed -5997.87 kg CO<sub>2</sub>, which is unusual. This may be another case of carbon crediting or an error in modeling treated water as a sequestration process. It's unclear why this occurs, but it could relate to how the model interprets water treatment. Only two components had positive direct CO<sub>2</sub> emissions: steel cold-rolled coil (5836.67 kg) and engineering steel (430.86 kg). These are likely due to the energy-intensive process of manufacturing the steel tank. Overall, while direct emissions are substantial, the large negative emissions may significantly offset the total.

For groundwater emissions, treated drinking water contributed 100% of the total:  $8.3 \times 10^5$  m<sup>3</sup>. This suggests that nearly all input groundwater ends up as output, with minimal upstream savings. Negative groundwater emissions from rolled coil steel (-0.009 m<sup>3</sup>) and engineering steel (-4.172 m<sup>3</sup>) were minor and likely reflect recycling credits again. Direct contributions were slightly positive (4.4 m<sup>3</sup>) for rolled coil steel and 0.59 m<sup>3</sup> for engineering steel). This is likely due to water use in steel production, but overall small compared to the treated water contribution.

One key limitation is that hazardous waste (PFAS-contaminated GAC) shows no emissions contribution. This is clearly inaccurate, as disposal (especially in a landfill) would produce some emissions. This omission, along with the lack of carbon-based emissions, points to a limitation in the software. As it stands, this model may not be ideal for accurately representing a GAC contactor system.

#### 10.4 Backwash LCA

A life cycle assessment (LCA) was conducted for the backwash tank using a mix of hand calculations and estimates, due to limitations in OpenLCA software usability. The main environmental impacts associated with the backwash tank are primarily related to emissions and energy use. The largest contributor in this case is the emissions due to transportation. This is likely due to the assumption that the tank is made in Texas and transported completely by truck, which contributed approximately 2,654 kg of CO<sub>2</sub>. [76]. In addition, steel production using electric arc furnaces (EAF) results in an estimated 780 kg of CO<sub>2</sub> emissions, and an additional 209.6 kg comes from electricity used during tank manufacturing [77]. While EAF is an electric furnace and typically more environmentally friendly than blast furnaces—since it uses recycled steel and consumes less energy—it can still result in high emissions if powered by coal-based electricity. EAF is also the reason why steel production is so energy intensive, consuming around 987 kWh [78] for the amount of steel used in this tank. Switching to renewable energy sources during manufacturing could significantly reduce this carbon footprint.

Steel production, especially through EAF, remains a considerable contributor to overall environmental impact across most manufacturing processes. The transportation emissions from trucking are also high, particularly over long distances, and alternative logistics such as rail transport may offer improved fuel efficiency. Additionally, while water use during manufacturing of steel was estimated at 7.2 m<sup>3</sup> [79], it is relatively modest compared to emissions. No design changes were made solely for environmental reasons, although the findings suggest that sourcing tanks locally and selecting manufacturers that use renewable energy could be future improvements.

## 11. Final Economic Analysis (Including Economic Hazards)

The project involves a total capital investment of just over \$6.8 million in year one, with cash flow beginning in year two. The largest portion of this investment is dedicated to land, buildings, and offsite facilities, which account for 50 percent of the total, or about \$3.98 million. The second largest cost comes from the GAC unit operations, including the contactor tanks and the initial supply of virgin media, totaling \$1.49 million. The ground well pumps represent the third most significant cost at approximately \$563,000. The cost of equipment was estimated using the methods outlined in Chapter 16 of Product and Process Design Principles, supplemented by data from reputable online sources featured in the final excel sheet.

In year two, the REAL water treatment plant purchases its second supply of virgin GAC media, leading to net earnings of \$1.95 million. By year three, the plant switches to using reactivated GAC media, increasing net earnings to \$2.08 million. This increase is due to a \$134,000 cost savings from reactivating media instead of purchasing new. After the second year, the plant will have two sets of GAC media. From this point on, it will alternate between the two, using one set while the other is being reactivated. The largest annual expense is for operations at \$1.66 million, with operators and engineers earning an average of \$40 per hour. The team estimated this cost by taking an average of wages for water plant operators and managers in Tucson. In addition to annual labor costs, they used a combination of the presentations provided during class to estimate our maintenance, operating overhead, depreciation costs, and general expenses.

The plant earns revenue by selling its water for \$10 per 100 cubic feet. This is based on the rates Tucson residents pay for their water [80]. Fortunately, as the REAL water treatment plant operates as a municipal entity, its revenue is not subject to taxation. While one potential method of increasing revenue would be to raise the cost of water, this approach is not preferred due to its impact on residents.

It is important to note that maintenance costs were estimated by halving the operational cost associated with using 20,000 pounds of reactivated GAC every six months. This approach was chosen because the only change in the system was an increase in both media quantity and tank size, which is expected to reduce maintenance needs by decreasing the frequency of media replacement. Specifically, the team reduced the maintenance cost by half, as the system now uses 30,000 pounds of media and replaces it half as often as the 20,000-pound baseline. This adjustment was not reflected in the standard cost estimation method presented in lecture, which assumes maintenance costs are 4.55% of the total depreciable capital for fluid handling processes.

Additionally, a potential factor that could influence profitability is the exclusion of chlorination and distribution costs. These components are considered outside the scope of this project, as there is currently no available data to estimate the cost of a distribution system or the duration over which the treated water would need to be stored and chlorinated.

The REAL water treatment project is profitable based on its Net Present Value (NPV) and Internal Rate of Return (IRR). NPV measures how much value a project adds in today's dollars by discounting future cash flows using a set interest rate. In this case, a 10% discount rate was used, and the project's NPV is approximately \$7 million, indicating that it generates more money than it costs over its 20-year lifetime. The IRR is the interest rate at which the NPV becomes zero. It represents the project's expected rate of return over its entire lifespan. For this project, the IRR is 24.52% over a 20-year period. This confirms that the investment is financially strong. The project begins generating positive cash flow in year two and pays back the initial investment in under 10 years, making it both cost-effective and sustainable in the long run.

Year	Investment						Net Earn	Cash	Cum PV	IRR
	fCTDC	fCPI	CWC	D	C excl D	S		Flow	\$ 0	\$ 0
1	\$ (5,099,366)	\$ (630,543)	\$ (1,145,982)	\$ -	\$ -	\$ -	\$ -	\$ (6,875,891)	\$ (6,250,810)	\$ (5,521,884)
2	\$ -	\$ -	\$ -	\$ 353,104	\$ (2,872,423)	\$ 5,855,615	\$ 1,953,764	\$ 1,600,660	\$ (4,927,950)	\$ (4,489,560)
3	\$ -	\$ -	\$ -	\$ 353,104	\$ (2,738,066)	\$ 5,855,615	\$ 2,088,122	\$ 1,735,018	\$ (3,624,405)	\$ (3,590,935)
4	\$ -	\$ -	\$ -	\$ 353,104	\$ (2,738,066)	\$ 5,855,615	\$ 2,088,122	\$ 1,735,018	\$ (2,439,365)	\$ (2,869,267)
5	\$ -	\$ -	\$ -	\$ 353,104	\$ (2,738,066)	\$ 5,855,615	\$ 2,088,122	\$ 1,735,018	\$ (1,362,055)	\$ (2,289,711)
6	\$ -	\$ -	\$ -	\$ 353,104	\$ (2,738,066)	\$ 5,855,615	\$ 2,088,122	\$ 1,735,018	\$ (382,683)	\$ (1,824,281)
7	\$ -	\$ -	\$ -	\$ 353,104	\$ (2,738,066)	\$ 5,855,615	\$ 2,088,122	\$ 1,735,018	\$ 507,656	\$ (1,450,504)
8	\$ -	\$ -	\$ -	\$ 353,104	\$ (2,738,066)	\$ 5,855,615	\$ 2,088,122	\$ 1,735,018	\$ 1,317,054	\$ (1,150,332)
9	\$ -	\$ -	\$ -	\$ 353,104	\$ (2,738,066)	\$ 5,855,615	\$ 2,088,122	\$ 1,735,018	\$ 2,052,871	\$ (909,270)
10	\$ -	\$ -	\$ -	\$ 353,104	\$ (2,738,066)	\$ 5,855,615	\$ 2,088,122	\$ 1,735,018	\$ 2,721,796	\$ (715,678)
11	\$ -	\$ -	\$ -	\$ 353,104	\$ (2,738,066)	\$ 5,855,615	\$ 2,088,122	\$ 1,735,018	\$ 3,329,909	\$ (560,209)
12	\$ -	\$ -	\$ -	\$ 353,104	\$ (2,738,066)	\$ 5,855,615	\$ 2,088,122	\$ 1,735,018	\$ 3,882,739	\$ (435,354)
13	\$ -	\$ -	\$ -	\$ 353,104	\$ (2,738,066)	\$ 5,855,615	\$ 2,088,122	\$ 1,735,018	\$ 4,385,312	\$ (335,086)
14	\$ -	\$ -	\$ -	\$ 353,104	\$ (2,738,066)	\$ 5,855,615	\$ 2,088,122	\$ 1,735,018	\$ 4,842,196	\$ (254,563)
15	\$ -	\$ -	\$ -	\$ 353,104	\$ (2,738,066)	\$ 5,855,615	\$ 2,088,122	\$ 1,735,018	\$ 5,257,546	\$ (189,897)
16	\$ -	\$ -	\$ -	\$ 353,104	\$ (2,738,066)	\$ 5,855,615	\$ 2,088,122	\$ 1,735,018	\$ 5,635,136	\$ (137,964)
17	\$ -	\$ -	\$ -	\$ 353,104	\$ (2,738,066)	\$ 5,855,615	\$ 2,088,122	\$ 1,735,018	\$ 5,978,400	\$ (96,259)
18	\$ -	\$ -	\$ -	\$ 353,104	\$ (2,738,066)	\$ 5,855,615	\$ 2,088,122	\$ 1,735,018	\$ 6,290,458	\$ (62,766)
19	\$ -	\$ -	\$ -	\$ 353,104	\$ (2,738,066)	\$ 5,855,615	\$ 2,088,122	\$ 1,735,018	\$ 6,574,148	\$ (35,868)
20	\$ -	\$ -	\$ 1,145,982	\$ 353,104	\$ (2,738,066)	\$ 5,855,615	\$ 2,088,122	\$ 2,881,000	\$ 7,002,390	\$ 0

TABLE 1210: CASH FLOW FOR THE FIRST 20 YEARS OF PLANT OPERATION.

## 11.1 Economic Hazards

The REAL WTP's revenue lies solely in household water demand. The demand for water is relatively constant because it is a fundamental resource. However, volatility exists mostly in raw materials purchased for the GAC and AOP unit operations.

### *11.1.1 GAC Cost*

As GAC as a treatment method for PFAS becomes increasingly popular in more municipalities the cost of tanks and media will increase. This could also be the opposite case where more novel PFAS remediation approaches popularize, leading to a decrease in demand for GAC. However, the economic viability of reactivation is poised to strengthen, particularly as Calgon Carbon's full-scale testing has demonstrated that reactivation destroys >99.99% of PFAS while restoring GAC to a near-virgin state. This high destruction efficiency, coupled with lower environmental liability, may shift demand from virgin GAC toward reactivation services, potentially tightening the supply chain for thermal reactivation facilities and driving up associated service costs.

### *11.1.2 1,4-dioxane treatment*

The treatment of 1,4-dioxane using AOP can present significant economic challenges and hazards for water treatment facilities due to its high energy demands and costs. The AOP used for treatment is powered by UV light, which requires substantial power to generate the reactive species needed to degrade 1,4-dioxane effectively. This energy-intensive process can lead to increased electricity costs, particularly in hotter months when energy prices are higher. This can be characterized as a hazard due to the volatility of electricity rates, which can pose even greater operational costs if the rates were to increase significantly. Additionally, the parts, maintenance, and replacement of the AOP components, such as the UV lamps, further add to the financial burden. Sourcing parts for maintenance or replacement can pose economic risks due to the increasingly expensive costs of the UV lamps. The overall energy cost of AOP consumption, which can be found in the Energy Balance, is roughly \$20,000/yr.

Although there is no federal MCL regulation on 1,4-Dioxane at this moment, the EPA is working towards it [81]. This means that other municipalities will be looking towards purchasing the UV-Phox AOP unit, resulting in increased prices and limited availability for raw materials like the UV-light replacements and hydrogen peroxide.

## **12. Global, Social, Cultural, and Public Health Impacts**

While most emissions are associated with the REAL WTP during the manufacturing of hydrogen peroxide, GAC media, and steel tanks, the plant itself generates minimal local emissions. The majority of environmental burdens stem from the production and transport of these materials rather than from on-site operations, meaning there is limited direct harm to the surrounding community. However, energy use remains a significant factor, particularly in the

AOP unit. Despite these demands, the plant uses groundwater efficiently, with no net water loss during treatment.

The mining and processing of raw materials like steel also come with broader global impacts, including emissions, water use, land disruption, and the potential for exploitative labor practices [82]. Components in the system, including those used in tanks and vessels, are durable (with a design life of over 10 years) and recyclable at end-of-life, thereby minimizing landfill waste and resource depletion.

Hydrogen peroxide production is particularly energy-intensive and is often tied to fossil fuel-based electricity, contributing significantly to upstream emissions, roughly 60,000 kg CO<sub>2</sub>/year. While its production is carbon-intensive, it decomposes completely during the AOP treatment process. Any remaining trace amounts are adsorbed by the GAC and do not leach into treated water or the environment. GAC also captures degradation byproducts, ensuring that hydrogen peroxide does not pose a public health risk to consumers. As such, it is considered a non-issue during operation.

The primary waste concern of the system lies in the disposal of PFAS-contaminated spent GAC, which is classified as hazardous waste. If landfilled, this waste carries a risk of leaching and long-term contamination of groundwater resources. However, the REAL WTP mitigates this risk by practicing high-temperature reactivation, which effectively destroys PFAS compounds. This method does generate emissions, but it significantly reduces the risk of long-term environmental contamination and a cyclical problem for the surrounding area.

Although she serves Tucson's Southside, another impacted community, Unified Community Advisory Board (UCAB) Co-chair Yolanda Herrera emphasized that "Clean, Safe Water IS Life!" Naturally occurring water is not enough to meet the basic needs and rights of Summit residents. Clean water from REAL WTP will lend the means for residents to participate fully in society, improve quality of life, and serve as a scalable model for other communities facing similar environmental justice challenges. In doing so, it reflects a broader commitment to valuing human life and promoting equity through infrastructure.

### 13. Conclusions and Recommendations

The design of the REAL Water Treatment Plant successfully integrates multiple treatment technologies to address PFAS and 1,4-dioxane contamination in Summit, Arizona and its surrounding area. Optimization efforts centered on extending breakthrough in GAC contactors, increasing the time until media replacement, which in turn minimized long-term costs and environmental impact. Additionally, the cyclic nature of PFAS waste was addressed by implementing thermal reactivation to the spent GAC media, reducing both cost and environmental impact.

The GAC media weight was optimized to balance cost and performance, with 30,000 pounds identified as the ideal GAC weight based on breakthrough modeling and feasibility limitations. Breakthrough modeling using Freundlich isotherms integrated into an RStudio precision model, allowed for a realistic prediction of breakthrough time of PFOS and PFOA, providing an estimation of media replacement time of every 12 months. After further investigation of the various factors that affect adsorption behavior, it was found that bituminous coal-based GAC (Calgon F400) proved to be the most effective media, demonstrating superior adsorption performance due to its favorable pore structure and high surface area.

Currently water treatment plants in the surrounding area that have implemented GAC as a remediation for PFAS dump their spent GAC into landfills. A main goal of the project was to eliminate the potential for PFAS to reenter the environment. To address this major concern, third party spent GAC reactivation served as an effective way to prevent the cyclical problem. By thermal reactivation, the spent media is restored to a near-virgin state, achieving PFAS destruction efficiencies exceeding 99.99%. This advancement not only allows for the reuse of media, which is economically viable, but slashes the environmental impact of landfill waste and emissions. Over a one year period, virgin GAC generates nearly ten times more CO<sub>2</sub> emissions and consumes significantly more energy (93.5 kg COE vs. 255 kg COE) than reactivated GAC. Additionally, reactivation also reduces environmental impacts across categories like acidification, ozone formation, eutrophication, and toxicity by 50–90%.

To maintain safety and compliance each unit operation underwent a HAZOP assessment, where a multitude of safety controls were implemented into the design. The AOP unit operation flagged as the most dangerous because of the use of hydrogen peroxide. To optimize safety in the future, an AOP using chlorine could be further researched. Due to multitude of side reactions that would release other contaminants into the water, it was not chosen for the process at this time.

The project requires an initial capital investment of \$6.8 million, with the largest costs attributed to land acquisition and GAC unit operations. Annual operating costs total \$1.66 million, primarily driven by labor at \$40/hour. Revenue begins in Year 2 at \$1.95 million and increases to \$2.08 million in Year 3 with the use of reactivated GAC. Reactivation is projected to save \$134,000 annually compared to virgin GAC. Over a 20-year period, the project yields a net present value of approximately \$7 million and an internal rate of return of 24.52%, with payback achieved in under 10 years.

Although the project is financially viable, the driving force behind it is not profit, it is necessity. Residents are paying for clean water because they have no choice. Conversations with the UCAB made it obvious that the fight for clean water is universal, and its urgency transcends economics. Delivering safe drinking water to Summit, Arizona is only a fraction of the solution, but it is a critical one. As a historically underserved community directly affected by contamination from the Davis-Monthan Air Force Base, the REAL WTP and Summit now can become a model for environmental justice. This project stands not just as a treatment plant, but as a testament to equity, accountability, and the right to clean water.

## 14. References

- [1] “PFAS: Forever Chemicals.” Accessed: Dec. 10, 2024. [Online]. Available: <https://www.tucsonaz.gov/Departments/Water/Water-Quality/PFAS>
- [2] “PFAS,” CT.gov - Connecticut’s Official State Website. Accessed: Dec. 10, 2024. [Online]. Available: <https://portal.ct.gov/dph/environmental-health/pfas/pfas>.
- [3] “Understanding organofluorine chemistry. An introduction to the C–F bond - Chemical Society Reviews (RSC Publishing).” Accessed: Dec. 10, 2024. [Online]. Available: <https://pubs.rsc.org/en/content/articlelanding/2008/cs/b711844a>
- [4] C. L. Leo, “UCAB 3Q 2024 TARP AOP QUARTERLY PROGRESS UPDATE”.
- [5] K. E. Pelch, A. Reade, T. A. M. Wolffe, and C. F. Kwiatkowski, “PFAS health effects database: Protocol for a systematic evidence map,” *Environ. Int.*, vol. 130, p. 104851, Sep. 2019, doi: 10.1016/j.envint.2019.05.045.
- [6] S. Brendel, É. Fetter, C. Staude, L. Vierke, and A. Biegel-Engler, “Short-chain perfluoroalkyl acids: environmental concerns and a regulatory strategy under REACH,” *Environ. Sci. Eur.*, vol. 30, no. 1, p. 9, Feb. 2018, doi: 10.1186/s12302-018-0134-4.
- [7] “TUCSON INTERNATIONAL AIRPORT AREA | Superfund Site Profile | Superfund Site Information | US EPA.” Accessed: Dec. 10, 2024. [Online]. Available: <https://cumulis.epa.gov/supercpad/SiteProfiles/index.cfm?fuseaction=second.cleanup&id=0900684>
- [8] “Story of Tucson’s Water – Sustainable Tucson.” Accessed: Dec. 10, 2024. [Online]. Available: <https://sustainabletucson.org/committees-working-groups/water-committee/the-story-of-tucson-water/>
- [9] “TECHNICAL FACT SHEET - 1,4-DIOXANE”.
- [10] “Groundbreaking study shows unaffordable costs of PFAS cleanup from wastewater | Minnesota Pollution Control Agency.” Accessed: Dec. 11, 2024. [Online]. Available: <https://www.pca.state.mn.us/news-and-stories/groundbreaking-study-shows-unaffordable-costs-of-pfas-cleanup-from-wastewater>
- [11] “Solvent stabilizers white paper - prepublication copy”.
- [12] “State-by-State Regulation of 1,4-Dioxane in Drinking Water,” JD Supra. Accessed: Dec. 10, 2024. [Online]. Available: <https://www.jdsupra.com/legalnews/state-by-state-regulation-of-1-4-8538403/>
- [13] “Remediation and Treatment Technologies – 14d.” Accessed: Dec. 10, 2024. [Online]. Available: <https://14d-1.itrcweb.org/remediation-and-treatment-technologies/>

- [14] A. Boonya-atichart, S. K. Boontanon, and N. Boontanon, “Study of hybrid membrane filtration and photocatalysis for removal of perfluorooctanoic acid (PFOA) in groundwater,” *Water Sci. Technol.*, vol. 2017, no. 2, pp. 561–569, Apr. 2018, doi: 10.2166/wst.2018.178.
- [15] “PFAS.” Accessed: May 02, 2025. [Online]. Available: <https://www.kemi.se/en/chemical-substances-and-materials/pfas>
- [16] R. C. Buck *et al.*, “Perfluoroalkyl and polyfluoroalkyl substances in the environment: Terminology, classification, and origins,” *Integr. Environ. Assess. Manag.*, vol. 7, no. 4, pp. 513–541, Oct. 2011, doi: 10.1002/ieam.258.
- [17] “Current Review of Increasing Animal Health Threat of Per- and Polyfluoroalkyl Substances (PFAS): Harms, Limitations, and Alternatives to Manage Their Toxicity.” Accessed: May 02, 2025. [Online]. Available: <https://www.mdpi.com/1422-0067/24/14/11707>
- [18] M. P. Krafft and J. G. Riess, “Selected physicochemical aspects of poly- and perfluoroalkylated substances relevant to performance, environment and sustainability—Part one,” *Chemosphere*, vol. 129, pp. 4–19, Jun. 2015, doi: 10.1016/j.chemosphere.2014.08.039.
- [19] T. A. Saleh, “Chapter 2 - Adsorption technology and surface science,” in *Interface Science and Technology*, vol. 34, T. A. Saleh, Ed., in Surface Science of Adsorbents and Nanoadsorbents, vol. 34. , Elsevier, 2022, pp. 39–64. doi: 10.1016/B978-0-12-849876-7.00006-3.
- [20] E. Gagliano, M. Sgroi, P. P. Falciglia, F. G. A. Vagliasindi, and P. Roccaro, “Removal of poly- and perfluoroalkyl substances (PFAS) from water by adsorption: Role of PFAS chain length, effect of organic matter and challenges in adsorbent regeneration,” *Water Res.*, vol. 171, p. 115381, Mar. 2020, doi: 10.1016/j.watres.2019.115381.
- [21] X. Lei *et al.*, “A review of PFAS adsorption from aqueous solutions: Current approaches, engineering applications, challenges, and opportunities,” *Environ. Pollut.*, vol. 321, p. 121138, Mar. 2023, doi: 10.1016/j.envpol.2023.121138.
- [22] A. Gabelman, “Adsorption can be used to treat waste streams or purify valuable components of a feed. This article describes both equilibrium and mass-transfer considerations, and reviews the fundamentals of adsorption system design,” *Back Basics*, 2017.
- [23] “Effective Treatment Methods of PFAS - AQUALIS.” Accessed: May 02, 2025. [Online]. Available: <https://aqualisco.com/effective-treatment-methods-of-pfas/>
- [24] C. J. Liu, C. C. Murray, R. E. Marshall, T. J. Strathmann, and C. Bellona, “Removal of per- and polyfluoroalkyl substances from contaminated groundwater by granular activated carbon and anion exchange resins: a pilot-scale comparative assessment,” *Environ. Sci. Water Res. Technol.*, vol. 8, no. 10, pp. 2245–2253, 2022, doi: 10.1039/D2EW00080F.

- [25] C. J. Liu, D. Werner, and C. Bellona, "Removal of per- and polyfluoroalkyl substances (PFASs) from contaminated groundwater using granular activated carbon: a pilot-scale study with breakthrough modeling," *Environ. Sci. Water Res. Technol.*, vol. 5, no. 11, pp. 1844–1853, 2019, doi: 10.1039/C9EW00349E.
- [26] "Depth to Water Data | Arizona Department of Water Resources." Accessed: Dec. 10, 2024. [Online]. Available: <https://www.azwater.gov/hydrology/depth-water-data>
- [27] M. R. Islam and M. E. Hossain, *DRILLING ENGINEERING: TOWARDS ACHIEVING TOTAL SUSTAINABILITY*. Gulf Professional Publishing, 2020.
- [28] "The Engineering ToolBox." Accessed: Dec. 10, 2024. [Online]. Available: <https://www.engineeringtoolbox.com/>
- [29] "slurry density | Energy Glossary." Accessed: May 02, 2025. [Online]. Available: [https://glossary.slb.com/en/terms/s/slurry\\_density](https://glossary.slb.com/en/terms/s/slurry_density)
- [30] Town of Marana Picture Rocks Campus, "Operations and Maintenance Plan".
- [31] A. Tawfik, "Degradation pathways of 1,4-dioxane in biological and advanced oxidation processes," *Desalination Water Treat.*, vol. 178, pp. 360–386, Feb. 2020, doi: 10.5004/dwt.2020.24970.
- [32] M. I. Stefan and J. R. Bolton, "Mechanism of the Degradation of 1,4-Dioxane in Dilute Aqueous Solution Using the UV/Hydrogen Peroxide Process," *Environ. Sci. Technol.*, vol. 32, no. 11, pp. 1588–1595, Jun. 1998, doi: 10.1021/es970633m.
- [33] "Comparison of Activated Carbons for Removal of Perfluorinated Compounds From Drinking Water - McNamara - 2018 - Journal AWWA - Wiley Online Library." Accessed: Dec. 10, 2024. [Online]. Available: <https://awwa.onlinelibrary.wiley.com/doi/10.5942/jawwa.2018.110.0003>
- [34] C. C. Murray, R. E. Marshall, C. J. Liu, H. Vatankhah, and C. L. Bellona, "PFAS treatment with granular activated carbon and ion exchange resin: Comparing chain length, empty bed contact time, and cost," *J. Water Process Eng.*, vol. 44, p. 102342, Dec. 2021, doi: 10.1016/j.jwpe.2021.102342.
- [35] "ccc\_truth\_in\_the\_data.pdf." Accessed: Dec. 10, 2024. [Online]. Available: [https://www.calgoncarbon.com/app/uploads/ccc\\_truth\\_in\\_the\\_data.pdf](https://www.calgoncarbon.com/app/uploads/ccc_truth_in_the_data.pdf)
- [36] "av-project-profile\_tucson\_az.pdf." Accessed: Dec. 10, 2024. [Online]. Available: [https://www.aqueousvets.com/uploads/9/8/8/7/98870448/av-project-profile\\_tucson\\_az.pdf](https://www.aqueousvets.com/uploads/9/8/8/7/98870448/av-project-profile_tucson_az.pdf)
- [37] "funding\_forum2024.pdf." Accessed: May 02, 2025. [Online]. Available: [https://static.azdeq.gov/wqd/pfas/funding\\_forum2024.pdf](https://static.azdeq.gov/wqd/pfas/funding_forum2024.pdf)

- [38] “DS-FILTRA40018-EIN-E1.pdf.” Accessed: May 02, 2025. [Online]. Available: <https://www.calgoncarbon.com/app/uploads/DS-FILTRA40018-EIN-E1.pdf>
- [39] “EPA 832-F-00-017 - September 2000.”
- [40] “Hydrothermal Alkaline Treatment for a Closed-Loop, On-Site PFAS Treatment Solution.” Accessed: Dec. 10, 2024. [Online]. Available: <https://serdp-estcp.mil/projects/details/a4c6918a-fe3b-43d2-95cb-fa3dfa3a50a2/hydrothermal-alkaline-treatment-for-a-closed-loop-on-site-pfas-treatment-solution>
- [41] B. R. Pinkard, C. Austin, A. L. Purohit, J. Li, and I. V. Novosselov, “Destruction of PFAS in AFFF-impacted fire training pit water, with a continuous hydrothermal alkaline treatment reactor,” *Chemosphere*, vol. 314, p. 137681, Feb. 2023, doi: 10.1016/j.chemosphere.2022.137681.
- [42] R. S. Kookana, D. A. Navarro, S. Kabiri, and M. J. McLaughlin, “Key properties governing sorption–desorption behaviour of poly- and perfluoroalkyl substances in saturated and unsaturated soils: a review,” *Soil Res.*, vol. 61, no. 2, pp. 107–125, Dec. 2022, doi: 10.1071/SR22183.
- [43] Y. Nakazawa, K. Kosaka, M. Asami, and Y. Matsui, “Maximum desorption of perfluoroalkyl substances adsorbed on granular activated carbon used in full-scale drinking water treatment plants,” *Water Res.*, vol. 254, p. 121396, May 2024, doi: 10.1016/j.watres.2024.121396.
- [44] Z. Du *et al.*, “Adsorption behavior and mechanism of perfluorinated compounds on various adsorbents—A review,” *J. Hazard. Mater.*, vol. 274, pp. 443–454, Jun. 2014, doi: 10.1016/j.jhazmat.2014.04.038.
- [45] H.-K. Chung, W.-H. Kim, J. Park, J. Cho, T.-Y. Jeong, and P.-K. Park, “Application of Langmuir and Freundlich isotherms to predict adsorbate removal efficiency or required amount of adsorbent,” *J. Ind. Eng. Chem.*, vol. 28, pp. 241–246, Aug. 2015, doi: 10.1016/j.jiec.2015.02.021.
- [46] Z. Zaafouri, D. Bauer, G. Batôt, C. Nieto-Draghi, and B. Coasne, “Cooperative Effects Dominating the Thermodynamics and Kinetics of Surfactant Adsorption in Porous Media: From Lateral Interactions to Surface Aggregation,” *J. Phys. Chem. B*, vol. 124, no. 47, pp. 10841–10849, Nov. 2020, doi: 10.1021/acs.jpccb.0c08226.
- [47] H.-K. Chung, W.-H. Kim, J. Park, J. Cho, T.-Y. Jeong, and P.-K. Park, “Application of Langmuir and Freundlich isotherms to predict adsorbate removal efficiency or required amount of adsorbent,” *J. Ind. Eng. Chem.*, vol. 28, pp. 241–246, Aug. 2015, doi: 10.1016/j.jiec.2015.02.021.
- [48] M. Pranić, L. Carlucci, A. van der Wal, and J. E. Dykstra, “Kinetic and isotherm study for the adsorption of per- and polyfluoroalkyl substances (PFAS) on activated carbon in the

low ng/L range,” *Chemosphere*, vol. 370, p. 143889, Feb. 2025, doi: 10.1016/j.chemosphere.2024.143889.

- [49] J. B. Burkhardt, N. Burns, D. Mobley, J. G. Pressman, M. L. Magnuson, and T. F. Speth, “Modeling PFAS Removal Using Granular Activated Carbon for Full-Scale System Design,” *J. Environ. Eng.*, vol. 148, no. 3, p. 04021086, Mar. 2022, doi: 10.1061/(ASCE)EE.1943-7870.0001964.
- [50] M. Chiban, A. Soudani, F. Sinan, and M. Persin, “Single, binary and multi-component adsorption of some anions and heavy metals on environmentally friendly *Carpobrotus edulis* plant,” *Colloids Surf. B Biointerfaces*, vol. 82, no. 2, pp. 267–276, Feb. 2011, doi: 10.1016/j.colsurfb.2010.09.013.
- [51] Y. Qu, C. Zhang, F. Li, X. Bo, G. Liu, and Q. Zhou, “Equilibrium and kinetics study on the adsorption of perfluorooctanoic acid from aqueous solution onto powdered activated carbon,” *J. Hazard. Mater.*, vol. 169, no. 1, pp. 146–152, Sep. 2009, doi: 10.1016/j.jhazmat.2009.03.063.
- [52] S. Sukeesan, N. Boontanon, S. Fujii, and S. K. Boontanon, “Evaluation of the adsorption behavior of mixed perfluoroalkyl and polyfluoroalkyl substances onto granular activated carbon and styrene-divinylbenzene resins,” *Remediat. J.*, vol. 33, no. 4, pp. 297–308, 2023, doi: 10.1002/rem.21766.
- [53] B. C. Moore *et al.*, “Changes in GAC pore structure during full-scale water treatment at Cincinnati: a comparison between virgin and thermally reactivated GAC,” *Carbon*, vol. 39, no. 6, pp. 789–807, May 2001, doi: 10.1016/S0008-6223(00)00097-X.
- [54] B. C. Moore *et al.*, “Changes in GAC pore structure during full-scale water treatment at Cincinnati: a comparison between virgin and thermally reactivated GAC,” *Carbon*, vol. 39, no. 6, pp. 789–807, May 2001, doi: 10.1016/S0008-6223(00)00097-X.
- [55] K. A. Mertz, F. Gobin, D. W. Hand, D. R. Hokanson, and J. C. Crittenden, “Manual Adsorption Design Software for Windows (AdDesignS<sup>2</sup>)”.
- [56] P. Bayer, E. Heuer, U. Karl, and M. Finkel, “Economical and ecological comparison of granular activated carbon (GAC) adsorber refill strategies,” *Water Res.*, vol. 39, no. 9, pp. 1719–1728, May 2005, doi: 10.1016/j.watres.2005.02.005.
- [57] “DEPARTMENT OF THE ARMY DG 1110-1-2,” 2001.
- [58] R. DiStefano, T. Feliciano, R. A. Mimna, A. M. Redding, and J. Matthis, “Thermal destruction of PFAS during full-scale reactivation of PFAS-laden granular activated carbon,” *Remediat. J.*, vol. 32, no. 4, pp. 231–238, 2022, doi: 10.1002/rem.21735.
- [59] “Thermal Regeneration of Spent Granular Activated Carbon Presents an Opportunity to Break the Forever PFAS Cycle | Environmental Science & Technology.” Accessed: May 02, 2025. [Online]. Available: <https://pubs.acs.org/doi/10.1021/acs.est.0c08224>

- [60] D. M. Kempisty, Y. Xing, and L. Racz, Eds., *Perfluoroalkyl Substances in the Environment: Theory, Practice, and Innovation*. Boca Raton: CRC Press, 2018. doi: 10.1201/9780429487125.
- [61] G. Abulikemu *et al.*, “Perfluoroalkyl chemical adsorption by granular activated carbon: Assessment of particle size impact on equilibrium parameters and associated rapid small-scale column test scaling assumptions,” *Water Res.*, vol. 271, p. 122977, Mar. 2025, doi: 10.1016/j.watres.2024.122977.
- [62] T. G. Mulugeta, M. S. Ersan, S. Garcia-Segura, and G. Ersan, “Predicting full-scale performance of adsorbents for per- and polyfluoroalkyl substances adsorption: The role of rapid small-scale column tests,” *Sci. Total Environ.*, vol. 974, p. 178944, Apr. 2025, doi: 10.1016/j.scitotenv.2025.178944.
- [63] G. Abulikemu *et al.*, “Perfluoroalkyl chemical adsorption by granular activated carbon: Assessment of particle size impact on equilibrium parameters and associated rapid small-scale column test scaling assumptions,” *Water Res.*, vol. 271, p. 122977, Mar. 2025, doi: 10.1016/j.watres.2024.122977.
- [64] “Pore-Surface Diffusion Model for Batch Adsorption Processes | Langmuir.” Accessed: May 02, 2025. [Online]. Available: <https://pubs.acs.org/doi/10.1021/la026624v>
- [65] H. Su, Q. Tian, C.-A. Hurd Price, L. Xu, K. Qian, and J. Liu, “Nanoporous core@shell particles: Design, preparation, applications in bioadsorption and biocatalysis,” *Nano Today*, vol. 31, p. 100834, Apr. 2020, doi: 10.1016/j.nantod.2019.100834.
- [66] “Pore size matters in the PFAS sorption by carbon adsorbents.” Accessed: May 02, 2025. [Online]. Available: <https://acs.digitellinc.com/p/s/pore-size-matters-in-the-pfas-sorption-by-carbon-adsorbents-601621>
- [67] “Product and Process Design Principles: Synthesis, Analysis and Evaluation, 4th Edition | Wiley,” Wiley.com. Accessed: May 02, 2025. [Online]. Available: <https://www.wiley.com/en-us/Product+and+Process+Design+Principles%3A+Synthesis%2C+Analysis+and+Evaluation%2C+4th+Edition-p-9781119282631>
- [68] L. Munla, T. Feliciano, R. A. Mimna, A. M. Redding, and J. Matthis, “Thermal destruction of PFAS during full-scale reactivation of PFAS-laden granular activated carbon,” *Remediat. J.*, vol. 32, no. 4, pp. 231–238, Sep. 2022, doi: 10.1002/rem.21735.
- [69] “PDS\_FILTRASORB-400.pdf.” Accessed: May 02, 2025. [Online]. Available: [https://www.treitelonline.com/wp-content/uploads/2021/03/PDS\\_FILTRASORB-400.pdf](https://www.treitelonline.com/wp-content/uploads/2021/03/PDS_FILTRASORB-400.pdf)
- [70] A. Vilén, P. Laurell, and R. Vahala, “Comparative life cycle assessment of activated carbon production from various raw materials,” *J. Environ. Manage.*, vol. 324, p. 116356, Dec. 2022, doi: 10.1016/j.jenvman.2022.116356.

- [71] “Packet\_20140520\_Facilities.pdf.” Accessed: May 02, 2025. [Online]. Available: [https://www.palmdalewater.org/wp-content/uploads/2014/08/Packet\\_20140520\\_Facilities.pdf](https://www.palmdalewater.org/wp-content/uploads/2014/08/Packet_20140520_Facilities.pdf)
- [72] “50,000 Gallon Bolted Steel Tank - National Storage Tank.” Accessed: May 02, 2025. [Online]. Available: <https://www.nationalstorage tank.com/product/50-000-gallon-carbon-bolted-steel-tank-low-profile-roof-diameter-33-peak-height-8/>
- [73] “Hydrogen Peroxide,” 2020.
- [74] C. Wang, N. Moore, K. Bircher, S. Andrews, and R. Hofmann, “Full-scale comparison of UV/H<sub>2</sub>O<sub>2</sub> and UV/Cl<sub>2</sub> advanced oxidation: The degradation of micropollutant surrogates and the formation of disinfection byproducts,” *Water Res.*, vol. 161, pp. 448–458, Sep. 2019, doi: 10.1016/j.watres.2019.06.033.
- [75] P. Alulema-Pullupaxi, Y. Zhang, N. B. Saleh, A. Venkatesan, and O. G. Apul, “Analyzing the Release of Per- and Polyfluoroalkyl Substances from Spent Granular Activated Carbons by Standard Leaching Procedures,” *Environ. Sci. Technol.*, Apr. 2025, doi: 10.1021/acs.est.4c12093.
- [76] Jason Mathers, “Green Freight Math: How to Calculate Emissions for a Truck Move,” EDF+Business. Accessed: May 02, 2025. [Online]. Available: <https://business.edf.org/insights/green-freight-math-how-to-calculate-emissions-for-a-truck-move/>
- [77] Vincent Doedee, “What is the carbon footprint of steel?,” Sustainable Ships. Accessed: May 02, 2025. [Online]. Available: <https://www.sustainable-ships.org/stories/2022/carbon-footprint-steel>
- [78] “Electric arc furnace,” *Wikipedia*. Apr. 23, 2025. Accessed: May 02, 2025. [Online]. Available: [https://en.wikipedia.org/w/index.php?title=Electric\\_arc\\_furnace&oldid=1286995701](https://en.wikipedia.org/w/index.php?title=Electric_arc_furnace&oldid=1286995701)
- [79] “Water-management-in-the-steel-industry.pdf.” Accessed: May 02, 2025. [Online]. Available: <https://worldsteel.org/wp-content/uploads/Water-management-in-the-steel-industry.pdf>
- [80] “Your Residential Water Bill.” Accessed: May 02, 2025. [Online]. Available: <https://www.tucsonaz.gov/Departments/Water/Your-Water-Bill/residential-bill>
- [81] “1,4-Dioxane State Groundwater Regulations,” BCLP - Bryan Cave Leighton Paisner - 1,4-Dioxane State Groundwater Regulations. Accessed: May 02, 2025. [Online]. Available: <https://www.bclplaw.com/en-US/events-insights-news/14-dioxane-state-groundwater-regulations.html>

[82] Laura, “Stop human rights violations in the steel industry.,” Climate Whistleblowers. Accessed: May 02, 2025. [Online]. Available: <https://www.climatewhistleblowers.org/stop-human-rights-violations-in-the-steel-industry/>

## 16. Appendices

### 16.1 Nomenclature

#### *16.1.1 Acronyms*

- **AOP** – Advanced Oxidation Process
- **BFD** – Block Flow Diagram
- **Cum PV** – Cumulative Present Value
- **EBCT** – Empty Bed Contact Time
- **EPA** – Environmental Protection Agency
- **GAC** – Granular Activated Carbon
- **HALT** – Hydrothermal Alkaline Treatment
- **IRR** – Internal Rate of Return
- **LPHO** – Low-Pressure High-Output (UV lamp type)
- **MCL** – Maximum Contaminant Level
- **NOM** – Natural Organic Matter
- **NPV** – Net Present Value
- **PFD** – Process Flow Diagram
- **PFAS** – Per- and Polyfluoroalkyl Substances
- **PFBS** – Perfluorobutane Sulfonic Acid
- **PFHxS** – Perfluorohexane Sulfonic Acid
- **PFNA** – Perfluorononanoic Acid
- **PFOA** – Perfluorooctanoic Acid
- **PFOS** – Perfluorooctane Sulfonic Acid
- **PSDFR** – Pore to Surface Diffusion Ratio
- **RO** – Reverse Osmosis
- **SRD** – Surface-Reticulated Design
- **TARP** – Tucson Airport Remediation Project
- **TSS** – Total Suspended Solids
- **UCAB** – Unified Community Advisory Board
- **UV** – Ultraviolet
- **WTP** – Water Treatment Plant

#### *16.1.2 Units*

- **µg/L** – Micrograms per liter
- **ng/L** – Nanograms per liter
- **ppt** – Parts per trillion
- **ppb** – Parts per billion
- **kWh** – Kilowatt-hour
- **ft<sup>3</sup>** – Cubic feet
- **psi** – Pounds per square inch
- **MPa** – Megapascal
- **gpd** – Gallons per day

- **mg/g** – Milligrams per gram
  - **L/mg** – Liters per milligram
- 16.1.3 Symbols

- **C-F bond**: Carbon-Fluorine bond
- **H<sub>2</sub>O**: Water
- **CO<sub>2</sub>**: Carbon Dioxide
- **H<sub>2</sub>O<sub>2</sub>**: Hydrogen Peroxide
- **•OH**: Hydroxyl Radicals

Symbol	Definition	Units
• <b>C<sub>e</sub></b>	Equilibrium concentration of solute in solution	μg/L or mg/L
• <b>q<sub>e</sub></b>	Adsorbed solute per unit mass of adsorbent	μg/g or mg/g
• <b>K<sub>f</sub></b>	Freundlich isotherm constant	(mg/g)(L/mg) <sup>n</sup>
• <b>n</b>	Freundlich isotherm exponent (adsorption intensity)	none

## 16.2 Final Calculations

### 16.2.1 Spread Sheets with Explanations

[443 Senior Design Calculations FINAL Optimization.xlsx](#)

### 16.2.3 Hand calculations that demonstrate correct order of magnitude for equipment

$$2 \text{H}_2\text{O}_2 \xrightarrow{\dot{e}_1} 2 \text{H}_2\text{O} + \text{O}_2$$

$$\text{C}_4\text{H}_8\text{O}_2 + 5 \text{O}_2 \xrightarrow{\dot{e}_2} 4 \text{CO}_2 + 4 \text{H}_2\text{O}$$

reaction

$$\begin{matrix} \text{H}_2\text{O} \\ \text{O}_2 \\ \text{CO}_2 \end{matrix}$$

Knowns:  
 $F_{1,\text{H}_2\text{O}_2} = 5.27$   
 $F_{1,\text{C}_4\text{H}_8\text{O}_2} = 1.1 \times 10^9$

$\text{H}_2\text{O}_2: F_{1,\text{H}_2\text{O}_2} - F_{2,\text{H}_2\text{O}_2} - \dot{e}_1 = 0 \rightarrow F_{1,\text{H}_2\text{O}_2} = \dot{e}_1 \rightarrow \boxed{\dot{e}_1 = 5.27}$   
 $\text{H}_2\text{O}: F_{1,\text{H}_2\text{O}} - F_{2,\text{H}_2\text{O}} + 2\dot{e}_1 + 4\dot{e}_2 = 0$   
 $\text{C}_4\text{H}_8\text{O}_2: F_{1,\text{C}_4\text{H}_8\text{O}_2} - F_{2,\text{C}_4\text{H}_8\text{O}_2} - \dot{e}_2 = 0 \rightarrow F_{1,\text{C}_4\text{H}_8\text{O}_2} = \dot{e}_2 \rightarrow \boxed{\dot{e}_2 = 1.1 \times 10^9}$   
 $\text{O}_2: F_{1,\text{O}_2} - F_{2,\text{O}_2} + \dot{e}_1 - 5\dot{e}_2 = 0$   
 $\text{CO}_2: F_{1,\text{CO}_2} - F_{2,\text{CO}_2} + 4\dot{e}_2 = 0$

$2\dot{e}_1 + 4\dot{e}_2 = F_{2,\text{H}_2\text{O}} \rightarrow 2(5.27) + 4(1.1 \times 10^9) \rightarrow \boxed{F_{2,\text{H}_2\text{O}} = 10.54}$   
 $F_{2,\text{CO}_2} = 4\dot{e}_2 \rightarrow \boxed{F_{2,\text{CO}_2} = 4.4 \times 10^9}$

Total:  $F_1 - F_2 - \cancel{\dot{e}_1} + 2\dot{e}_1 + 4\dot{e}_2 - \cancel{\dot{e}_2} + \cancel{\dot{e}_1} - 5\dot{e}_2 + 4\dot{e}_2 = 0$   
 $F_1 - F_2 + 2\dot{e}_1 + 2\dot{e}_2 = 0$

$F_1 = F_{1,\text{H}_2\text{O}_2} + F_{1,\text{C}_4\text{H}_8\text{O}_2} = 5.27 \rightarrow F_2 = 5.27 + 2(5.27) + 2(1.1 \times 10^9) = 15.81$   
 $F_2 = F_{2,\text{H}_2\text{O}} + F_{2,\text{H}_2\text{O}_2} + F_{2,\text{O}_2} + F_{2,\text{C}_4\text{H}_8\text{O}_2} + F_{2,\text{CO}_2}$   
 $15.81 = 10.54 + F_{2,\text{O}_2} + 4.4 \times 10^9$   
 $\boxed{F_{2,\text{O}_2} = 5.27}$

$F_{1,\text{O}_2} = 5(1.1 \times 10^9) - 5.27 + 5.27$   
 $\boxed{F_{1,\text{O}_2} = 5.5 \times 10^9}$

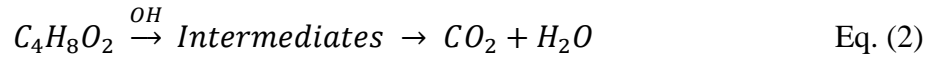
16.2.4 [Hand calculations for GAC Contactor Head loss from cut sheets](#)

16.2.5 *Additional Information*

Formation of Hydroxyl Radicals



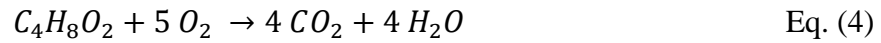
Complete Destruction Process of 1,4-dioxane



Balanced Equation of Breakdown of Hydrogen Peroxide



Balanced Equation of 1,4-dioxane



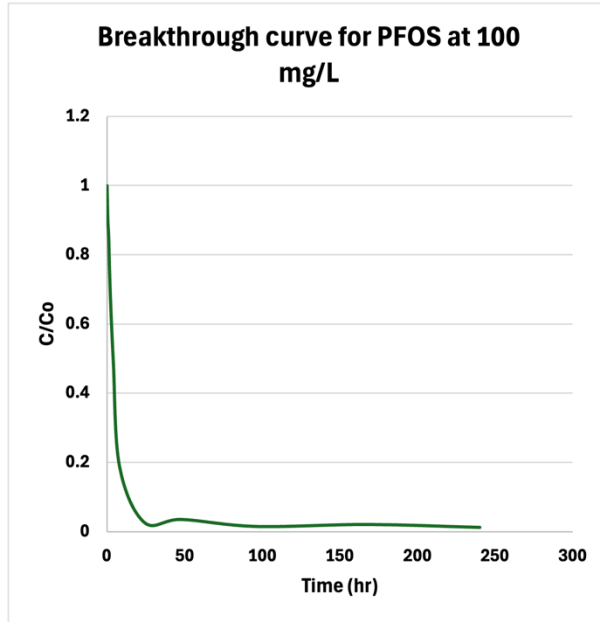
Langmuir (linearized)

$$\frac{1}{q_e} = \left( \frac{1}{K_L \cdot q_{max}} \right) \cdot \frac{1}{C_e} + \frac{1}{q_{max}}$$

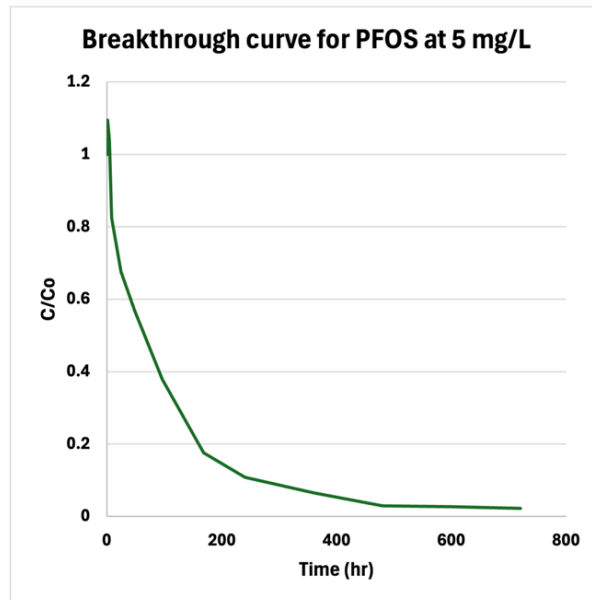
Freundlich (linearized)

$$\log q_e = \frac{1}{n} \log C_e + \log K_F$$

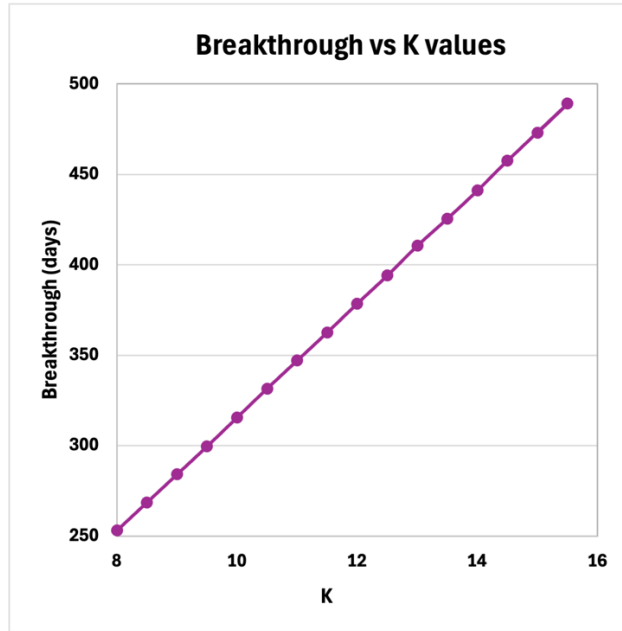
### 16.3 Figures



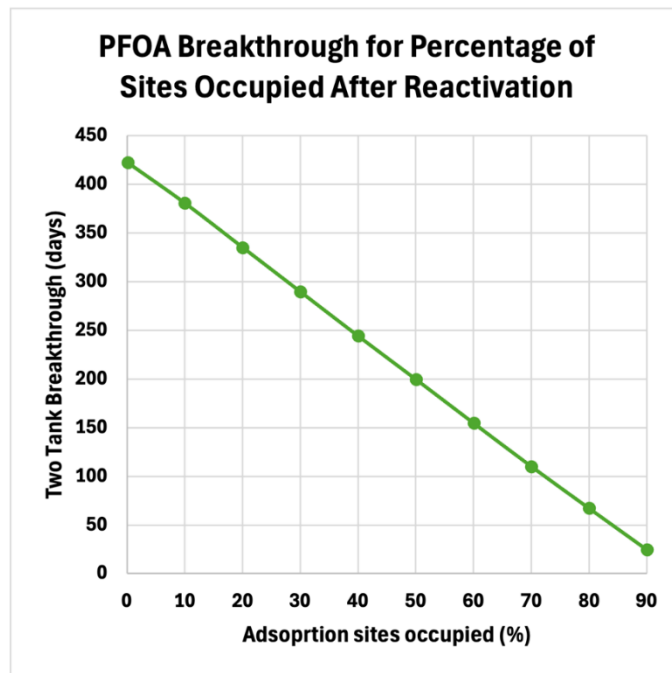
*A. Figure I* BREAKTHROUGH CURVE FOR PFOS AT AN INFLUENT CONCENTRATION OF 100 mg/L, SHOWING NORMALIZED CONCENTRATION ( $C/C_0$ ) OVER TIME. THE SHARP INITIAL DECLINE INDICATES RAPID ADSORPTION ONTO THE MEDIA, FOLLOWED BY A SUSTAINED LOW  $C/C_0$  VALUE, SUGGESTING EFFECTIVE PFOS REMOVAL AND MINIMAL BREAKTHROUGH OVER THE 250-HOUR DURATION.



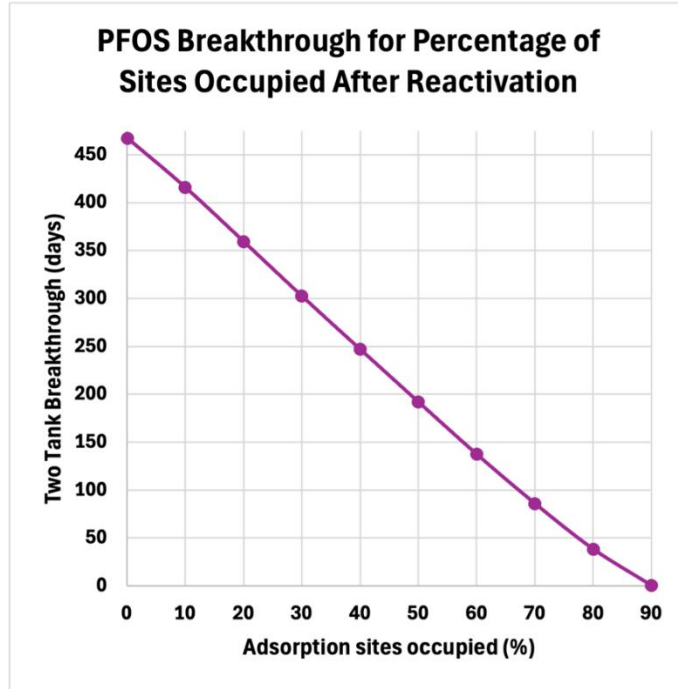
*A. Figure II* BREAKTHROUGH CURVE FOR PFOS AT AN INFLUENT CONCENTRATION OF 5 mg/L, ILLUSTRATING NORMALIZED CONCENTRATION ( $C/C_0$ ) VERSUS TIME. COMPARED TO HIGHER CONCENTRATIONS, THE SLOWER DECLINE IN  $C/C_0$  OVER ~750 HOURS REFLECTS A MORE GRADUAL ADSORPTION PROCESS, WITH EXTENDED MEDIA PERFORMANCE AND DELAYED BREAKTHROUGH UNDER LOWER LOADING CONDITIONS.



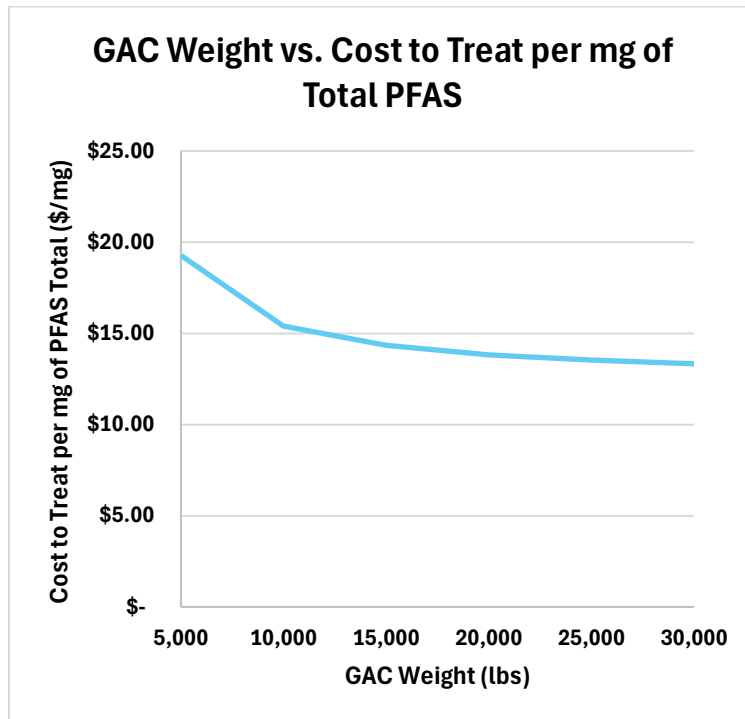
*A. Figure III* BREAKTHROUGH TIME AS A FUNCTION OF THE ADSORPTION COEFFICIENT (K). THE PLOT SHOWS A STRONG POSITIVE CORRELATION BETWEEN K VALUES AND BREAKTHROUGH TIME, INDICATING THAT HIGHER ADSORPTION AFFINITIES RESULT IN SIGNIFICANTLY LONGER MEDIA LIFESPANS BEFORE PFOS BREAKTHROUGH OCCURS.



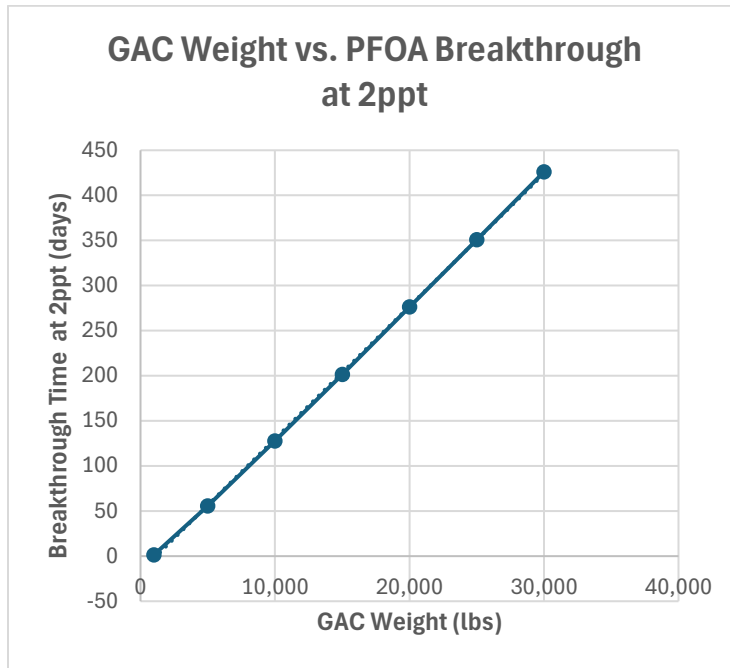
*A. Figure IV* TWO-TANK BREAKTHROUGH TIME FOR PFOA AS A FUNCTION OF ADSORPTION SITE OCCUPATION FOLLOWING GAC MEDIA REACTIVATION. THE INVERSE LINEAR RELATIONSHIP ILLUSTRATES THAT HIGHER PERCENTAGES OF OCCUPIED SITES SIGNIFICANTLY REDUCE SYSTEM LONGEVITY, EMPHASIZING THE IMPORTANCE OF THOROUGH REGENERATION FOR MAXIMIZING BREAKTHROUGH TIME.



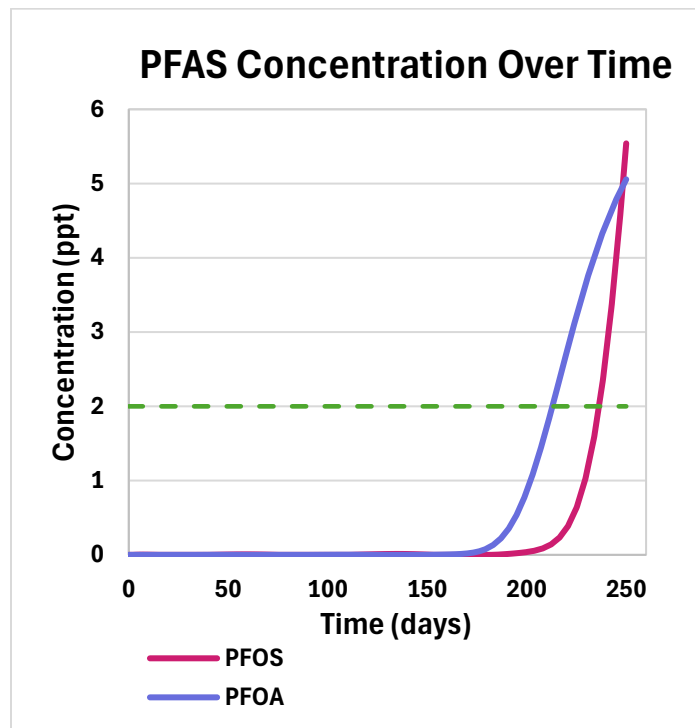
*A. Figure V* Two-TANK BREAKTHROUGH TIME FOR PFOS AS A FUNCTION OF ADSORPTION SITE OCCUPANCY AFTER MEDIA REACTIVATION. THE LINEAR DECREASE IN BREAKTHROUGH DURATION WITH INCREASING SITE OCCUPATION UNDERSCORES THE CRITICAL IMPACT OF INCOMPLETE REGENERATION ON TREATMENT SYSTEM PERFORMANCE AND LONGEVITY.



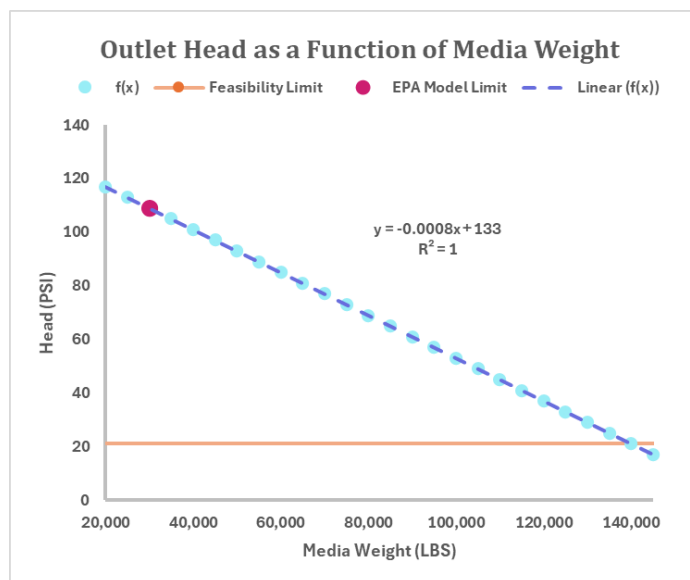
*A. Figure VI* COST TO TREAT PER MILLIGRAM OF TOTAL PFAS AS A FUNCTION OF GRANULAR ACTIVATED CARBON (GAC) WEIGHT. THE GRAPH DEMONSTRATES THAT INCREASING GAC WEIGHT LEADS TO A DECREASE IN TREATMENT COST PER MG OF PFAS, HIGHLIGHTING THE COST EFFECTIVENESS OF INCREASING MEDIA WEIGHT TO A CERTAIN POINT.



A. Figure VII RELATIONSHIP BETWEEN GAC MEDIA WEIGHT (LBS) AND PFOA BREAKTHROUGH TIME (DAYS). THIS INDICATES THE WEIGHT OF 30,000LBS RESULTED IN LONGEST TIME UNTIL BREAKTHROUGH.



A. Figure VIII BREAKTHROUGH CURVE OF PFOS AND PFOA, INDICATING THE TARGET MCL (2PPT) FOR MEDIA REPLACEMENT TIME. BREAKTHROUGH IS FOR STANDARD OPTIMIZED CONDITIONS OF 30,000LBS OF GAC MEDIA.



A. Figure IX OUTLET HEAD PRESSURE FROM THE FOUR GAC CONTACTORS AS A FUNCTION OF MEDIA WEIGHT. THE ORANGE LINE INDICATES THE MINIMUM HEAD REQUIRED TO TRANSFER WATER TO THE FINISHING TANKS, WHILE THE PINK DOT MARKS THE EPA MODEL'S FEASIBILITY LIMIT. THE LINEAR TREND LINE ( $R^2 = 1$ , SLOPE =  $-0.0008$ ) DEMONSTRATES A PERFECT INVERSE RELATIONSHIP. FEASIBILITY IS EXCEEDED AT 140,000 POUNDS OF GAC MEDIA.

#### 16.4 Tables

**Table I:** Breakthrough Times for PFOA Varying Flow, Media Weights, and Tank Heights.

PFOA					
Flow rate (gpm)	Height (m)	Weight of GAC (lbs)	Breakthrough at 2 ppt (days)	Breakthrough at 2 ppt (months)	Notes
1,664	9.76	40,000	66.00	2	Quadruple flow, double height, double weight
416	9.76	40,000	0	0	Double height, doubled weight
832	9.76	40,000	139.75	4.658	Double flow, height, weight
416	4.88	20,000	138.25	4.608	Standard conditions
832	4.88	20,000	65.25	2.175	Double flow

TABLE I: PFOA BREAKTHROUGH TIMES UNDER VARYING FLOW RATES, GAC WEIGHTS, AND COLUMN HEIGHTS AT A BREAKTHROUGH THRESHOLD OF 2 PPT. RESULTS SHOW THAT INCREASING GAC WEIGHT AND COLUMN HEIGHT GENERALLY EXTENDS BREAKTHROUGH TIME, WHILE HIGHER FLOW RATES REDUCE IT. THE STANDARD CONDITION (416 GPM, 4.88 M HEIGHT, 20,000 LBS GAC) YIELDS ~138 DAYS UNTIL BREAKTHROUGH. DOUBLING FLOW UNDER STANDARD GEOMETRY NEARLY HALVES THE BREAKTHROUGH TIME, WHILE DOUBLING BOTH HEIGHT AND WEIGHT RESTORES PERFORMANCE. AT QUADRUPLE FLOW WITH DOUBLE GEOMETRY, BREAKTHROUGH DROPS SIGNIFICANTLY, ILLUSTRATING NONLINEAR SCALING EFFECTS.

**Table II:** Breakthrough Times for PFOA Varying Flow, Media Weights, and Tank Heights.

PFOS					
Flow rate (gpm)	Height (m)	Weight of GAC (lbs)	Breakthrough at 2 ppt	Months at 2 ppt	Notes
1,664	9.76	40,000	66	2.2	Quadruple flow, double height, double weight
416	9.76	40,000	0	0	Double height, doubled weight
832	9.76	40,000	151.5	5.05	Double flow, height, weight
416	4.88	20,000	145	4.833	Standard conditions
832	4.88	20,000	61.75	2.0583	Double flow

TABLE II PFOS BREAKTHROUGH TIMES AT A THRESHOLD OF 2 PPT UNDER VARYING FLOW RATES, GAC WEIGHTS, AND COLUMN HEIGHTS. THE STANDARD SETUP (416 GPM, 4.88 M HEIGHT, 20,000 LBS GAC) ACHIEVES ~145 DAYS BEFORE BREAKTHROUGH. DOUBLING THE FLOW RATE UNDER THE SAME GEOMETRY REDUCES BREAKTHROUGH TO ~62 DAYS. WHEN BOTH THE COLUMN HEIGHT AND GAC WEIGHT ARE DOUBLED, BREAKTHROUGH TIME IS RESTORED AND IMPROVED. AT QUADRUPLE FLOW, DESPITE DOUBLED GEOMETRY, PERFORMANCE DROPS TO ~66 DAYS, UNDERSCORING THE COMPOUNDING EFFECTS OF HIGH FLOW ON ADSORPTION EFFICIENCY.

**Table III:** Breakthrough of PFOA at Various Occupied Site Percentages

PFOA					
GAC amount (lbs)	Height (m)	Radius (m)	One tank breakthrough (days)	Two tank breakthrough (days)	Notes
30,000	7.32	3.66	213	426	No site occupied at start (i.e. virgin GAC)
29,700	7.32	3.66	211	422	Assuming that 0.1% of sites are occupied after reactivation
27000	7.32	3.66	190.25	380.5	Assuming that 10% of sites are occupied after reactivation
24000	7.32	3.66	167.5	335	Assuming that 20% of sites are occupied after reactivation
21000	7.32	3.66	144.75	289.5	Assuming that 30% of sites are occupied after reactivation
18000	7.32	3.66	122	244	Assuming that 40% of sites are occupied after reactivation
15000	7.32	3.66	99.75	199.5	Assuming that 50% of sites are occupied after reactivation
12000	7.32	3.66	77.25	154.5	Assuming that 60% of sites are occupied after reactivation
9000	7.32	3.66	55	110	Assuming that 70% of sites are occupied after reactivation
6000	7.32	3.66	33.5	67	Assuming that 80% of sites are occupied after reactivation
3000	7.32	3.66	12.25	24.5	Assuming that 90% of sites are occupied after reactivation

TABLE III. PFOA ONE- AND TWO-TANK BREAKTHROUGH TIMES AT 2 PPT AS A FUNCTION OF GAC WEIGHT AND PERCENTAGE OF ADSORPTION SITES OCCUPIED AFTER REACTIVATION. ALL SCENARIOS MAINTAIN CONSTANT COLUMN GEOMETRY (7.32 M HEIGHT, 3.66 M RADIUS). VIRGIN GAC ACHIEVES A TWO-TANK BREAKTHROUGH OF 426 DAYS, WHILE BREAKTHROUGH TIME DECLINES LINEARLY WITH INCREASING SITE OCCUPATION. AT 90% SITE OCCUPATION, BREAKTHROUGH DROPS TO JUST 24.5 DAYS, EMPHASIZING THE CRITICAL IMPORTANCE OF REACTIVATION EFFICIENCY ON LONG-TERM TREATMENT PERFORMANCE.

**Table IV:** Breakthrough of PFOS at Various Occupied Site Percentages

PFOS					
GAC amount (lbs)	Height (m)	Radius (m)	One tank breakthrough (days)	Two tank breakthrough (days)	Notes
30,000	7.32	3.66	236.5	473	No site occupied at start (i.e. virgin GAC)
29,700	7.32	3.66	233.5	467	Assuming that 0.1% of sites are occupied after reactivation
27000	7.32	3.66	208	416	Assuming that 10% of sites are occupied after reactivation
24000	7.32	3.66	179.75	359.5	Assuming that 20% of sites are occupied after reactivation
21000	7.32	3.66	151.25	302.5	Assuming that 30% of sites are occupied after reactivation
18000	7.32	3.66	123.5	247	Assuming that 40% of sites are occupied after reactivation
15000	7.32	3.66	96	192	Assuming that 50% of sites are occupied after reactivation
12000	7.32	3.66	68.75	137.5	Assuming that 60% of sites are occupied after reactivation
9000	7.32	3.66	43	86	Assuming that 70% of sites are occupied after reactivation
6000	7.32	3.66	19.25	38.5	Assuming that 80% of sites are occupied after reactivation
3000	7.32	3.66	0.25	0.5	Assuming that 90% of sites are occupied after reactivation

TABLE IV. PFOS ONE- AND TWO-TANK BREAKTHROUGH TIMES AT 2 PPT AS A FUNCTION OF GAC WEIGHT AND PERCENTAGE OF ADSORPTION SITES OCCUPIED AFTER REACTIVATION. COLUMN GEOMETRY IS HELD CONSTANT (7.32 M HEIGHT, 3.66 M RADIUS). VIRGIN GAC ACHIEVES A TWO-TANK BREAKTHROUGH OF 473 DAYS. AS THE PERCENTAGE OF OCCUPIED ADSORPTION SITES INCREASES, BREAKTHROUGH TIME DECREASES SHARPLY, WITH ONLY 0.5 DAYS ACHIEVED AT 90% OCCUPATION. THIS HIGHLIGHTS THE DRAMATIC REDUCTION IN TREATMENT PERFORMANCE WHEN REACTIVATION IS INCOMPLETE, REINFORCING THE NEED FOR HIGH-EFFICIENCY REGENERATION PROCESSES.

**Table V:** Effect of PSDFR Parameter on PFOA Breakthrough

PFOA					
amount of GAC (lbs)	tank radius (m)	tank height (m)	PSDFR	one tank breakthrough (days)	two tanks breakthrough (days)
30,000	3.66	7.32	1	203.25	406.5
30,000	3.66	7.32	2	207.75	415.5
30,000	3.66	7.32	3	210.25	420.5
30,000	3.66	7.32	4	211.75	423.5
30,000	3.66	7.32	5	213	426
30,000	3.66	7.32	6	214	428
30,000	3.66	7.32	7	214.5	429
30,000	3.66	7.32	8	215.25	430.5
30,000	3.66	7.32	9	215.5	431
30,000	3.66	7.32	10	216	432

TABLE V. EFFECT OF PARTICLE SIZE DISTRIBUTION FIT RATIO (PSDFR) ON PFOA BREAKTHROUGH TIME USING 30,000 LBS OF GAC IN A FIXED TANK GEOMETRY (3.66 M RADIUS, 7.32 M HEIGHT). INCREASING PSDFR IMPROVES BREAKTHROUGH PERFORMANCE MODESTLY, WITH TWO-TANK BREAKTHROUGH TIME RISING FROM 406.5 DAYS AT PSDFR 1 TO 432 DAYS AT PSDFR 10. THIS TREND SUGGESTS THAT MORE FAVORABLE MEDIA PARTICLE SIZE DISTRIBUTIONS ENHANCE ADSORPTION KINETICS AND EXTEND OPERATIONAL LIFESPAN.

**Table VI:** Effect of PSDFR Parameter on PFOS Breakthrough

PFOS					
amount of GAC (lbs)	tank radius (m)	tank height (m)	PSDFR	one tank breakthrough (days)	two tanks breakthrough (days)
30,000	3.66	7.32	1	209.75	419.5
30,000	3.66	7.32	2	223	446
30,000	3.66	7.32	3	229.5	459
30,000	3.66	7.32	4	233.5	467
30,000	3.66	7.32	5	236.5	473
30,000	3.66	7.32	6	238.5	477
30,000	3.66	7.32	7	240	480
30,000	3.66	7.32	8	241.25	482.5
30,000	3.66	7.32	9	242	484
30,000	3.66	7.32	10	242.75	485.5

TABLE VI. PFOS BREAKTHROUGH TIMES AS A FUNCTION OF PARTICLE SIZE DISTRIBUTION FIT RATIO (PSDFR), WITH A CONSTANT 30,000 LBS OF GAC AND FIXED TANK GEOMETRY (3.66 M RADIUS, 7.32 M HEIGHT). AS PSDFR INCREASES FROM 1 TO 10, TWO-TANK BREAKTHROUGH TIME IMPROVES FROM 419.5 TO 485.5 DAYS. THIS UPWARD TREND INDICATES THAT OPTIMIZED PARTICLE SIZE DISTRIBUTION ENHANCES MASS TRANSFER AND ADSORPTION EFFICIENCY, THEREBY EXTENDING THE TREATMENT SYSTEM'S OPERATIONAL DURATION.

**Table VII: Effect of Particle Radius on PFOS Breakthrough**

PFOS							
standard particle radius (cm)	amount of GAC (lbs)	flow rate (gpm)	tank radius (m)	tank height (m)	one tank breakthrough (days)	two tank breakthrough (days)	notes
0.0513	30,000	416	3.66	7.32	236.5	473	OG size
0.0462	30,000	416	3.66	7.32	243.25	486.5	90% of OG size
0.0410	30,000	416	3.66	7.32	249.5	499	80% of OG size
0.0359	30,000	416	3.66	7.32	-	-	70% of OG size
0.0308	30,000	416	3.66	7.32	-	-	60% of OG size
0.0257	30,000	416	3.66	7.32	-	-	50% of OG size
0.0205	30,000	416	3.66	7.32	-	-	40% of OG size
0.0154	30,000	416	3.66	7.32	-	-	30% of OG size
0.0103	30,000	416	3.66	7.32	-	-	20% of OG size
0.0051	30,000	416	3.66	7.32	-	-	10% of OG size

TABLE VII. EFFECT OF STANDARD PARTICLE RADIUS ON PFOS BREAKTHROUGH TIMES WITH FIXED FLOW RATE (416 GPM), GAC MASS (30,000 LBS), AND TANK GEOMETRY (3.66 M RADIUS, 7.32 M HEIGHT). AS PARTICLE RADIUS DECREASES FROM THE ORIGINAL 0.0513 CM TO 80% OF THE ORIGINAL SIZE, BREAKTHROUGH TIME INCREASES, WITH TWO-TANK PERFORMANCE IMPROVING FROM 473 TO 499 DAYS. SMALLER PARTICLES LIKELY ENHANCE ADSORPTION KINETICS BY INCREASING SURFACE AREA AND REDUCING MASS TRANSFER RESISTANCE. BREAKTHROUGH DATA FOR PARTICLE SIZES SMALLER THAN 80% WAS NOT AVAILABLE, THOUGH FURTHER IMPROVEMENT MAY BE CONSTRAINED BY PRESSURE DROP AND OPERATIONAL FEASIBILITY. TOP OF FORM BOTTOM OF FORM

ADDITIONAL NOTE: WHEN THE PARTICLE DIAMETER IS 10-70% OF THE ORIGINAL SIZE, THE BREAKTHROUGH CURVES INCREASES PAST 0 PPT, THEN DECREASES BACK TO 0, AND THEN INCREASES AGAIN (INDICATING THAT THERE IS SOMETHING WRONG WITH THE MODEL (MAY NOT BE ABLE TO CALCULATE A PARTICLE THAT SMALL ACCURATELY) ALSO, AT 70% OF THE OG SIZE, IT GOES PAST 250 DAYS AND YOU CAN'T EVEN SEE BREAKTHROUGH AT 2 PPT BC RSTUDIO ABORTS PAST 250 DAYS.

**Table VIII: Effect of Particle Radius on PFOA Breakthrough**

PFOA							
standard particle radius (cm)	amount of GAC (lbs)	flow rate (gpm)	tank radius (m)	tank height (m)	one tank breakthrough (days)	two tank breakthrough (days)	notes
0.0513	30,000	416	3.66	7.32	213	426	OG size
0.0462	30,000	416	3.66	7.32	215.25	430.5	90% of OG size
0.0410	30,000	416	3.66	7.32	217.5	435	80% of OG size
0.0359	30,000	416	3.66	7.32	219.75	439.5	70% of OG size
0.0308	30,000	416	3.66	7.32	221.75	443.5	60% of OG size
0.0257	30,000	416	3.66	7.32	223.75	447.5	50% of OG size
0.0205	30,000	416	3.66	7.32	225.75	451.5	40% of OG size
0.0154	30,000	416	3.66	7.32	-	-	30% of OG size
0.0103	30,000	416	3.66	7.32	-	-	20% of OG size
0.0051	30,000	416	3.66	7.32	-	-	10% of OG size

TABLE VIII. EFFECT OF STANDARD PARTICLE RADIUS ON PFOA BREAKTHROUGH TIMES USING 30,000 LBS OF GAC AT 416 GPM AND FIXED TANK DIMENSIONS (3.66 M RADIUS, 7.32 M HEIGHT). AS PARTICLE SIZE DECREASES FROM THE ORIGINAL 0.0513 CM TO 40% OF THE ORIGINAL SIZE, BREAKTHROUGH TIME INCREASES STEADILY—REACHING 451.5 DAYS FOR TWO TANKS. SMALLER PARTICLES IMPROVE BREAKTHROUGH PERFORMANCE DUE TO INCREASED SURFACE AREA AND REDUCED DIFFUSION PATH LENGTHS. BREAKTHROUGH DATA FOR PARTICLES BELOW 30% OF THE ORIGINAL SIZE WAS NOT AVAILABLE, POTENTIALLY DUE TO OPERATIONAL CONSTRAINTS SUCH AS EXCESSIVE PRESSURE DROP OR MEDIA COMPACTION.

## 16.5 HAZOP

### *16.5.1 Solids Removal Zone*

[HAZOPForm\(desander\).docx](#)

### *16.5.2 AOP*

[HAZOPForm\(AOP\).docx](#)

### *16.5.3 GAC*

[GAC HAZOP](#)

### *16.5.4 Backwash*

[HAZOPForm\(Backwash\).docx](#)

## 16.6 LCA

### *16.6.1 Desander*

[OpenLCA.docx](#)

### *16.6.2 AOP*

[LCA Homework.docx](#)

### *16.6.3 GAC*

[LCA HW](#)

### *16.6.4 Backwash*

[Backwash LCA.docx](#)